

# ML in heliophysics

-

## Space weather

Peter Wintoft

**Swedish Institute of Space Physics**

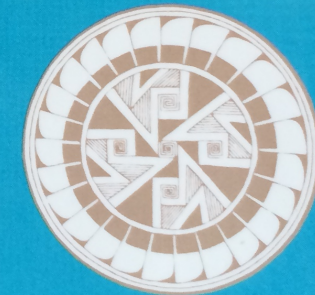
# Outline

- I. Heliophysics and space weather
- II. Machine learning with focus on neural networks applied to space weather
- III. Future challenges



# INTRODUCTION TO THE THEORY OF NEURAL COMPUTATION

*John Hertz  
Anders Krogh  
Richard G. Palmer*



A LECTURE NOTES VOLUME IN THE  
SANTA FE INSTITUTE STUDIES IN THE SCIENCES OF COMPLEXITY

## COMPLEX SYSTEMS: TURBULENCE, CHAOS, NEURAL NETWORKS

European-Nordic Summer School – Krogerup Højskole, Humlebæk, Denmark  
21 – 28 August 1993

Sponsored by Nordisk Forskerutdannigsakademi (NorFA) and EC Mobility Programme - Danish Research Academy



The aim of the school is to introduce graduate students and post-doctoral fellows into recent advances in physics of complex systems: chaos in low dimensional classical and quantum systems, turbulence in flows, neural networks, self-organized critical phenomena, fractals in oil research, interface growth.

**Lecturers:**

D. Rand (Warwick)  
P. Cvitanović (Copenhagen)  
I. Procaccia (Weizmann)

**J. Feder (Oslo)**

A. Libchaber (Princeton)  
S. Solla (AT&T)  
T. Bohr (Copenhagen)

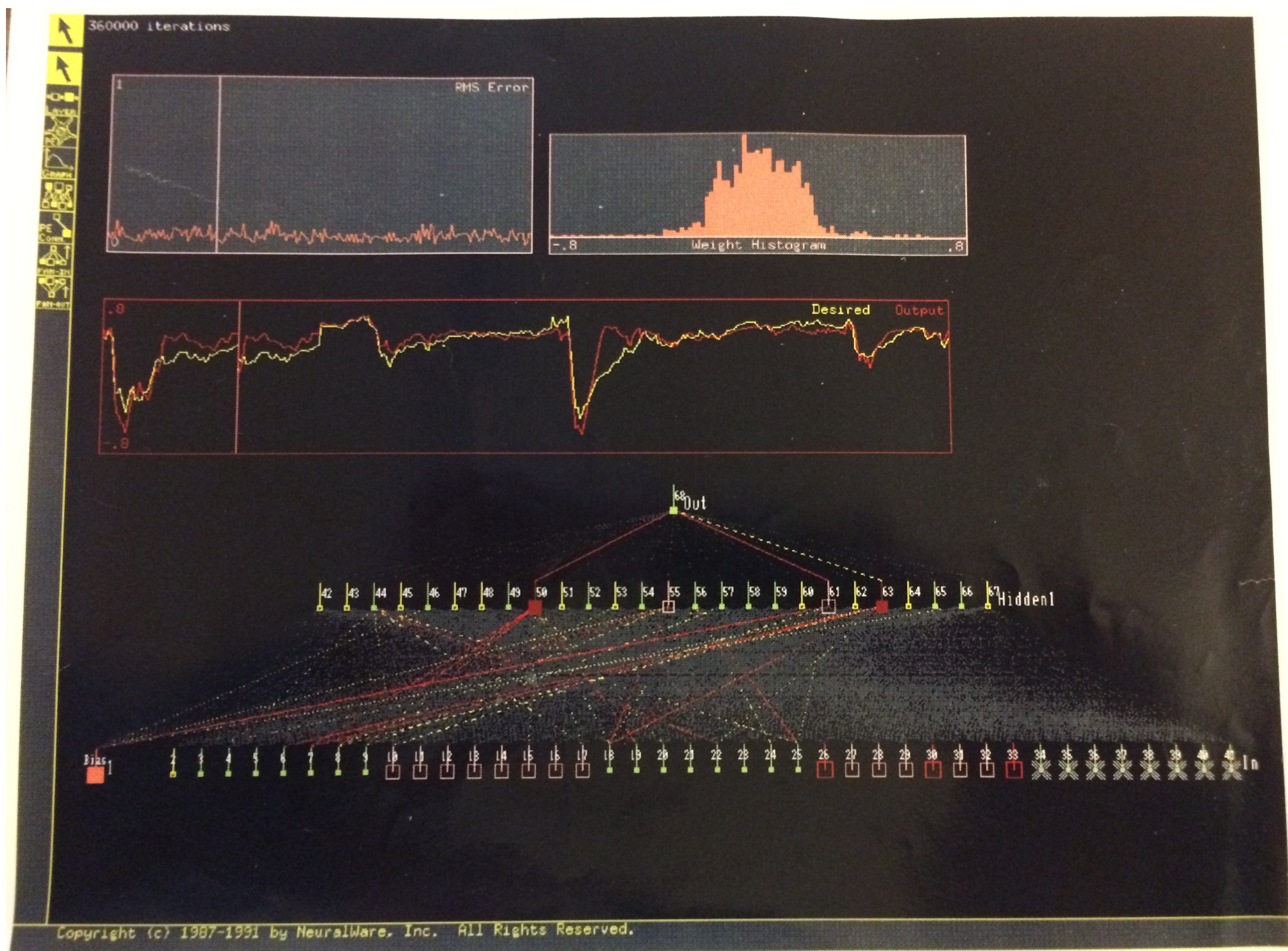
**P. Bak (Brookhaven)**

G. Grinstein (IBM)  
J. Hertz (Copenhagen)  
J. Krug (Jülich)

Scientific Direction: Mogens H. Jensen; T. Bohr, P. Cvitanović, J. Hertz, C. Peterson.

Applications, with brief C.V. and description of research interests, should reach this address before 1 May 1993. Applicants should also arrange for letter(s) of reference. Funding is available for students from EC, Nordic countries and Baltic republics. For information please contact:

Ellen Pedersen, NORDITA, Blegdamsvej 17, DK-2100 Copenhagen Ø, Denmark  
Tel: +45 : 31 42 16 16 / Fax: +45 : 31 38 91 57 / telex: 15216 nbi dk / e-mail: sum\_sch@nordita.dk



Proceedings of the International Workshop on  
Artificial Intelligence Applications in  
Solar-Terrestrial Physics

Lund, Sweden, 22–24 September 1993

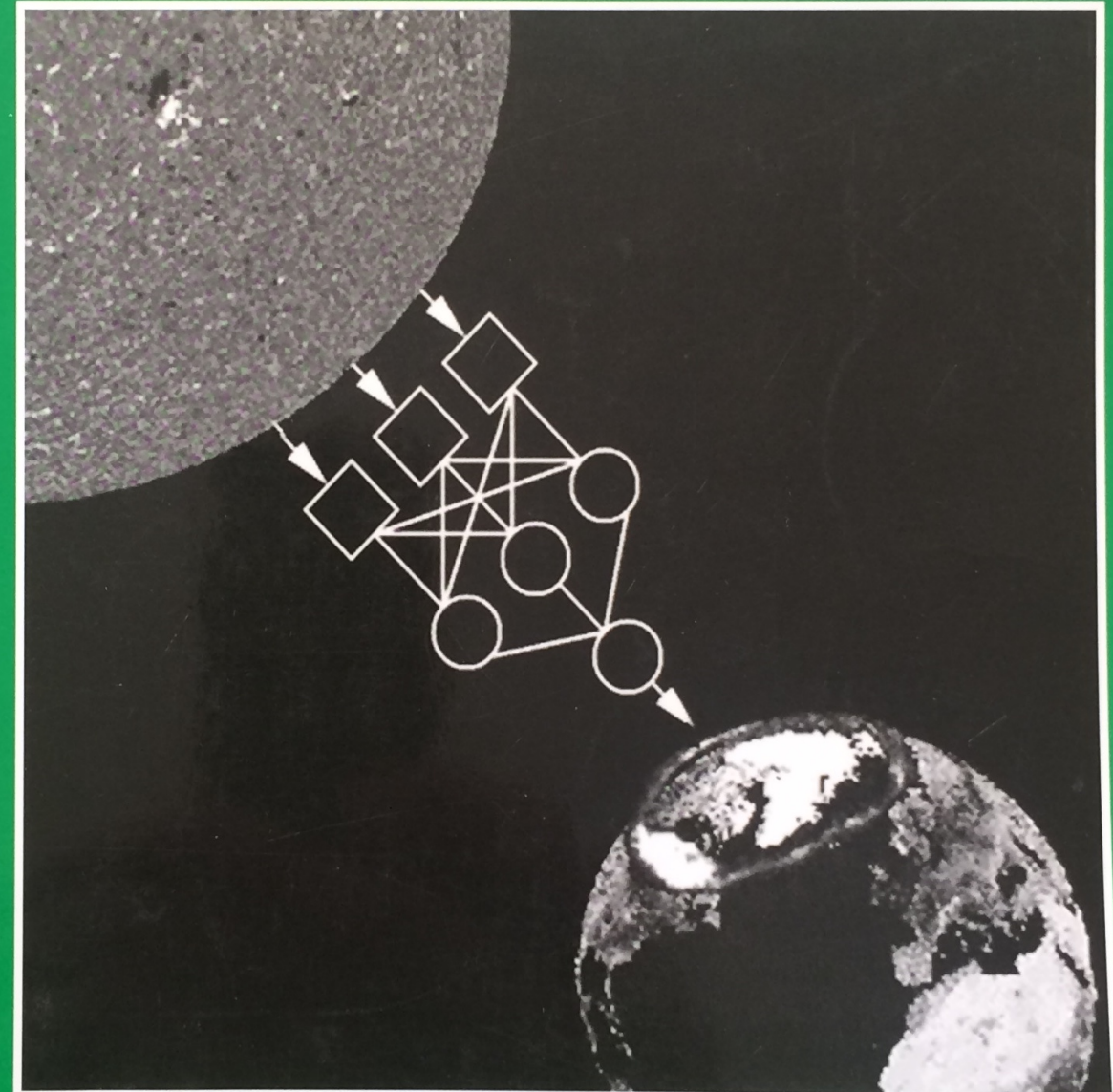
Edited by

JoAnn Joselyn, Henrik Lundstedt, and Joanna Trolinger

NOAA Space Environment Laboratory  
Boulder, Colorado, USA

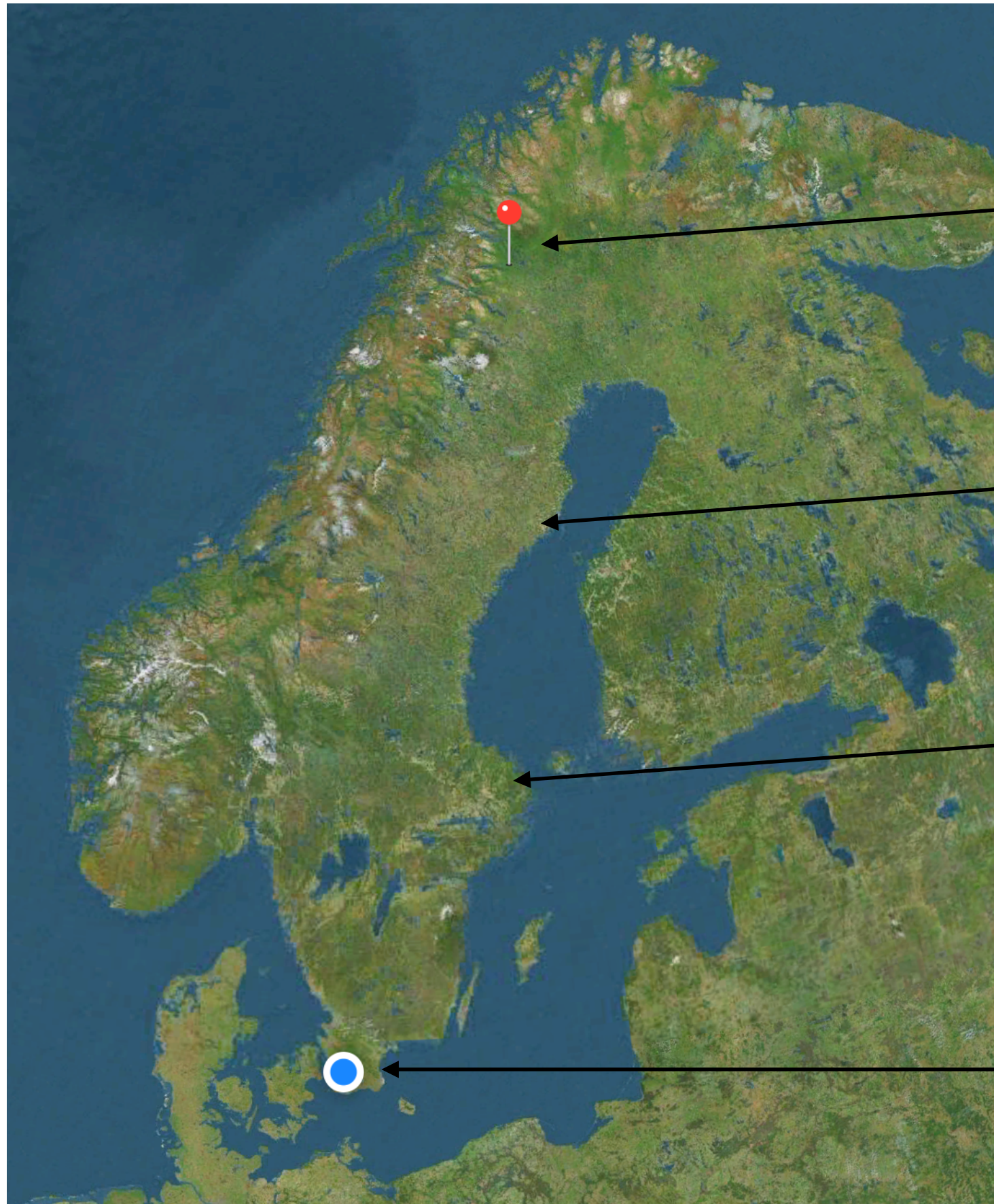


AI Applications in  
Solar-Terrestrial Physics



Lund, Sweden, 29-31 July 1997

# Institutet för rymdfysik



First AIDA school, Bologna, 2020-01-22

**Staff**

**57**



**Kiruna**

**2**



**Umeå**

**38**



**Uppsala**

**3**



**Lund**

**Total: 100**

# Solar Terrestrial and Atmospheric Research STAR

## STAR Kiruna staff:

Evgenia Belova  
Peter Dalin  
Johan Kero  
Hans Nilsson (50%)  
Tima Sergienko  
Peter Voelger  
Masatoshi Yamauchi (50%)

## KAGO (observatory) staff:

Urban Brändström  
Uwe Raffalski  
Daria Mikhaylova  
Lars-Göran Vanhainen

## PhD students:

Audrey Schillings  
Daniel Kastinen

## Postdoc:

Tikemani Bag

## STAR Uppsala staff:

Thomas Leyser

## STAR Umeå staff:

Peje Nilsson  
Fredrik Rutqvist  
Asta Pellinen-Wannberg (25%)

## STAR Lund staff:

Peter Wintoft  
Magnus Wik  
Juri Katkalov

## STAR EISCAT staff:

Peter Bergqvist  
Lennart Lövqvist

Solar photosphere

Corona

Solar wind

Bow shock

Magnetopause

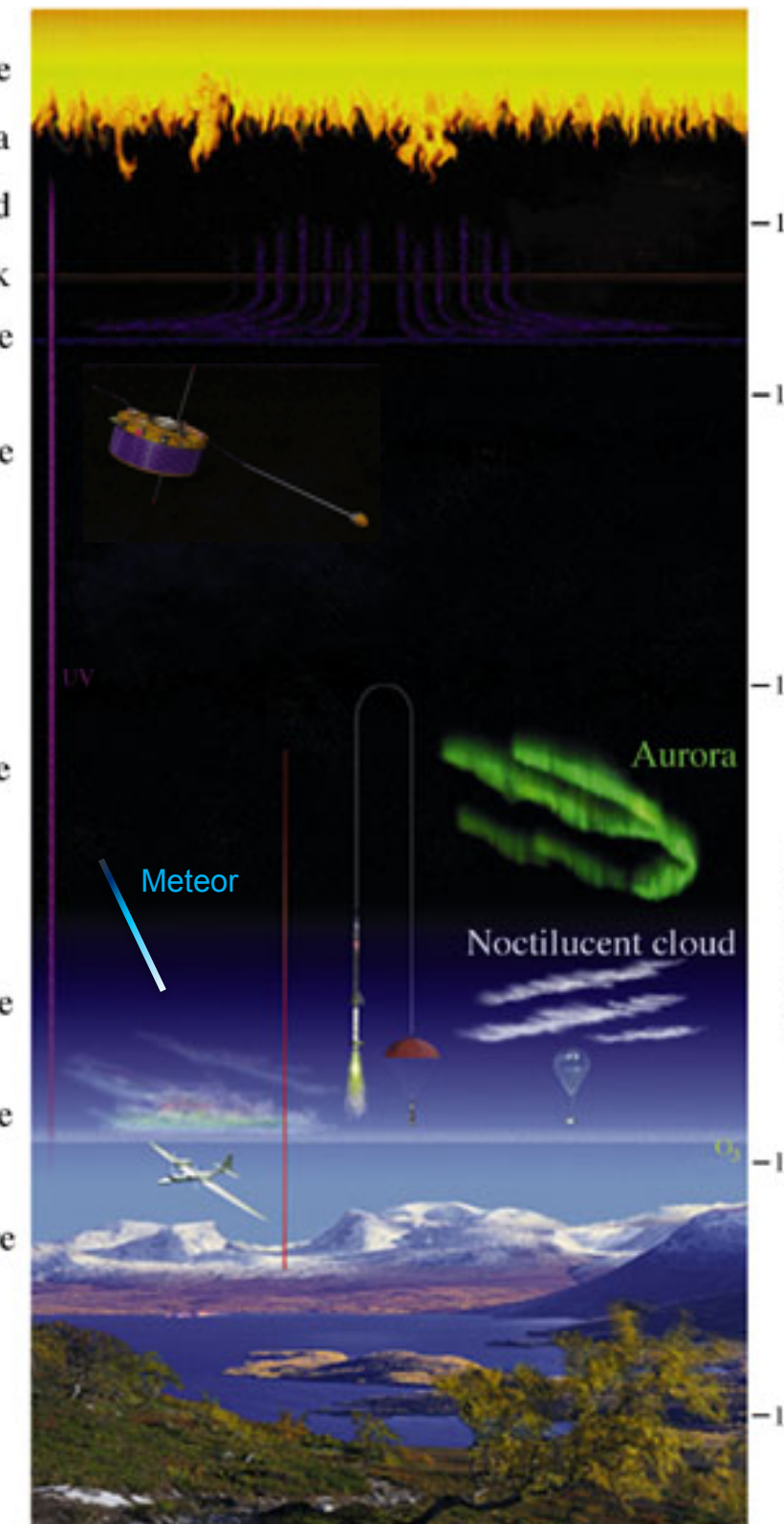
Magnetosphere

Ionosphere

Mesosphere

Stratosphere

Troposphere



# Heliophysics and space weather

- Wikipedia: “Heliophysics is the science of the Sun and the physical connections between the Sun and the solar system.”
- Wikipedia: “Space weather is a branch of space physics and aeronomy, or heliophysics, concerned with the time varying conditions within the Solar System, including the solar wind, emphasizing the space surrounding the Earth, including conditions in the magnetosphere, ionosphere, thermosphere, and exosphere.”

## (US) National Space Weather definition

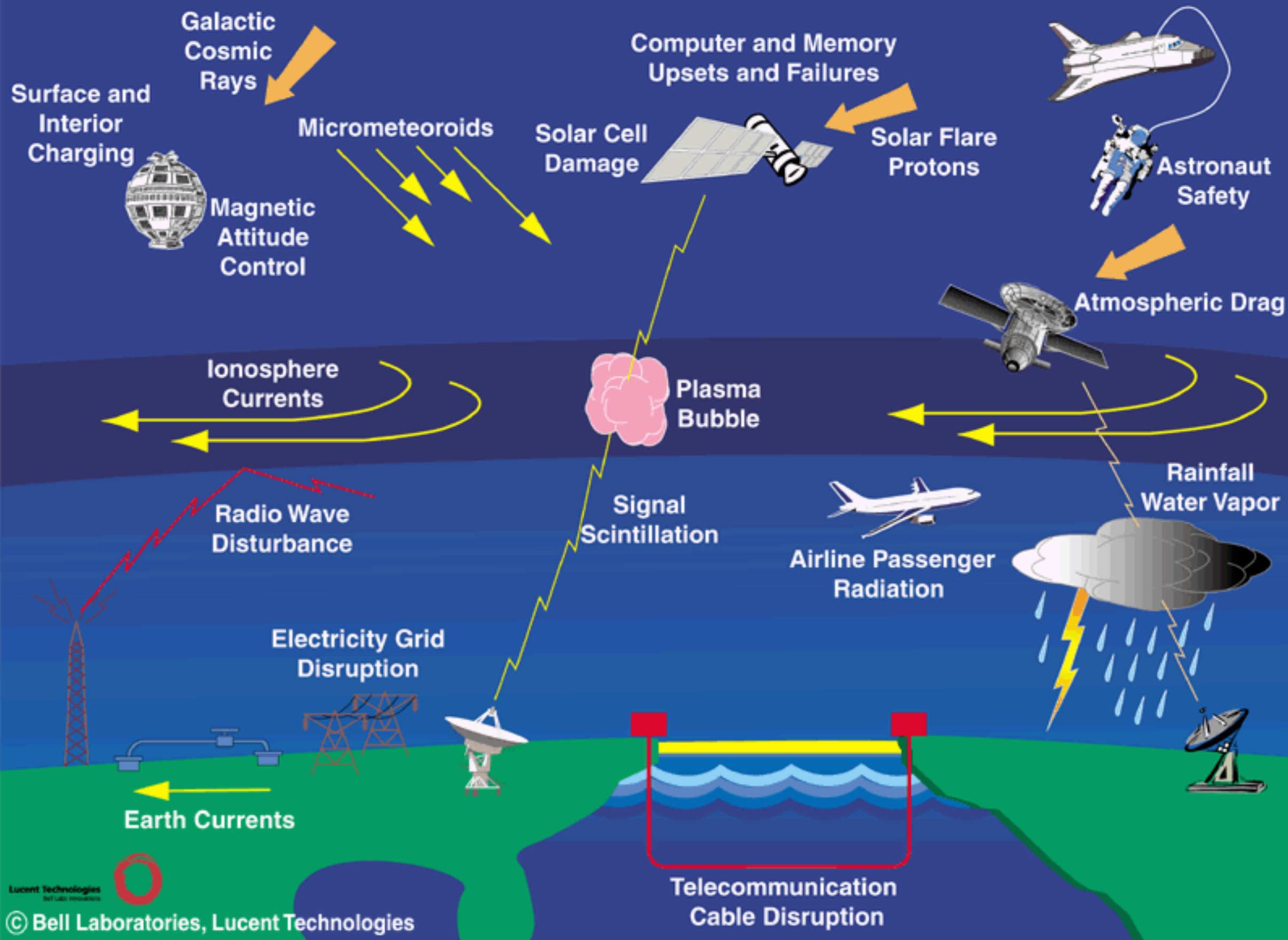
Space weather refers to conditions on the Sun and in the solar wind, magnetosphere, ionosphere, and thermosphere that can influence the performance and reliability of space-borne and ground-based technological systems and can endanger human life or health.

## COST 724 Space Weather definition

(European Cooperation in Science and Technology)

Space weather is the physical and phenomenological state of natural space environments. The associated discipline aims, through observation, monitoring, analysis and modelling, at understanding and predicting the state of the Sun, the interplanetary and planetary environments, and the solar and non-solar driven perturbations that affect them, and also at forecasting and nowcasting the potential impacts on biological and technological systems.

# Space Weather



# Some space weather events

- May 1921
- August 1972
- March 1989
- Oct-Nov 2003
- Dec 2006

# May 1921

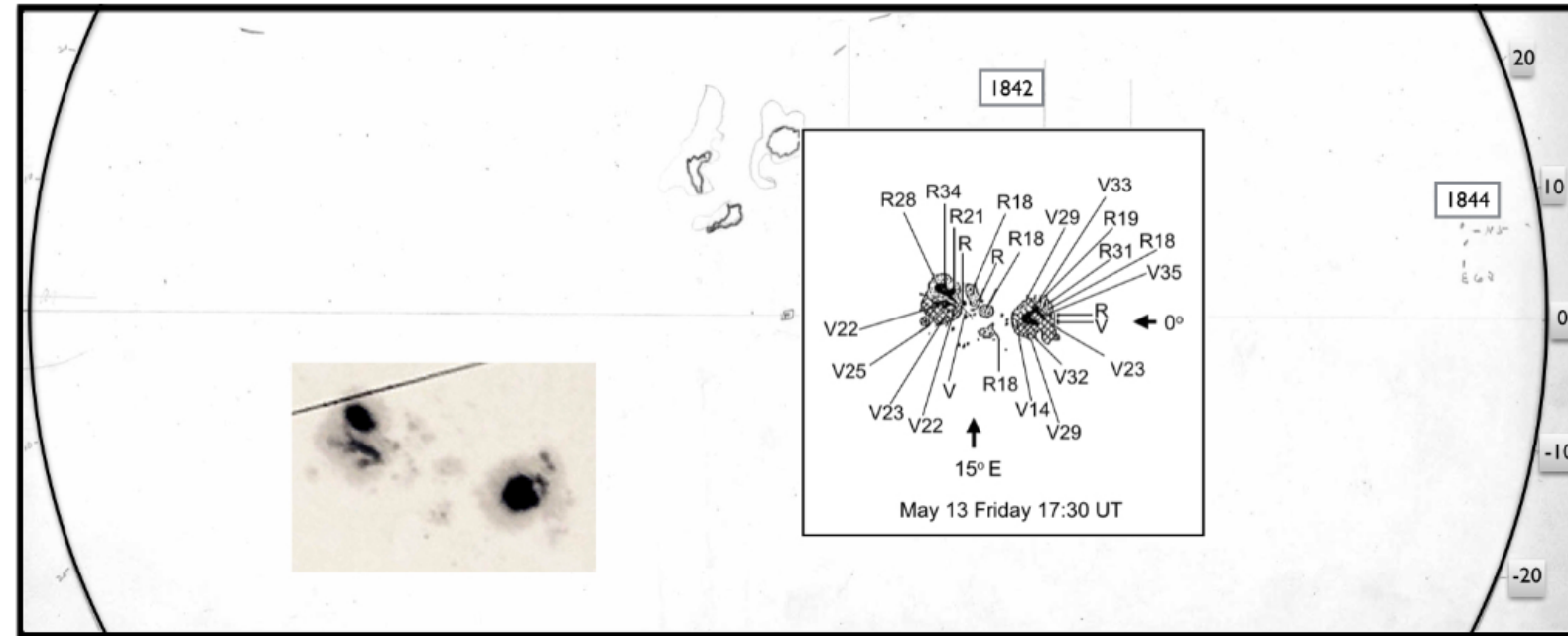
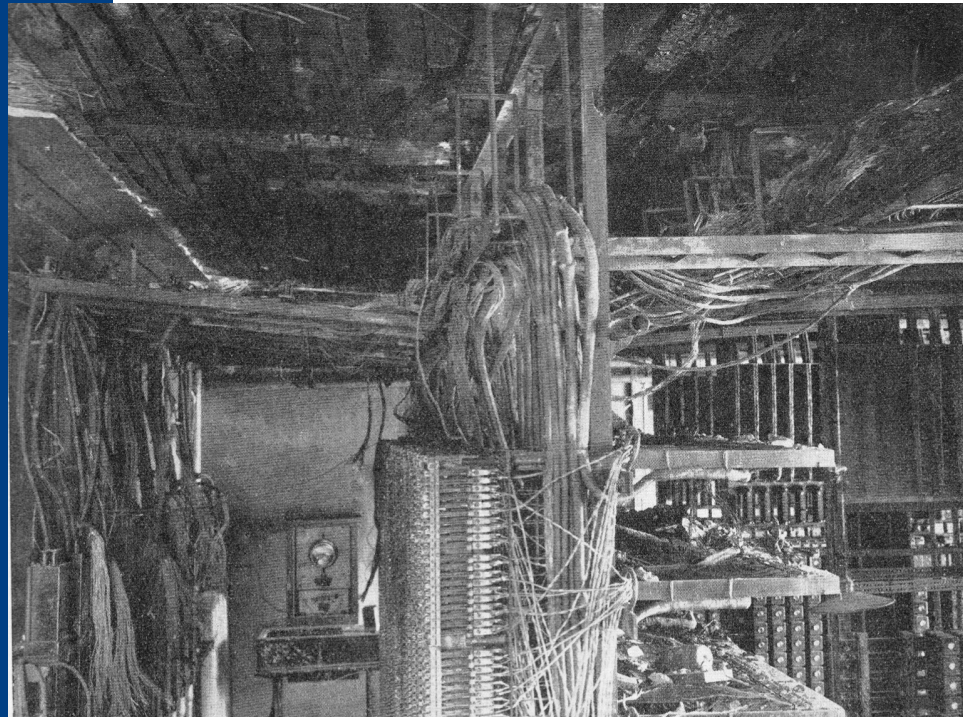


**Figure 1.** Mount Wilson drawing of active regions occurring on 13 May 1921 at 17:30 UT and to the left, a white-light observation by Royal Greenwich Observatory (RGO) at 09:55 UT.

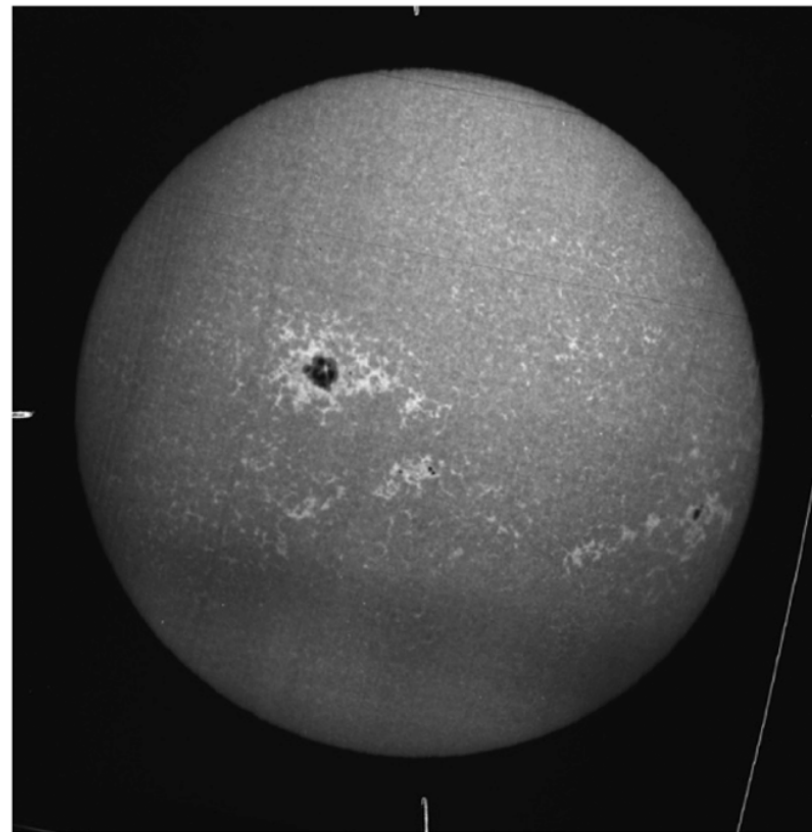
The extreme solar storm of May 1921: observations and a complex topological model  
 H. Lundstedt and T. Persson and V. Andersson  
*Annales Geophysicae* 33 109–116 (2015)



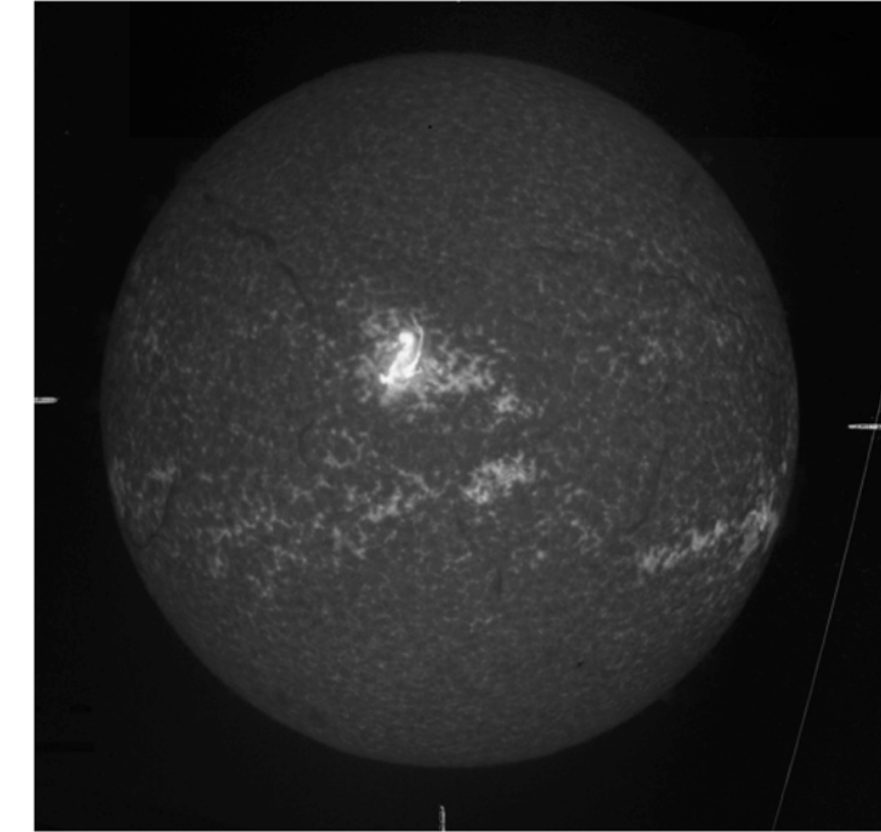
**At 00:00 UT (02:00 local time) in the morning of 15 May a fire occurred in a telegraph station in Karlstad, Sweden (Em, 1921).**

# August 1972

a) Calcium Emission, 3 August 1972



b) Hydrogen- $\alpha$  Emission, 4 August 1972



## 1.4. Naval Effects

Tucked away in the history of the Vietnam War is a likely associated effect of the extraordinary 4 August IP disturbance: The sudden detonation of a *large number* of U.S. Navy magnetic-influence sea mines (designated as Destructors, DSTs) dropped into the coastal waters of North Vietnam only 3 months earlier (Greer, 1997). See Appendix for additional context. Tucker (2006, Chap. 15, p. 177) wrote that "... on 4 August (1972) TF-77 aircraft reported some two dozen explosions in a minefield near Hon La over a thirty-second time span...Ultimately the Navy concluded that the explosions had been caused by the magnetic perturbations of solar storms, the most intense in more than two decades."

Knipp, D. J., Fraser, B. J., Shea, M. A., & Smart, D. F. (2018). On the little-known consequences of the 4 August 1972 ultra-fast coronal mass ejecta: Facts, commentary, and call to action. *Space Weather*, 16, 1635–1643. <https://doi.org/10.1029/2018SW002024>

# March 1989

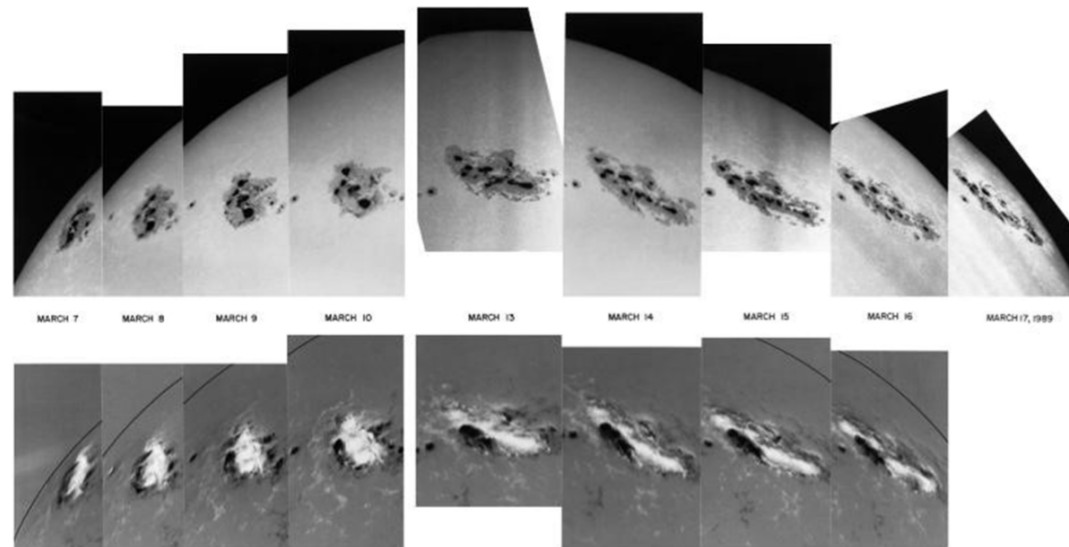


**Figure 1.** White light images (top row) and solar magnetograms (bottom row) showing the passage of Region 5395 across the face of the Sun between 7 and 17 March 1989. The solar magnetograms show the strong magnetic fields directed inward (black) and outward (white) in the sunspot group. Images from the Kitt Peak Observatory.

"In Québec, because of the high ground resistivity, this produced large electric fields that drove geomagnetically induced currents (GICs) across the Hydro-Québec power system, causing transformer saturation, harmonic generation and increased reactive power consumption by the transformers. The harmonics caused Static VAR Compensators to trip out and without the reactive power support they were designed to provide the system went unstable and protection relays operated to shut down the system (Bolduc, 2002; Czech et al., 1989; Guillon et al., 2016)."

A 21st Century View of the March 1989 Magnetic Storms  
D. H. Boteler  
Space Weather 17 (2019)

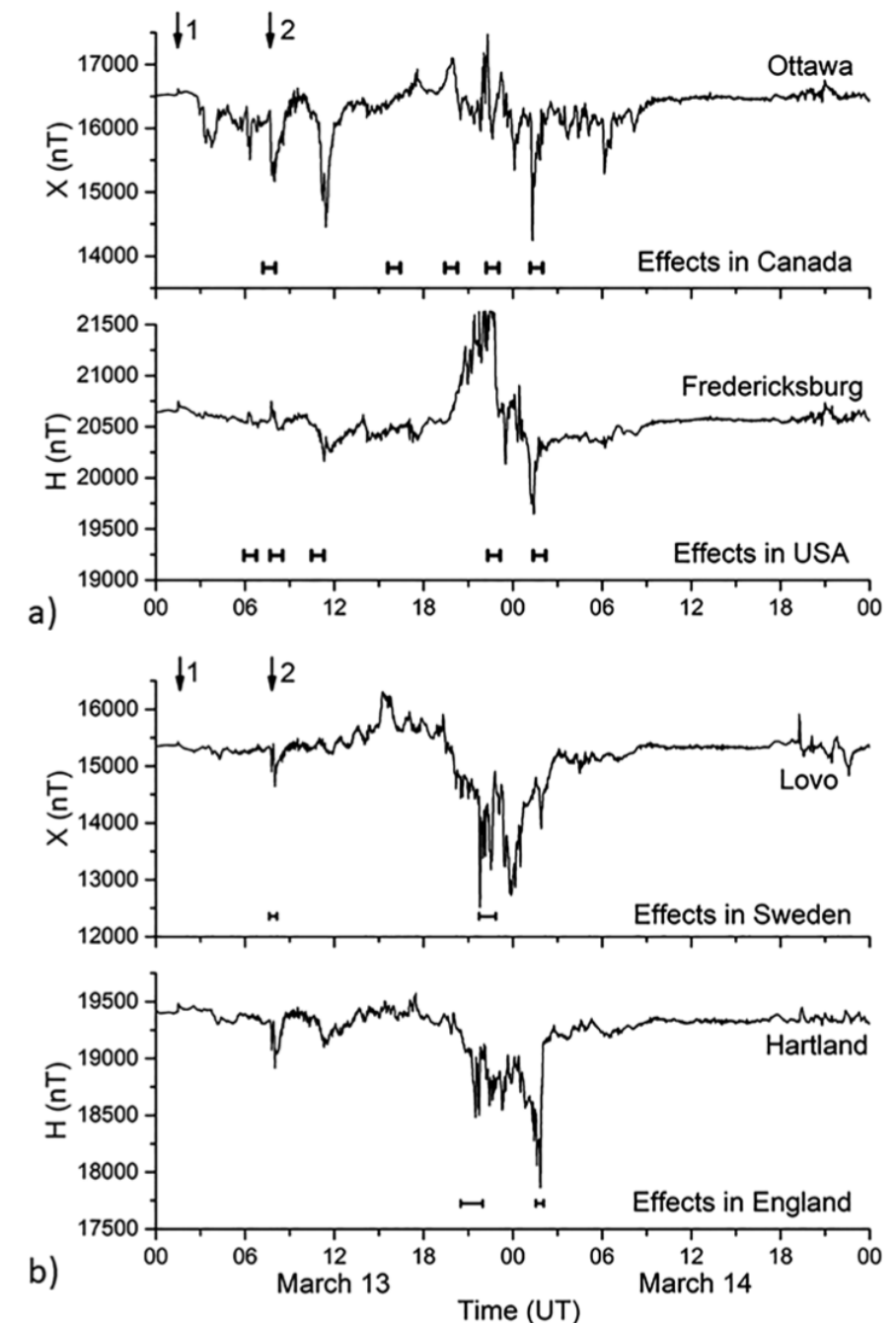


**Figure 8.** Magnetic disturbances and effects on power systems during 13–14 March 1989 in (a) North America and (b) Europe (the different vertical scales). Horizontal bars indicate the times of power system effects. Black arrows indicate the times of the storm sudden commencement.

# Oct 2003

## PM Malmöhus

[Start](#)[Program A-Ö](#)[Tablå](#)[Låtlistor](#)[Arkiv](#)[Om ...](#)[Tips!](#)

## Stort strömavbrott i centrala Malmö

**Strax efter klockan 21.00 drabbades stora delar av centrala Malmö av ett stort strömavbrott. Som mest var 50 000 hushåll utan el. Orsaken kan ha varit solmagnetisk störning.**

Publicerat fredag 31 oktober 2003 kl 06:48

 [DELA](#)

Det var en 130 kilovoltsledning som slogs ut. Efter ungefär en timme var strömmen tillbaka när Sydkraft lyckats göra omkopplingar. Strömavbrottet drabbade ett 20-tal tåg vid Malmö central. I olika fastigheter fastnade sammanlagt sju personer i hissar och fick hjälpas ut. Sydsvenska Dagbladet fick problem med tryckningen av tidningen. Under strömavbrottet skedde också en trafikolycka mellan en personbil och en brandbil under utryckning vid Triangeln i Malmö. Två personer skadades, dock bara lindrigt. På fredagsmorgonen var strömförsörjningen åter helt normal i Malmö. Orsaken till avbrottet är inte helt klarlagd. Det kan ha varit solmagnetisk störning som slog ut spänningen.

<http://sverigesradio.se/sida/artikel.aspx?programid=96&artikel=315130>

**Table 1.** Problems due to GIC in ground-based technological systems in Sweden.

Date	Effects
2 Sep 1859	Problems with the telegraph system in Gothenburg
13–15 May 1921	Fires in telegraph equipment
11 Feb 1958	Fires with severe damage in telegraph equipment
13 Nov 1960	30 line circuit breakers tripped in the high-voltage power network
13–14 Jul 1982	4 transformers and 15 lines tripped in the high-voltage power system. Railway traffic lights turned erroneously to red. Telecommunications were also affected.
8–9 Feb 1986	5 events in the high-voltage power system, 1–3 lines tripped per event
13–14 Mar 1989	5 130 kV lines tripped, 5-degree temperature increase in a generator
24 Mar 1991	9 220 kV lines and a transformer tripped
9 Nov 1991	One 220 kV line tripped. Large pipe-to-soil voltages in a pipeline
1999	Radio communication for protection lost in the power system
2000	Voltage drop in the 400 kV system
6 Apr 2000	Largest GIC ever measured in a transformer (about 300 A)
30 Oct 2003	Power blackout in Malmö, excess heating in a transformer
8 Nov 2004	GIC of over 100 A measured in a transformer in southern Sweden

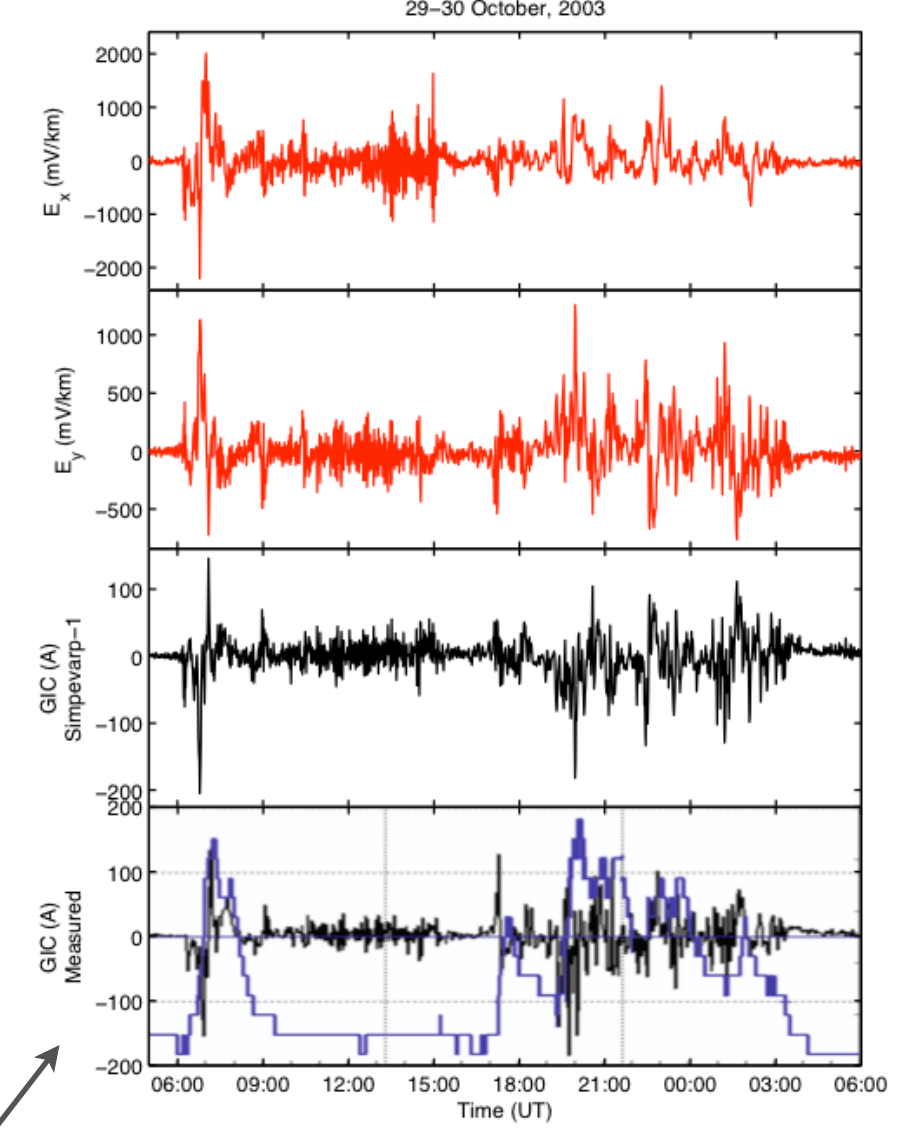


**Fig. 8.** The bottom panel shows measured GIC (black curve) and transformer temperature (blue curve) at Simpevarp-1 (#20 in Fig. 2) from 05:00 UT on 29 October to 06:00 UT on 30 October 2003. The total range from bottom to top in the figure for the temperature is roughly ten degrees. There are no measurements at later times on 30 October due to a problem with the monitoring system (private communication with H. Swahn). The second panel from the bottom presents calculated GIC at Simpevarp-1. The two upper panels refer to the calculated geoelectric field at the more southern red grid point in Fig. 1.

Wik, M., R. Pirjola, H. Lundstedt, A. Viljanen, P. Wintoft, and A. Pulkkinen, Space weather events in July 1982 and October 2003 and the effects of geomagnetically induced currents on Swedish technical systems, *Ann. Geophys.*, 27, 1775–1787, 2009.

# DEC 2006

:Product: 1212RSGA.txt

:Issued: 2006 Dec 12 2204 UTC

# Prepared jointly by the U.S. Dept. of Commerce, NOAA,

# Space Environment Center and the U.S. Air Force.

#

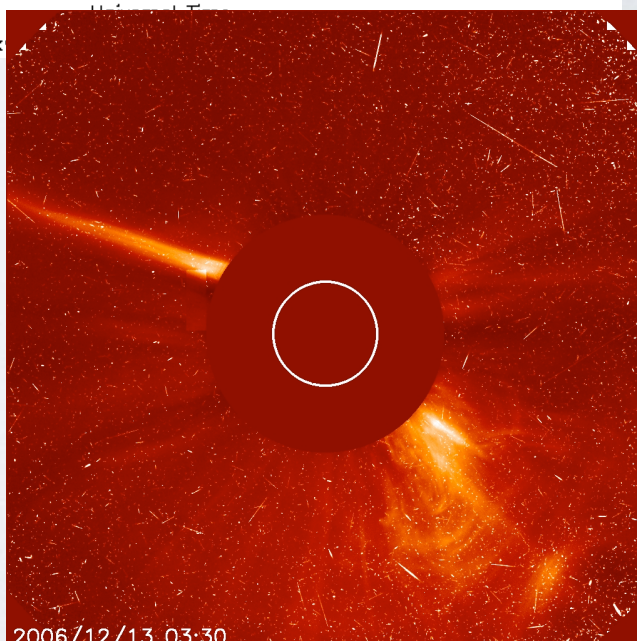
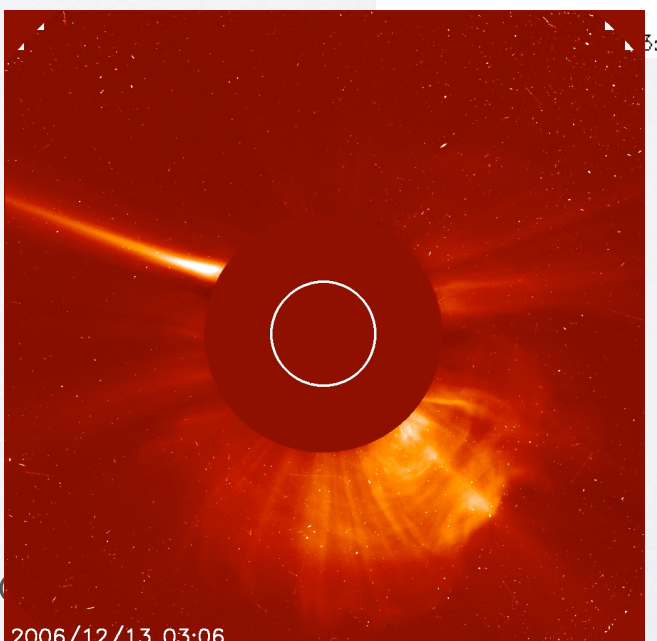
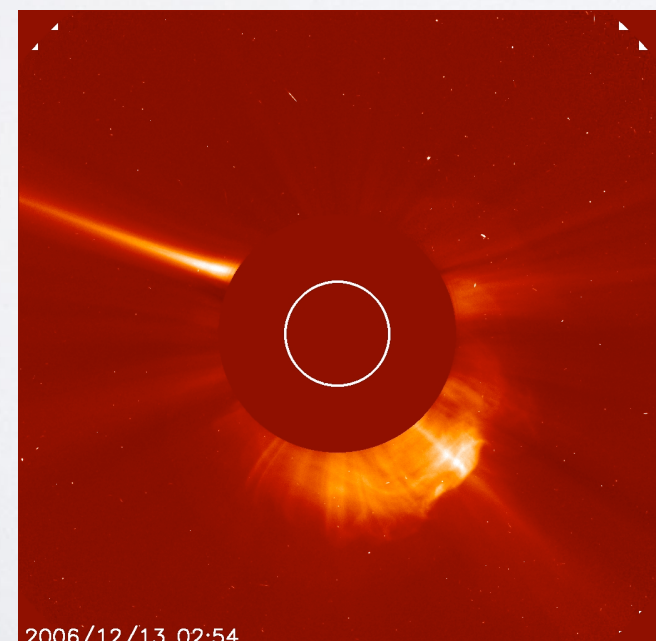
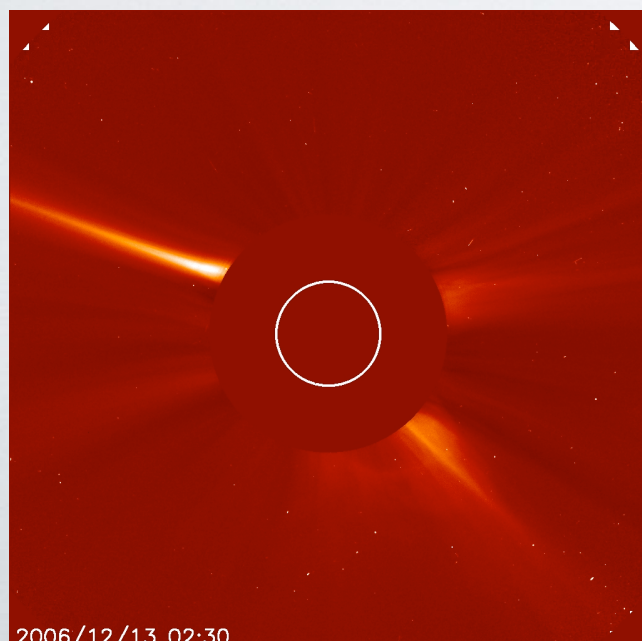
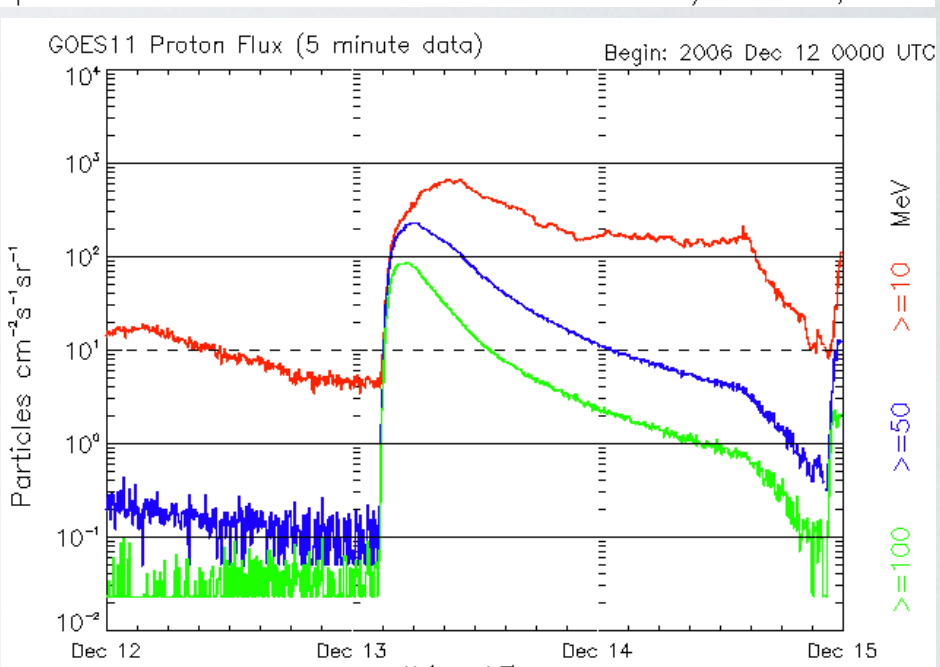
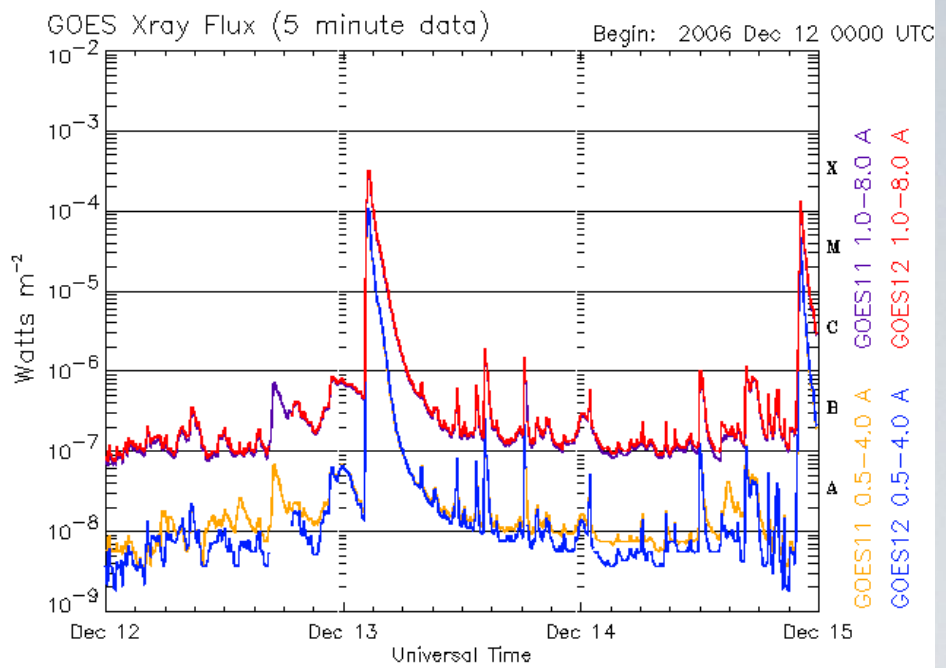
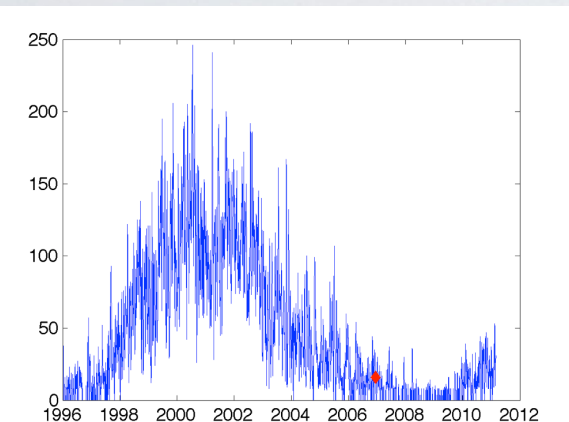
### III. Event Probabilities 13 Dec-15 Dec

Class M 25/25/25

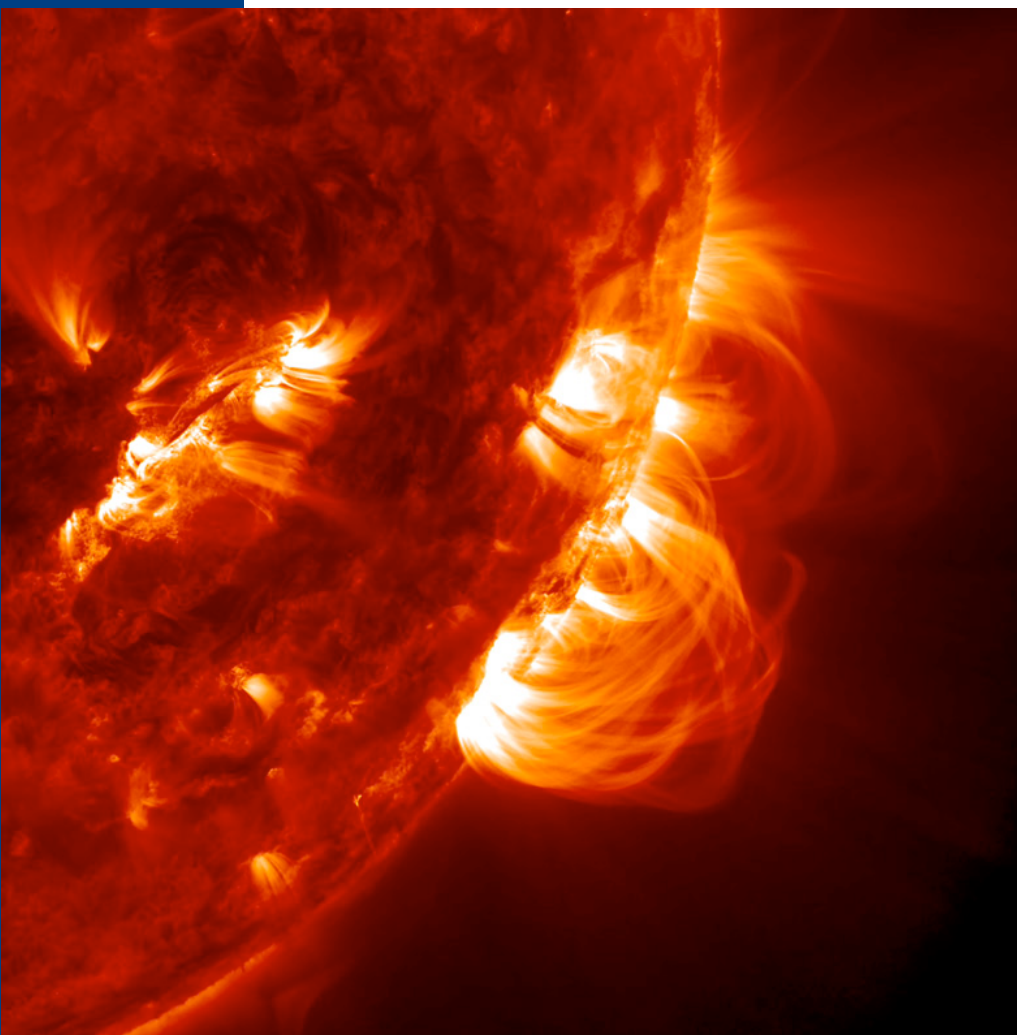
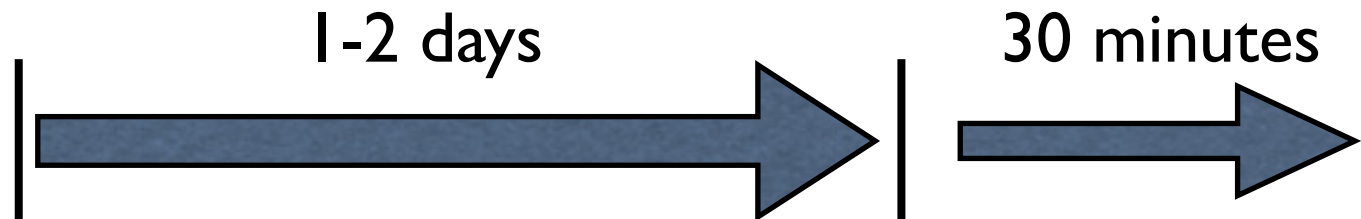
Class X 10/10/10

Proton 10/10/10

PCAF yellow



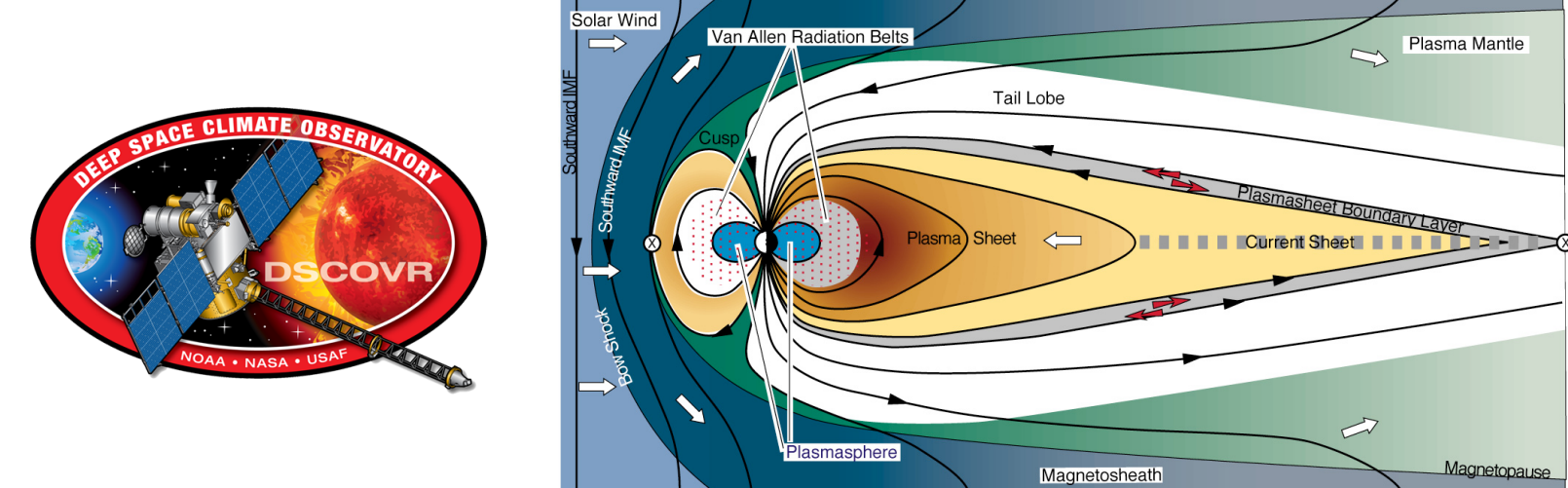
# Sun–solar wind–Earth



SDO

<http://sdo.gsfc.nasa.gov>

L1



Magnetosphere

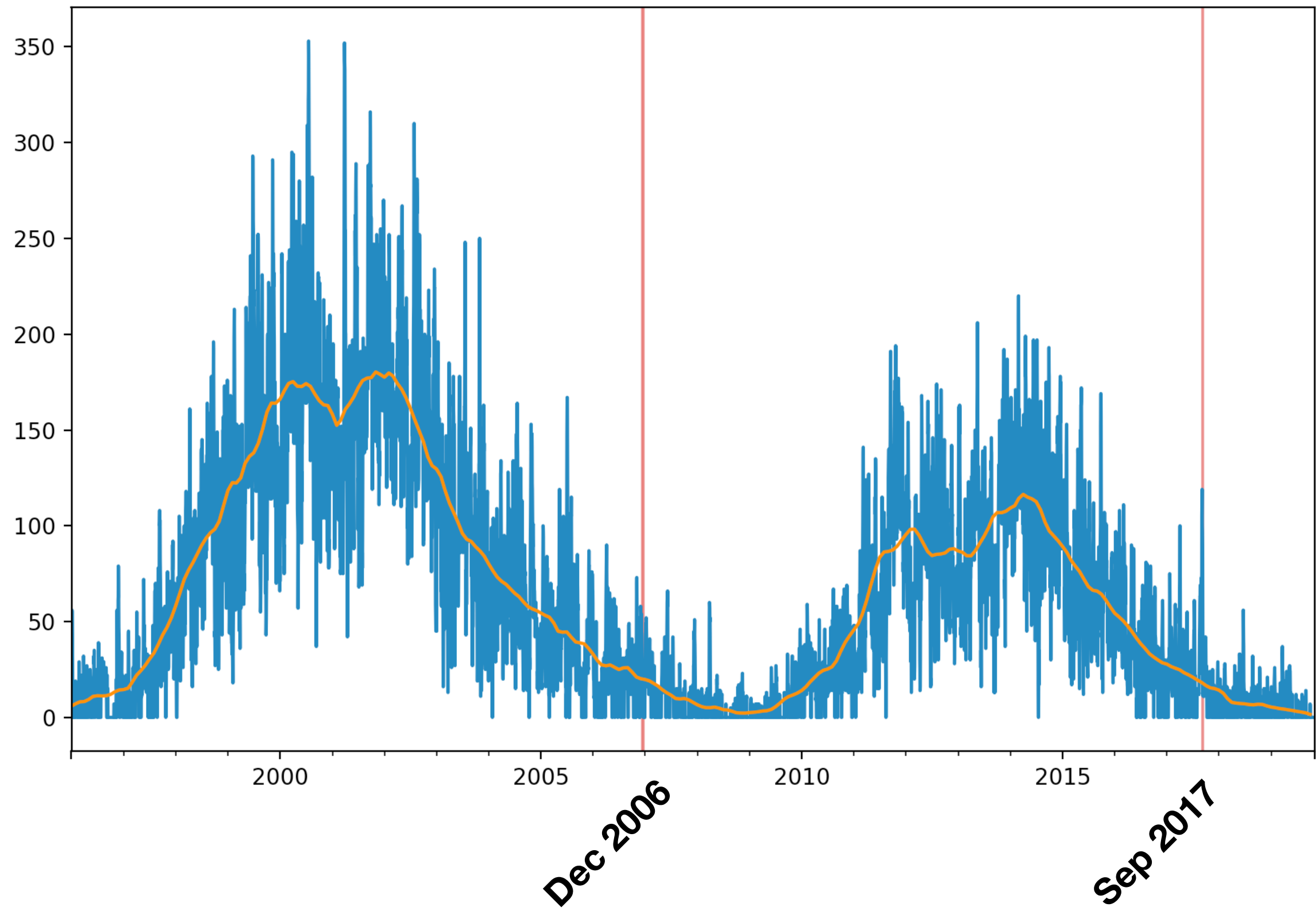
<http://space.rice.edu/IMAGE/>

DSCOVR

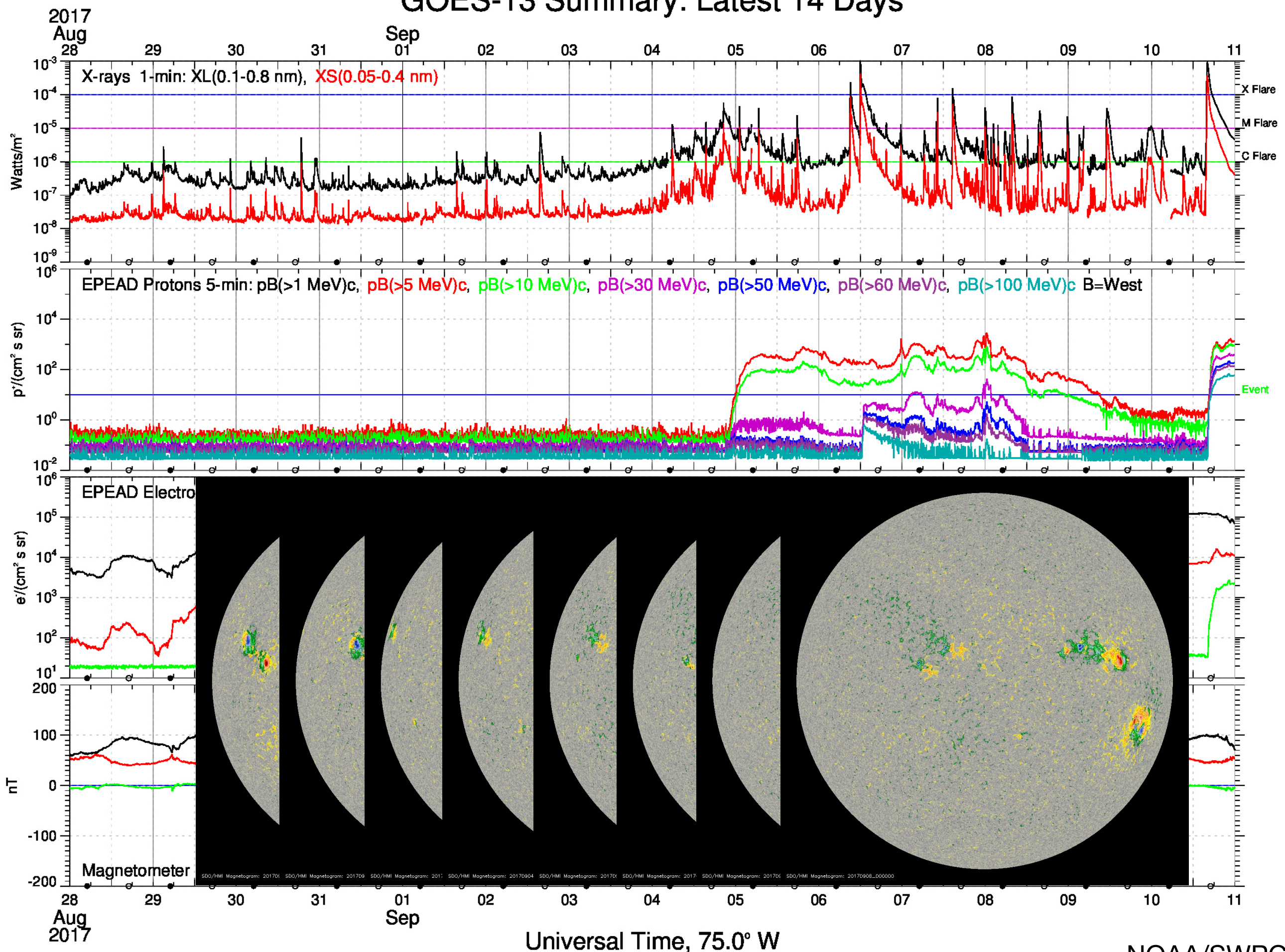
<https://www.nesdis.noaa.gov/content/dscovr-deep-space-climate-observatory>

**And many more spacecraft and observations, and derived products spanning decades or more.**

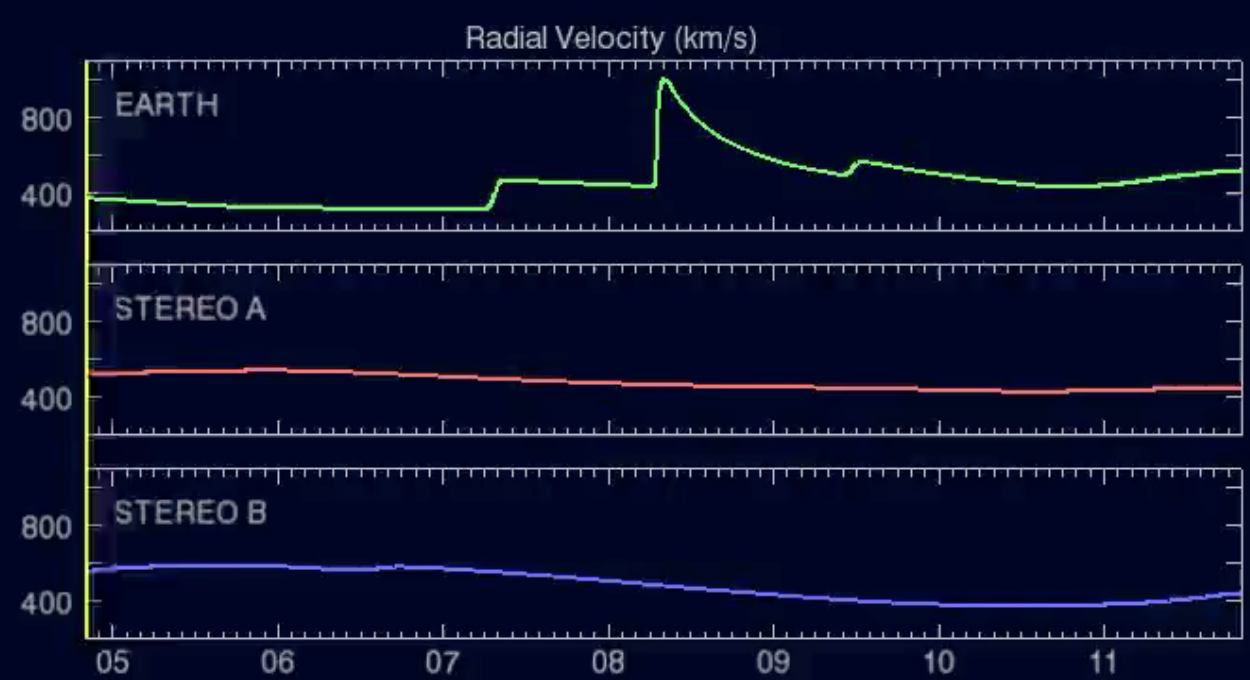
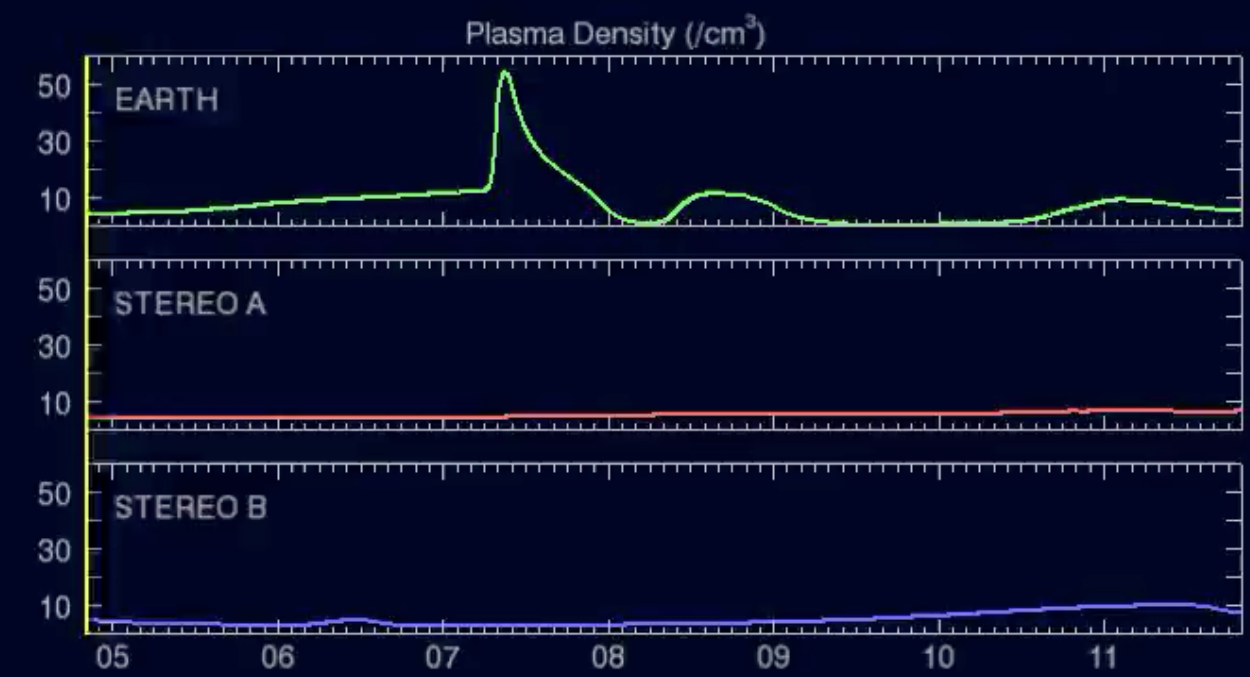
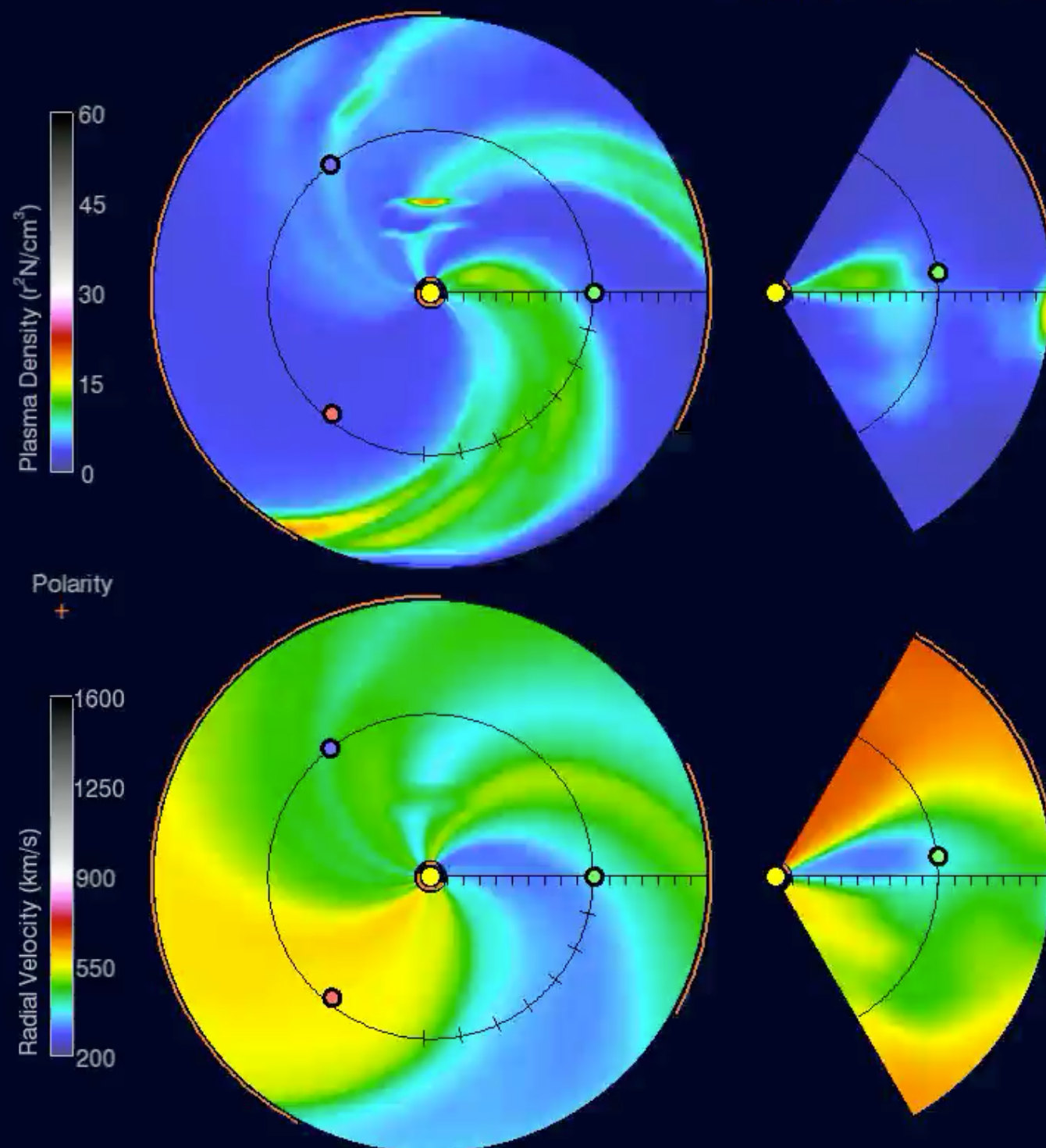
# Déjà vu



# GOES-13 Summary: Latest 14 Days



2017-09-04 20:00:00



© Crown copyright. Met Office

Run Time: 2017-09-06 20:00 UT Mode: CME

Image Created: 2017-09-06 23:54 UT

<https://www.metoffice.gov.uk/weather/specialist-forecasts/space-weather>

<https://www.swpc.noaa.gov>

Modeling 3-D solar wind structure

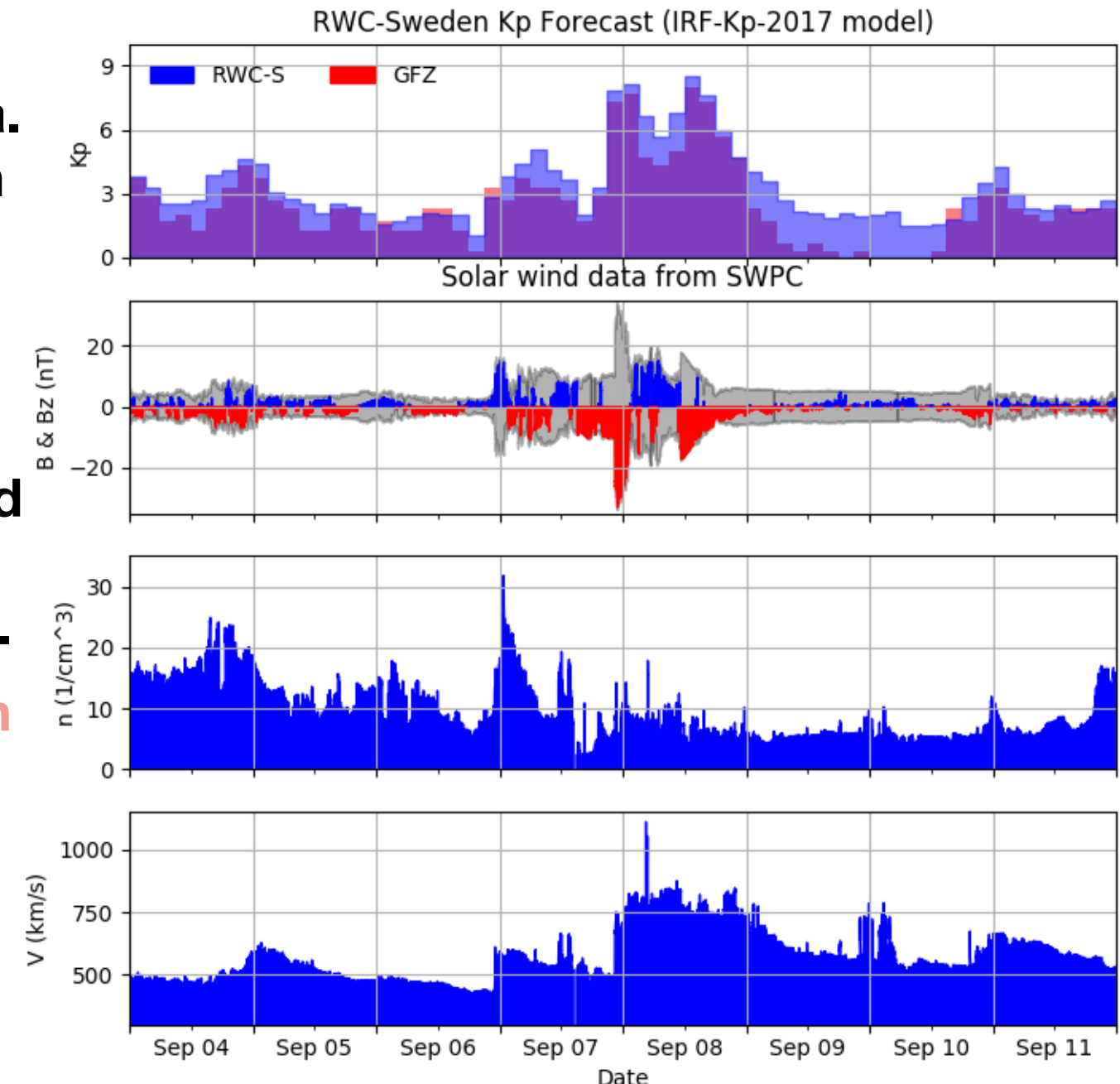
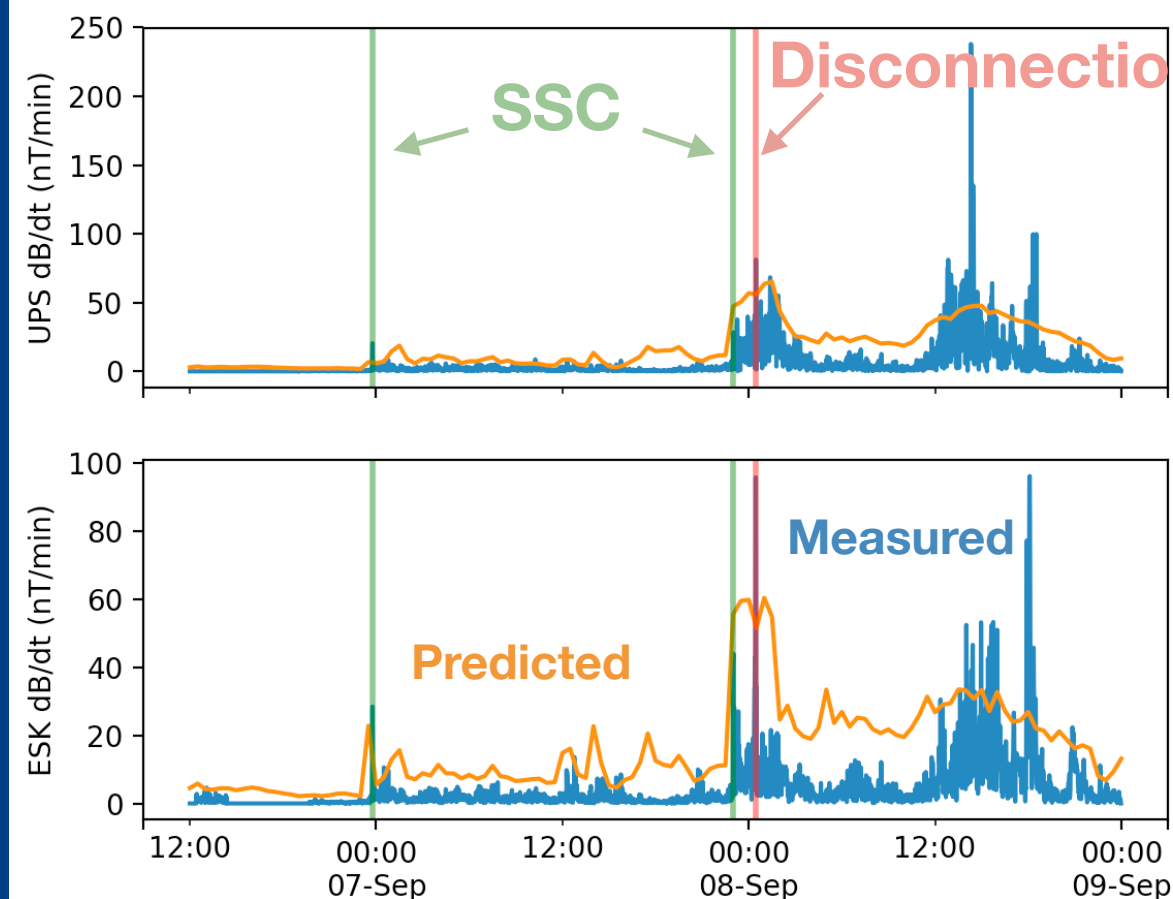
D. Odstrcil

Advances in Space Research 32 497-506 (2003)

First AIDA school, Bologna, 2020-01-22

# Sep 2017 events, Earth

- Monitoring of predictions.
- Monitoring of geomagnetic data.
- Continued reporting to SvK with feedback on possible effects.
- Wrap-up after event:
  - No effects on SvK grid.
  - Disconnection of one transformer on local grid, and immediately reconnected, possibly related to this event.



Forecasting Kp from solar wind data: input parameter study  
 using 3-hour averages and 3-hour range values  
 P. Wintoft and M. Wik and J. Matzka and Y. Shprits  
 Journal of Space Weather and Space Climate 7 A29 (2017)

# Geomagnetically induced current (GIC)

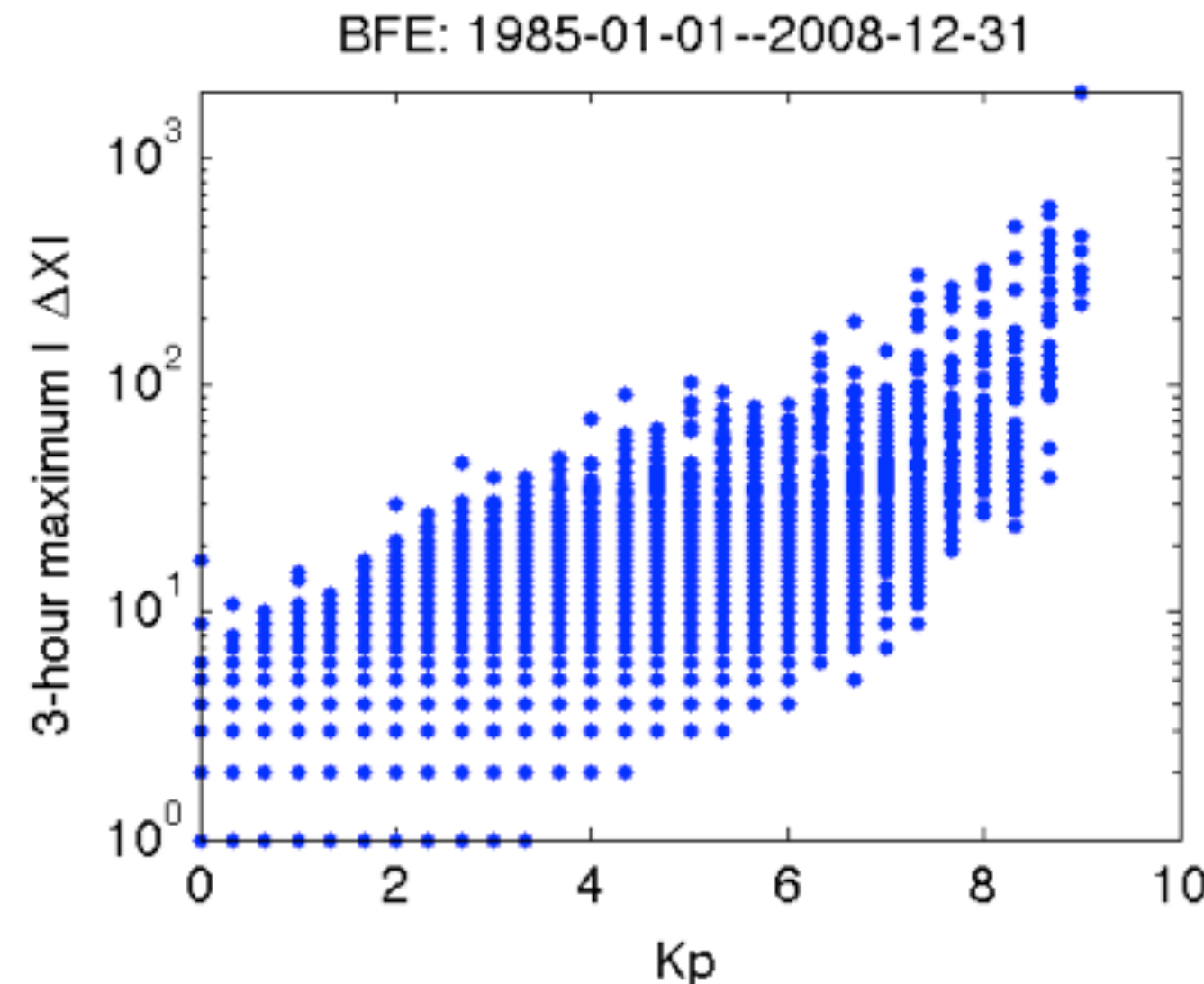
$$\nabla \times \mathbf{E} = -\frac{\partial \mathbf{B}}{\partial t}$$

Maxwell-Faraday

Plane wave  
assumption

$$E_y(t) = -\frac{1}{\sqrt{\pi \mu_0 \sigma}} \int_{t'=-\infty}^t \frac{\partial B_x(t')/\partial t}{\sqrt{t-t'}} dt'$$

R. Pirjola, A. Viljanen, A. Pulkkinen, S. Kilpua, and O. Amm. Ground effects of space weather, chapter Space weather effects on electric power transmission grids and pipelines. NATO Science Series. Kluwer Academic Publishers, 2004.



Movie of E-field: <https://www.swpc.noaa.gov/products/geoelectric-field-1-minute>

# Indices

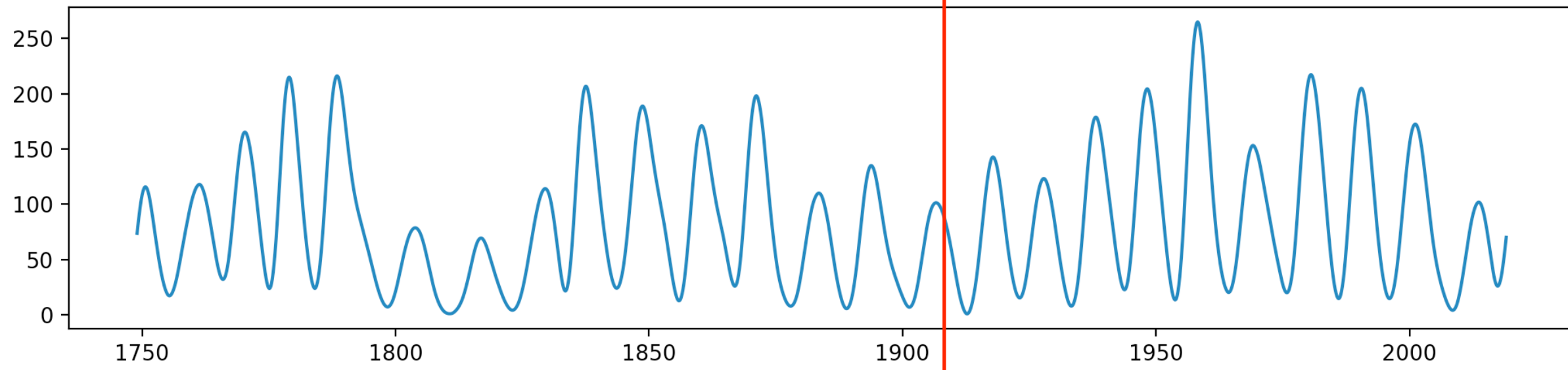
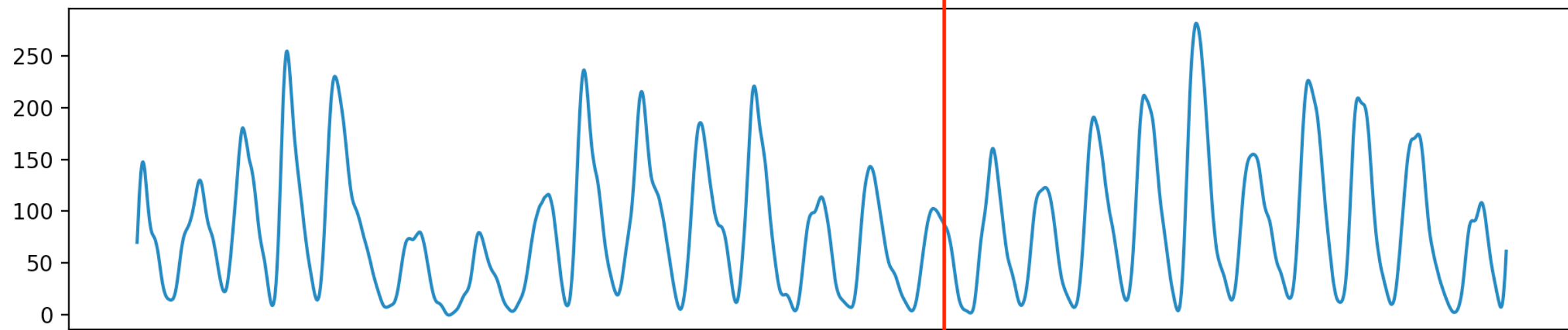
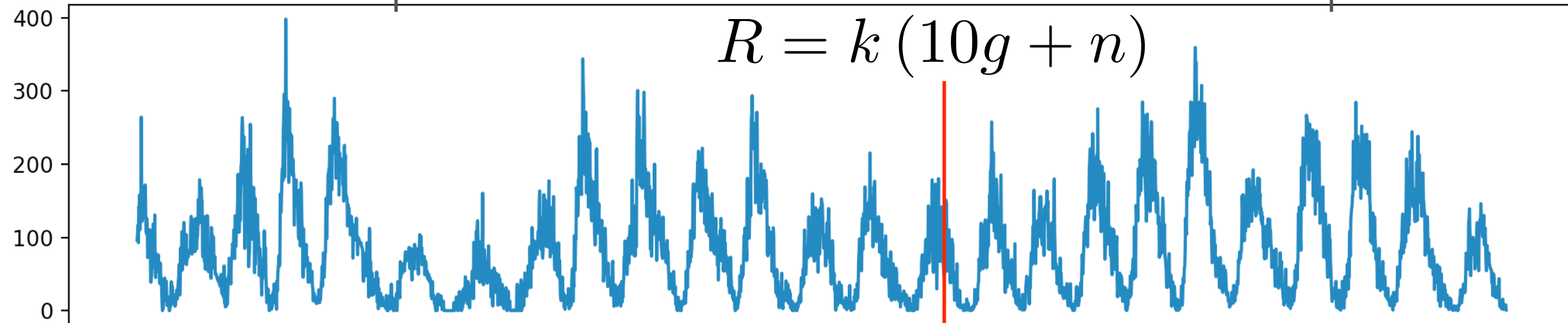
“Basically, an index aims at giving summarised information in a continuous way concerning a more or less complex phenomenon which varies with time ...”

“Any geomagnetic index should correspond, as much as possible, to a single well-defined phenomenon ...”

Derivation, meaning, and use of geomagnetic indices, P. N. Mayaud, AGU Monograph 22, 1980.

The sunspot number  $\neq$  the number of sunspots

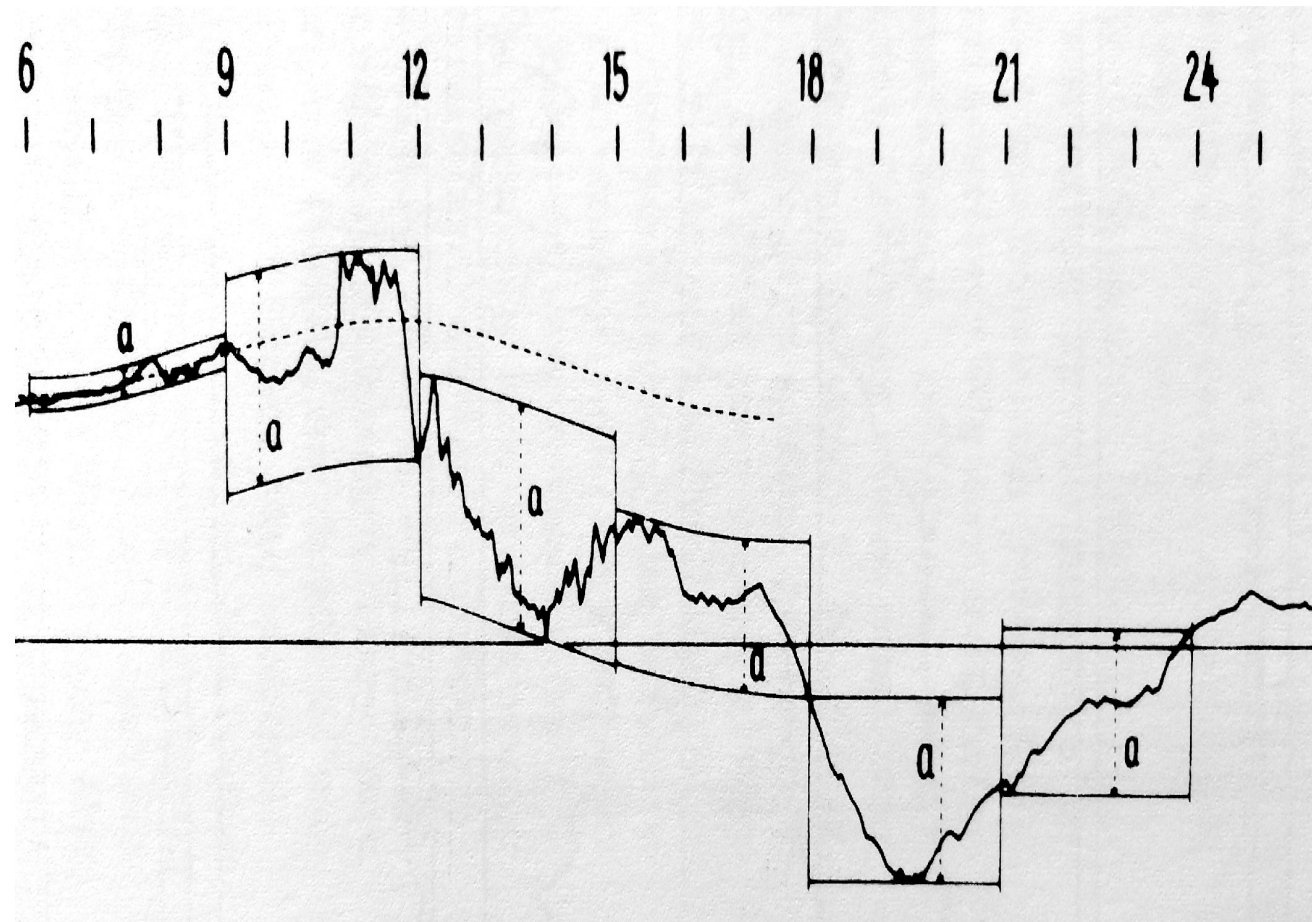
$$R = k(10g + n)$$



Data from WDC-SILSO, Royal Observatory of Belgium

Zeeman effect (Hale, 1908)

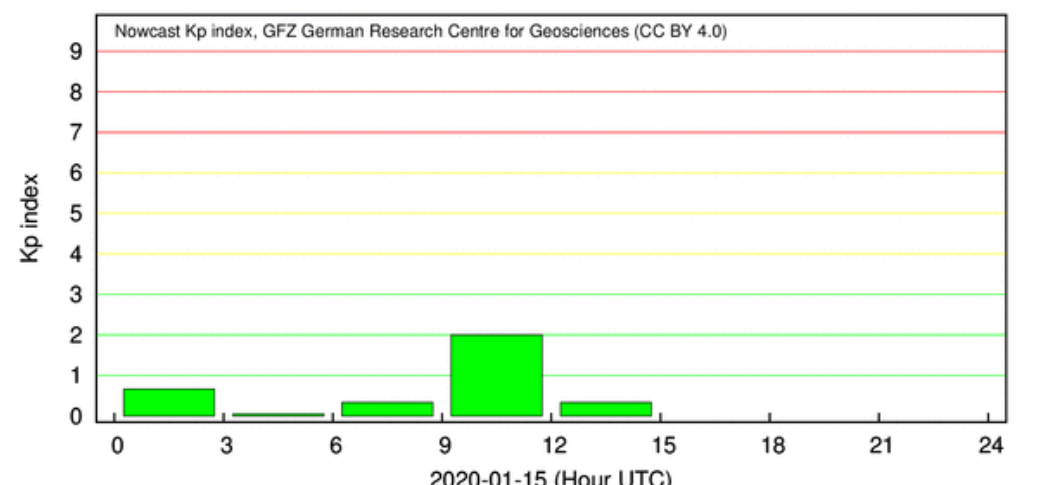
# Kp: planetarische Kennziffer



Derivation, meaning, and use of geomagnetic indices, P. N. Mayaud, AGU, 22, 1980.

- Sensitivity to sub-3-hour variations.
- High-pass filtered storm dynamics

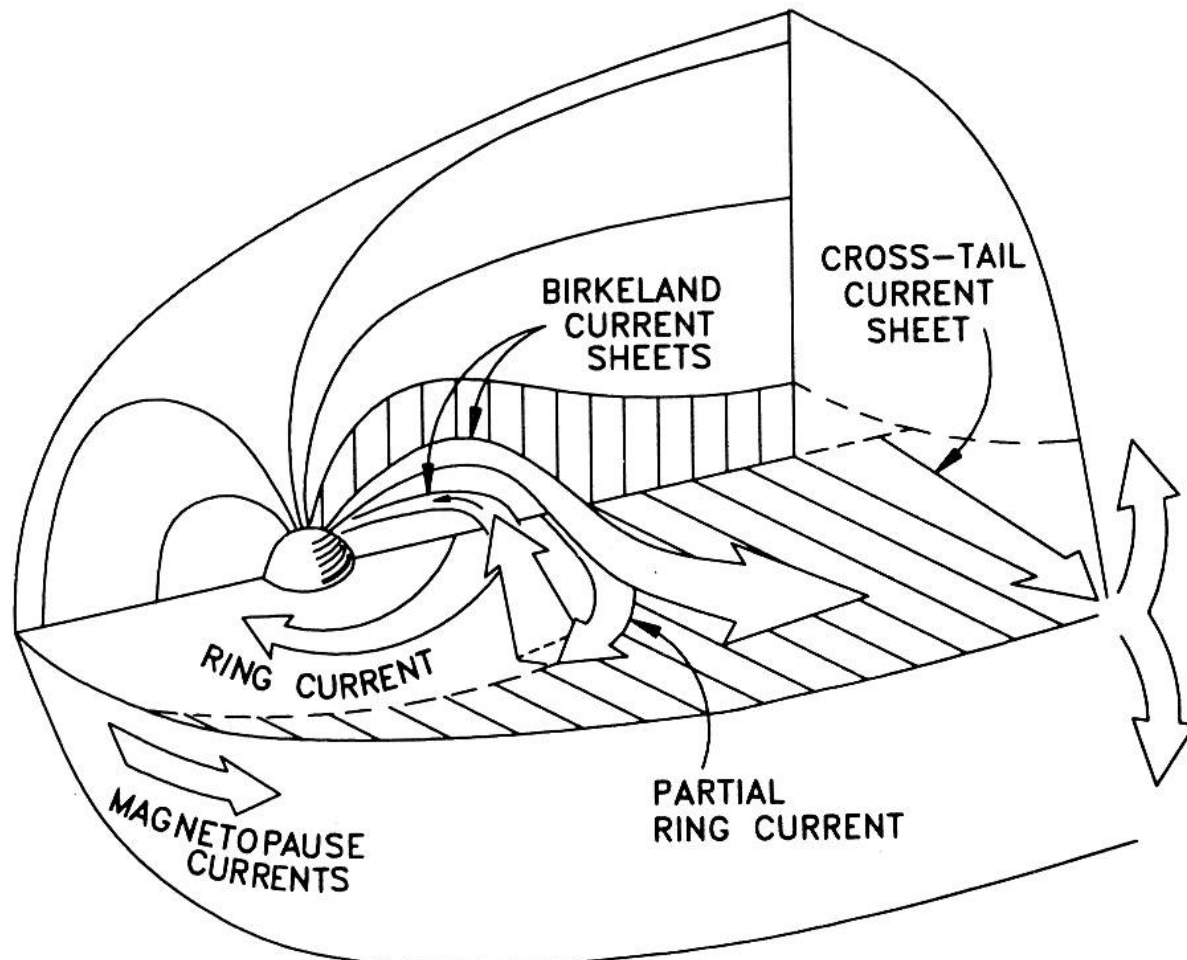
Maximum range in horizontal components over each 3-hour interval is quasi-logarithmically scaled to integer values 0, … 9. Data from 13 mid-latitude observatories are combined into Kp that has 28 levels (0o, 0+, 1-, 1o, 1+, ..., 9o).



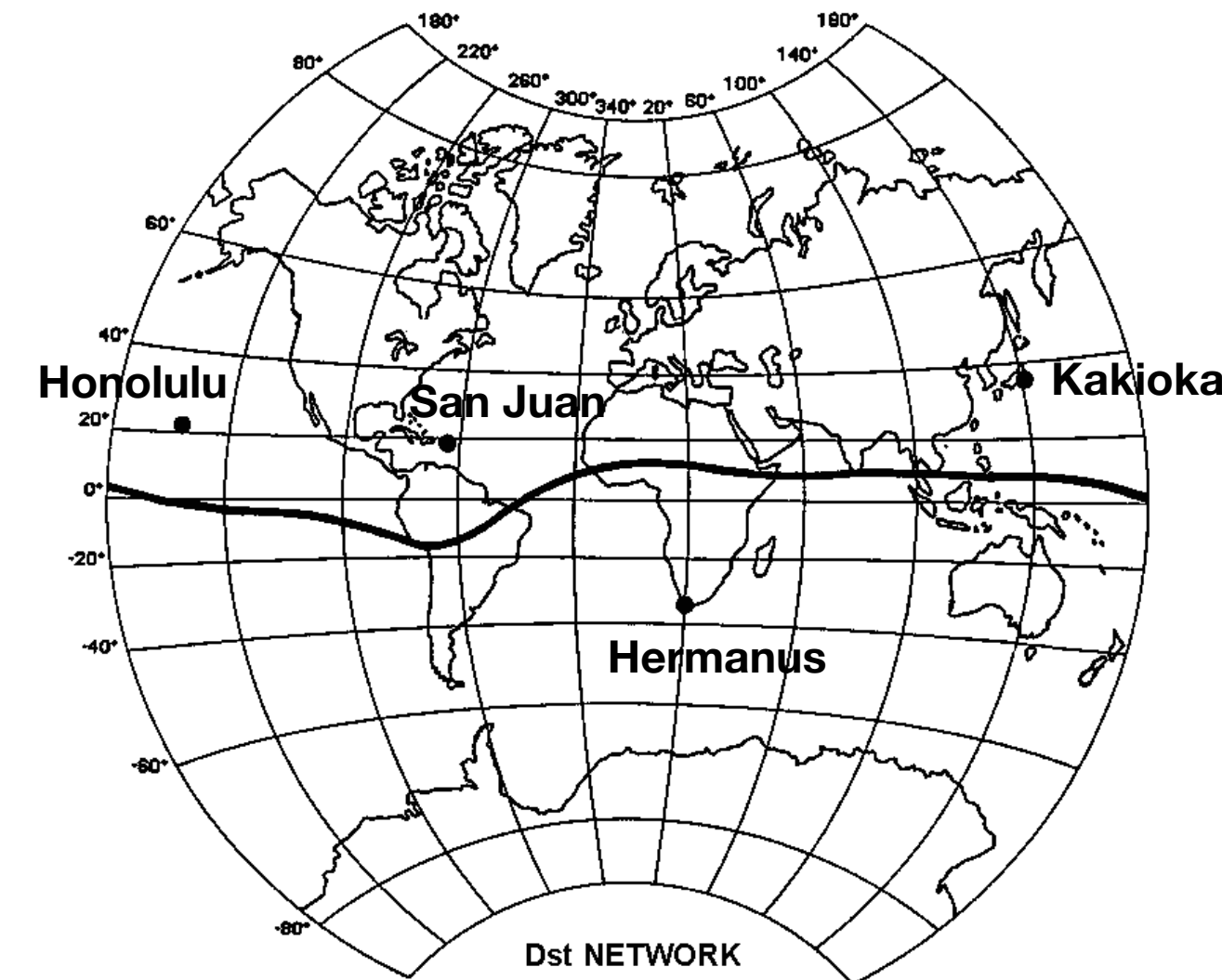
Why Kp is such a good measure of magnetospheric convection  
M. F. Thomsen  
Space Weather 2 S11004 (2004)



# Dst: Disturbance storm time index

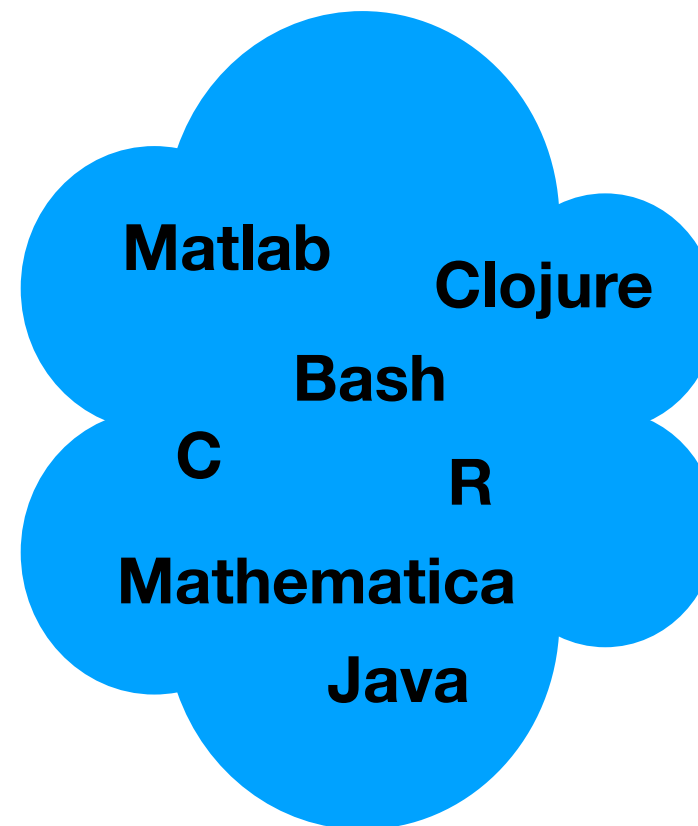


David P. Stern, 1994: "The art of mapping the magnetosphere"  
Journal of Geophysical Research, doi:10.1029/94JA01239



<http://wdc.kugi.kyoto-u.ac.jp/dstdir/dst2/onDstindex.html>

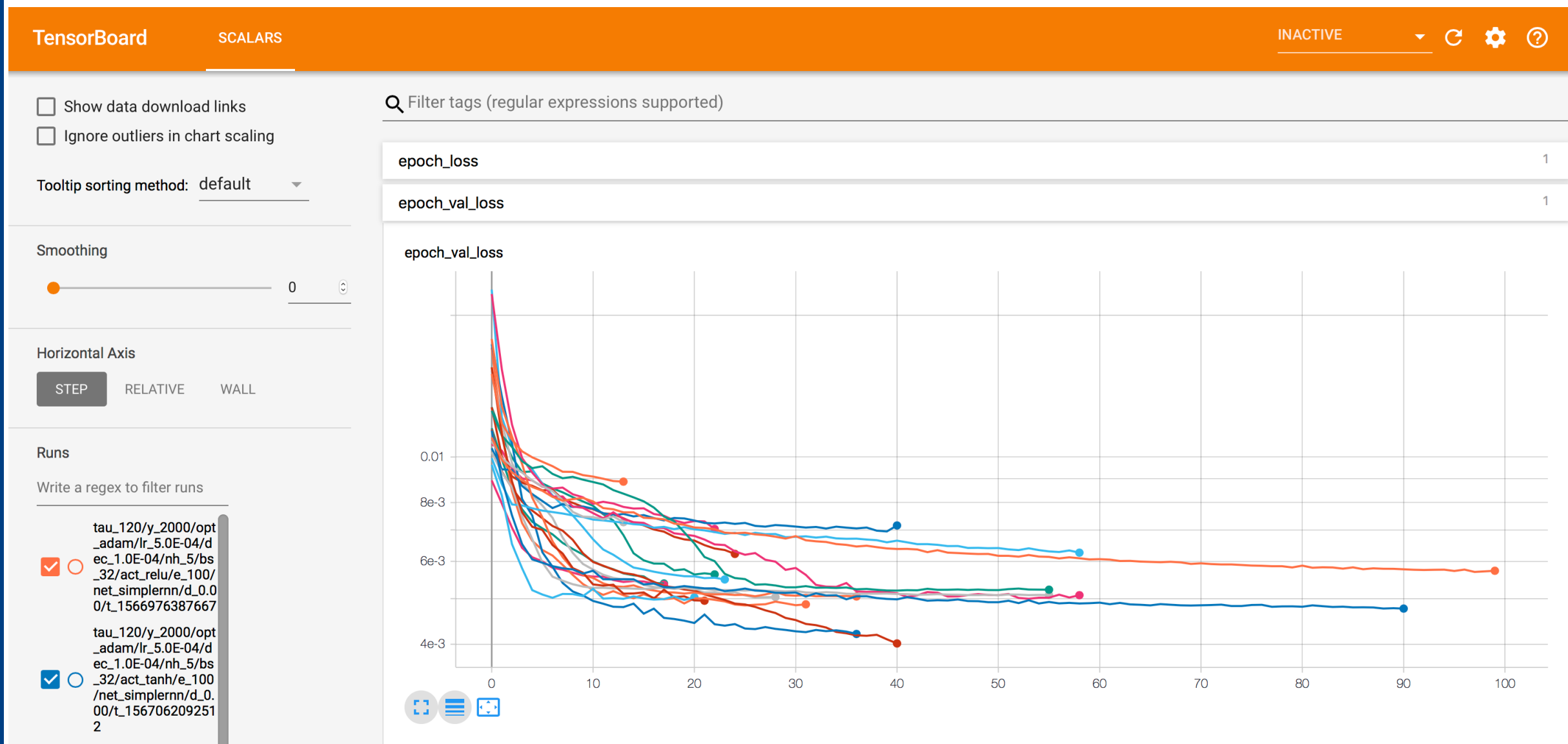




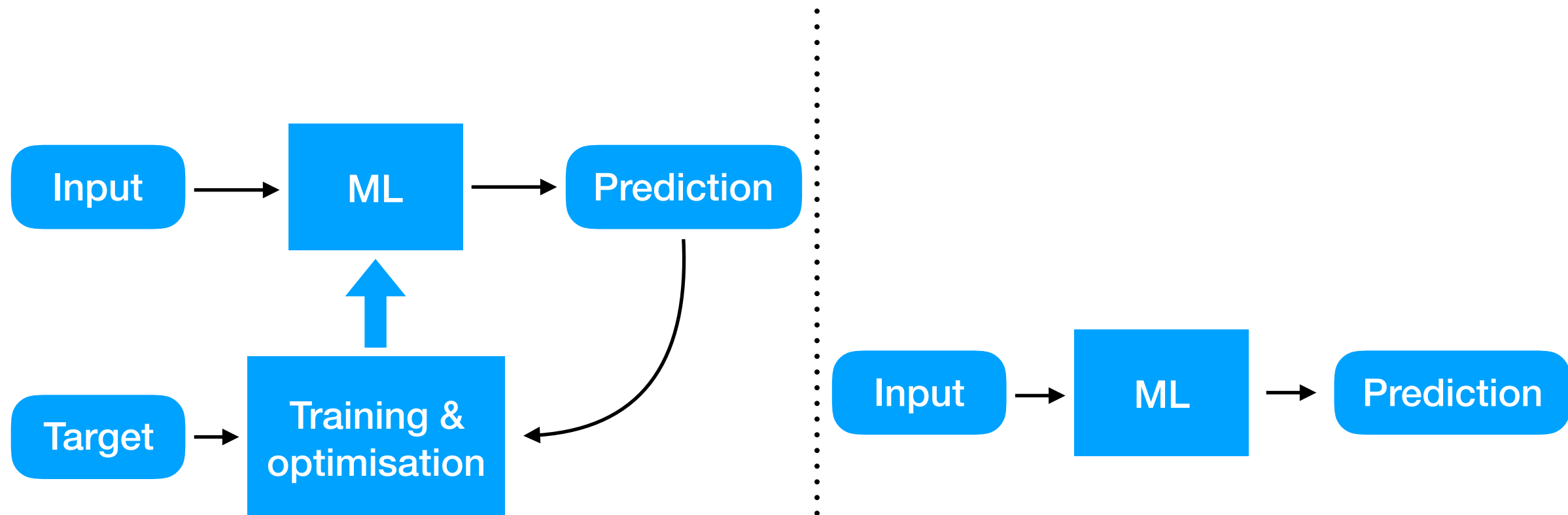
# Tools

## Python

- **Tensorflow/Tensorboard/Keras**
- **PyMC3 (4)**
- **Scikit**
- **Matplotlib, Scipy, Numpy, Pandas, Seaborn, ...**
- **PyCharm**
- **Git**



# Machine Learning (ML)



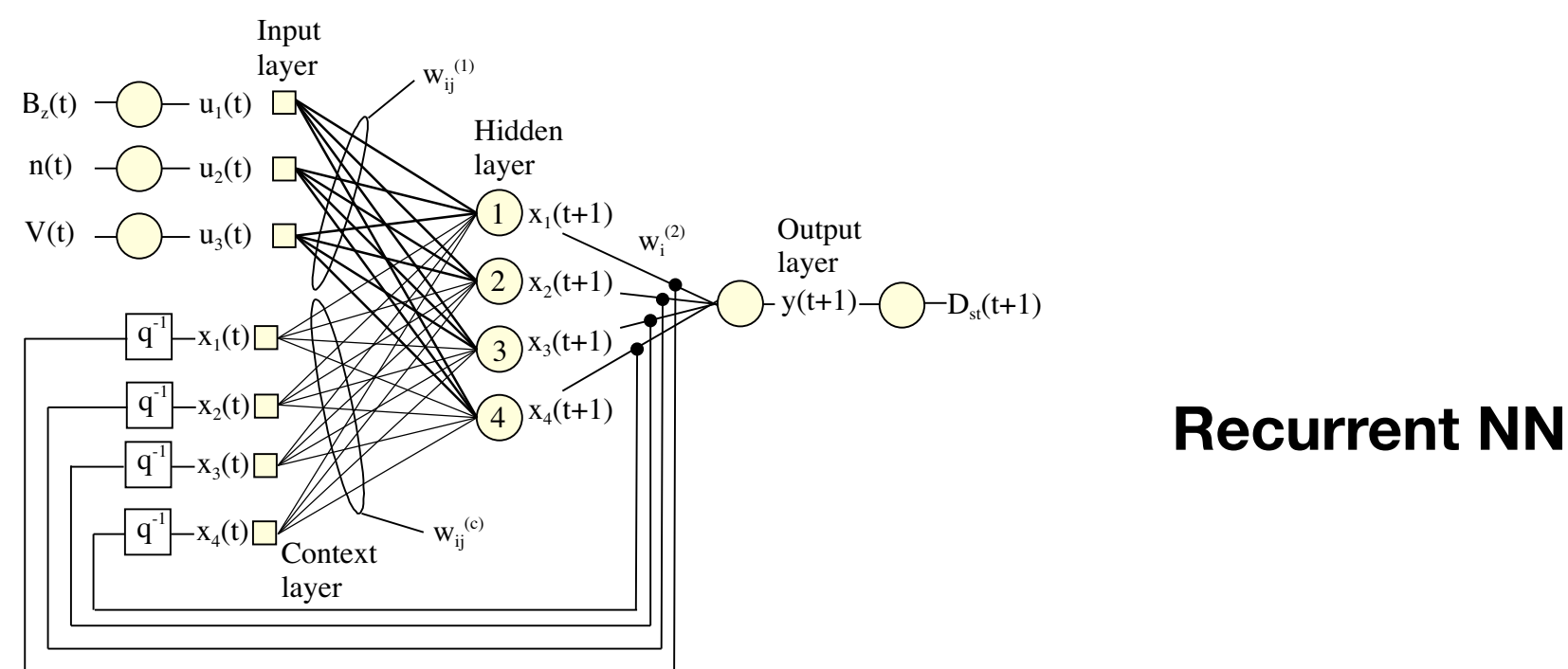
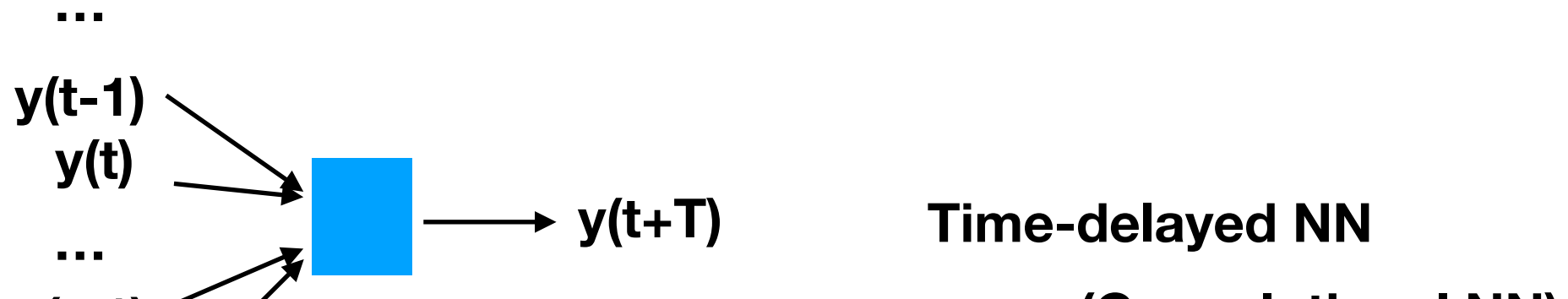
# Neural network

- Inputs - target (supervised).
- Architecture.
- Hyperparameters.
- Training, validation, and test sets.
- Timeseries and causality.

# Two ways to capture dynamics

- Time delays on inputs
  - Equivalent to non-linear ARX
  - Cannot model chaotic systems (in principle)
- Recurrent connections
  - Vanishing gradient problems, but now new functions to mitigate that
  - Can model chaotic systems (how about learning?)

# Dynamical NN (NNs with memory)



# A sunspot maximum prediction using neural network, H. C. Koons and D. J. Gorney, Eos Transactions AGU 71 677-688 (1990)

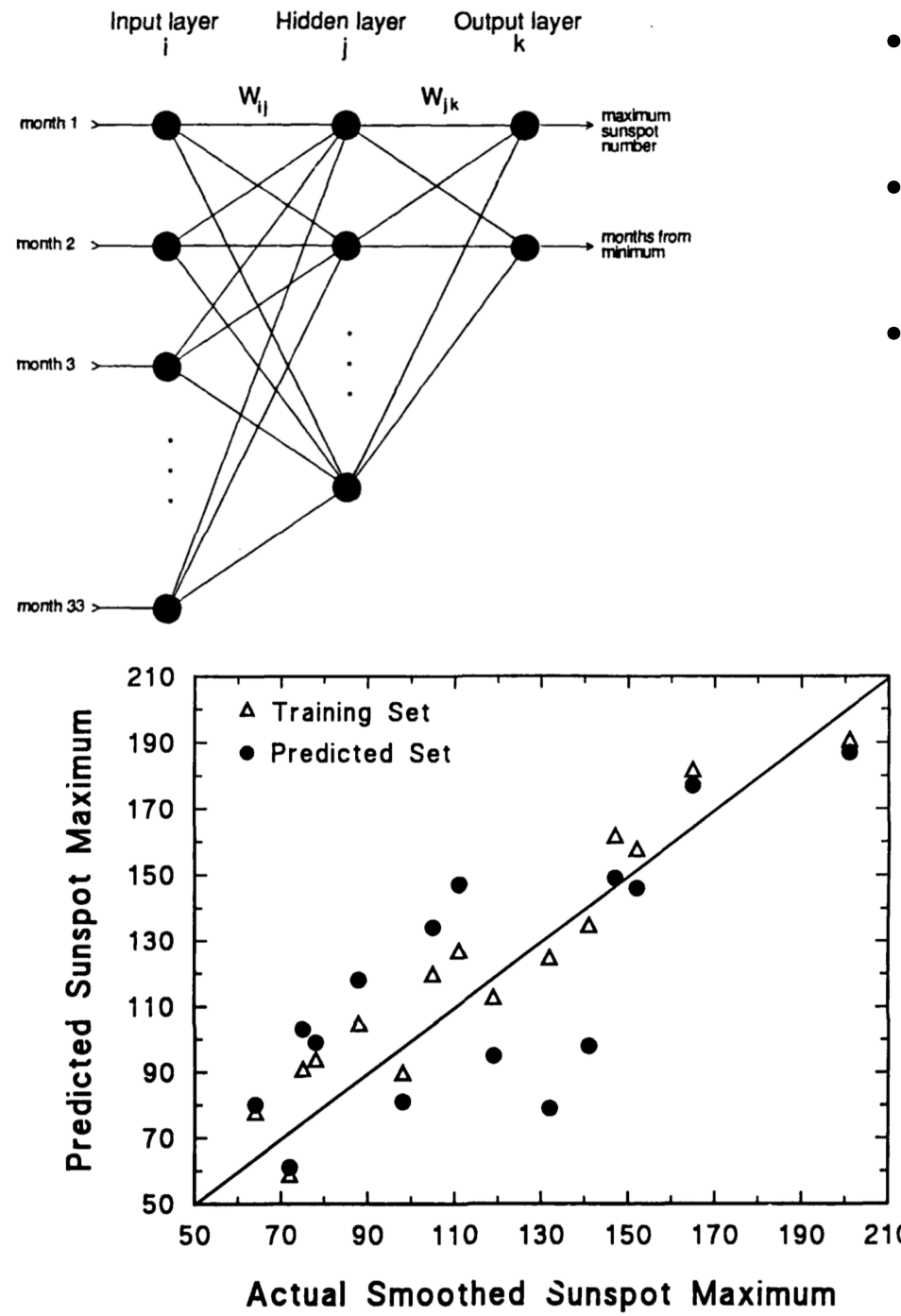


Fig. 2. A Scatter Diagram Showing the Predicted Sunspot Maximum vs the Actual Sunspot Maximum for the Solar Cycles from 7 Through 21. The triangles include the entire training set used to predict the sunspot maximum for cycle 22. The circles show the prediction for a cycle when that cycle is removed from the training set.

$\Delta$  Training set

$\circ$  Test points

- Requires time of minima based on 13-month running average SSN.
- 33 past monthly 3-month averages from time of minima.
- Predicts coming 13-month maxima and number of months after minima.

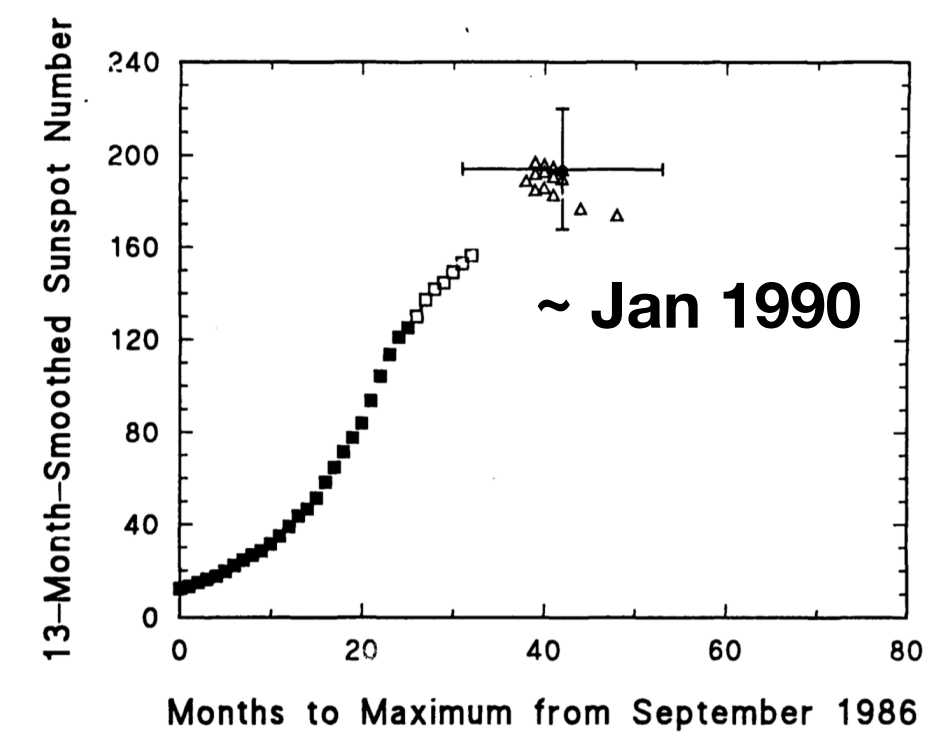


Fig. 3. The Prediction of the Maximum 13-Month-Smoothed Sunspot Number for Solar Cycle 22. The triangles show the predictions obtained as each cycle is individually removed from the training set. The squares show the actual values observed for cycle 22. The solid squares show the data available at the time the neural network prediction was made.

Inputs are daily values for past 3 days and 27 days based on:

- Solar flare classes and locations
- CMEs and locations
- Radio bursts
- Proton events
- Coronal holes
- Past geomagnetic activity

Data set from March 1990 to July 1991 (518 days)

Output is 4 classes of different geomagnetic storm levels.

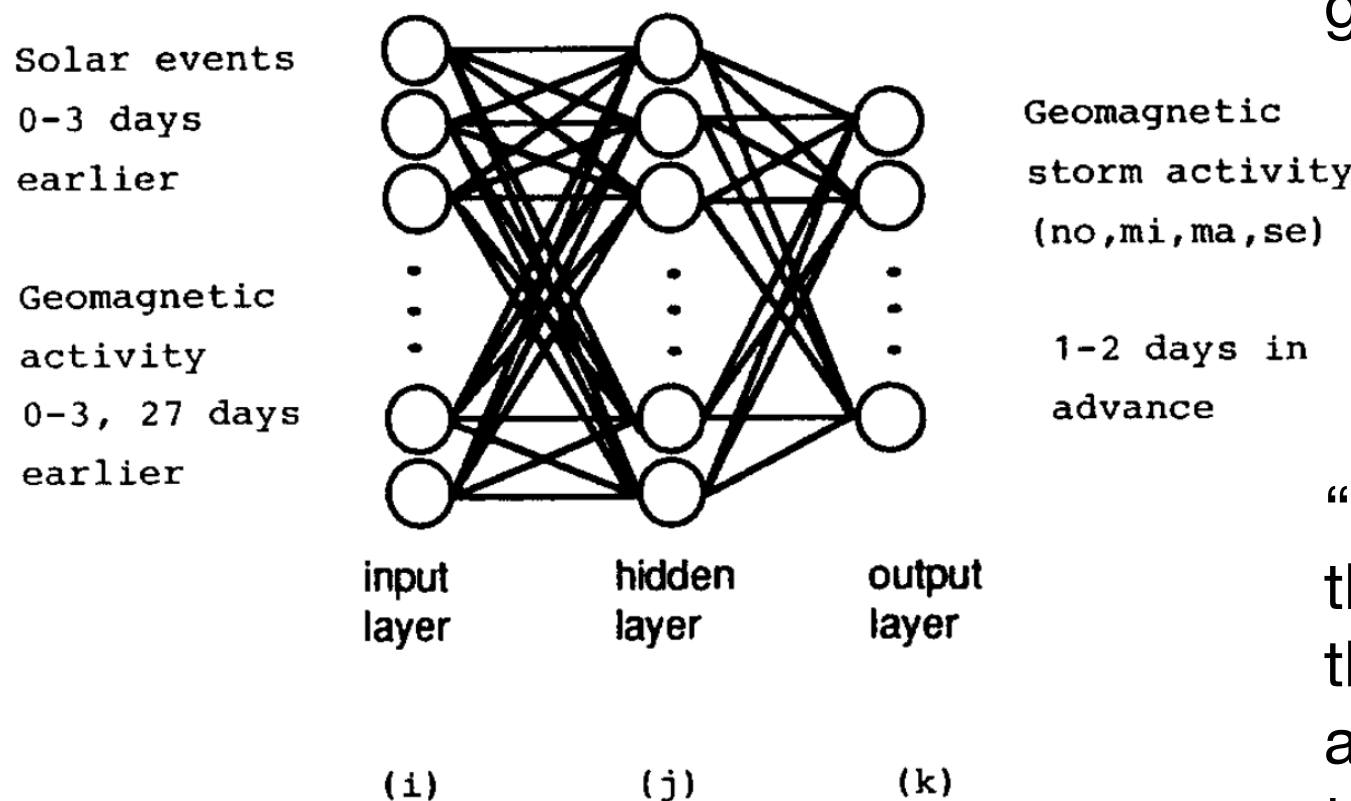


FIG. 3. MULTILAYER BACK-PROPAGATION NETWORK ARCHITECTURE.

“If the learning rate was 1.0, the momentum factor 0.9 and the error tolerance was chosen as 0.1, then training typically took 30 minutes on a PC-386 with a mathematical coprocessor ...”

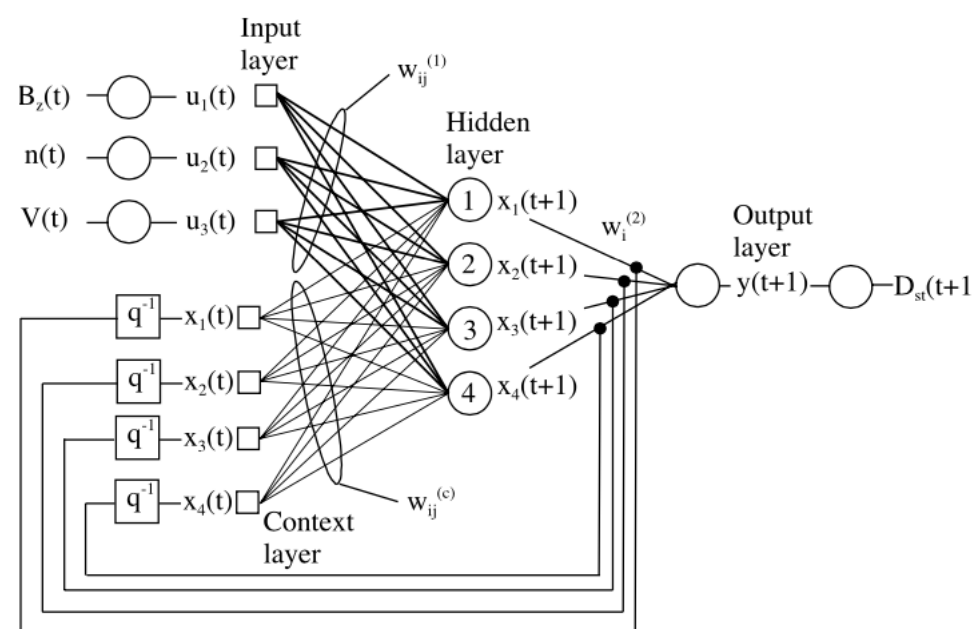
Neural networks and predictions of solar-terrestrial effects, H. Lundstedt, Planetary and Space Science 40 457-464 (1992)



Prediction of geomagnetic storms from solar wind data with the use of a neural network  
 H. Lundstedt and P. Wintoft  
*Annales Geophysicae* 12 19--24 (1994)

“The network is trained on data covering a total of **8700** h, extracted from the 25-year period from 1963 to 1987, taken from the NSSDC data base. The performance of the network is examined with test data, not included in the training set, which covers **386** h and includes four different storms.”

**Elman NN** Neural network modeling of solar wind-magnetosphere interaction  
 J.-G. Wu and H. Lundstedt  
*Journal of Geophysical Research* 102 14,457-14,466 (1997)



$$\mathbf{W}^{(c)} = \begin{pmatrix} 0.6099 & 0.2223 & -0.4379 & 0.0053 \\ 0.7935 & 0.5000 & -1.2654 & -0.0428 \\ -0.3496 & 0.1024 & 0.3605 & 0.1790 \\ -0.2067 & 0.2270 & 0.5446 & 0.1019 \end{pmatrix}$$

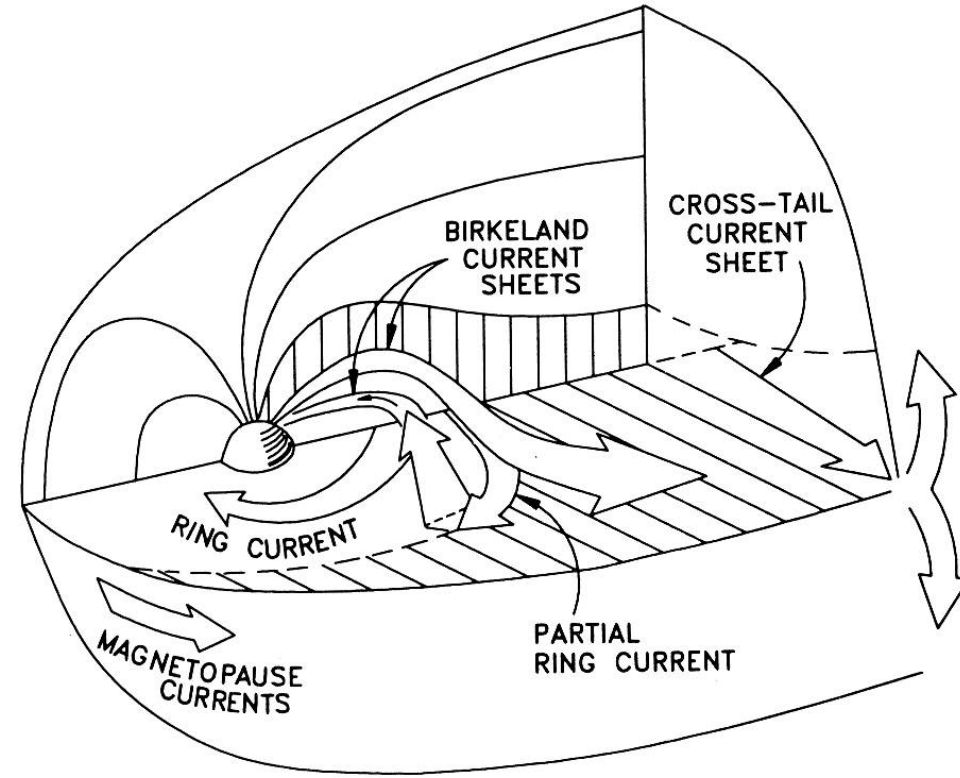
$$\mathbf{b}^{(1)} = \begin{pmatrix} -0.1081 \\ -0.7252 \\ -0.2307 \\ 0.5406 \end{pmatrix}$$

$$\mathbf{w}^{(2)} = (0.2535 \quad 0.3172 \quad -0.4860 \quad -0.2346)$$

$$\mathbf{b}^{(2)} = \mathbf{0.0712}$$

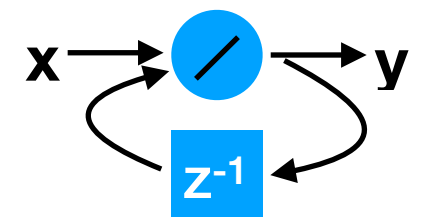
Operational forecasts of the geomagnetic Dst index  
 H. Lundstedt and H. Gleisner and P. Wintoft  
*Geophysical Research Letters* 29 34-1--4 (2002)

# Why Elman NN?



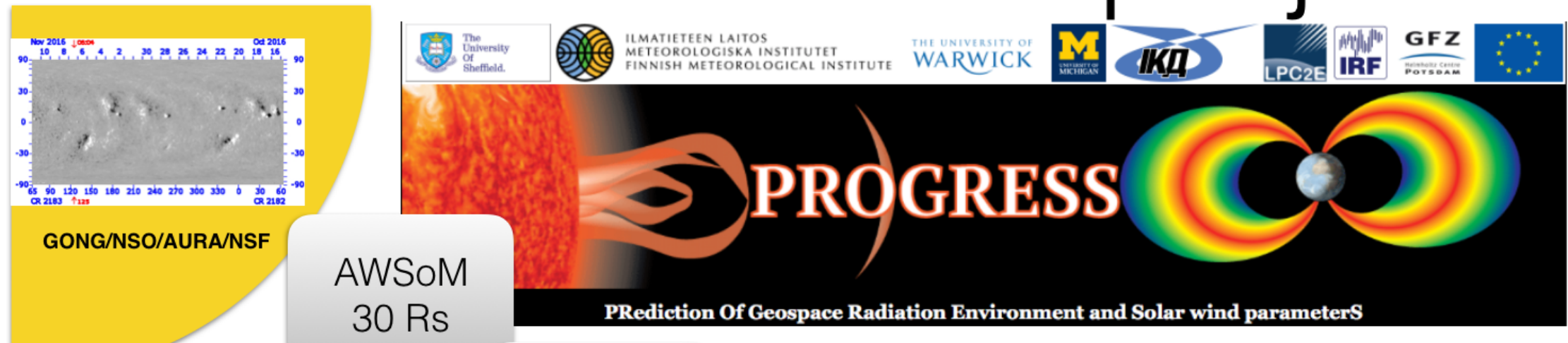
David P. Stern, 1994: "The art of mapping the magnetosphere"  
Journal of Geophysical Research, doi:10.1029/94JA01239

$$\frac{dDst^*}{dt} = Q(t) - \frac{Dst^*}{\tau}$$



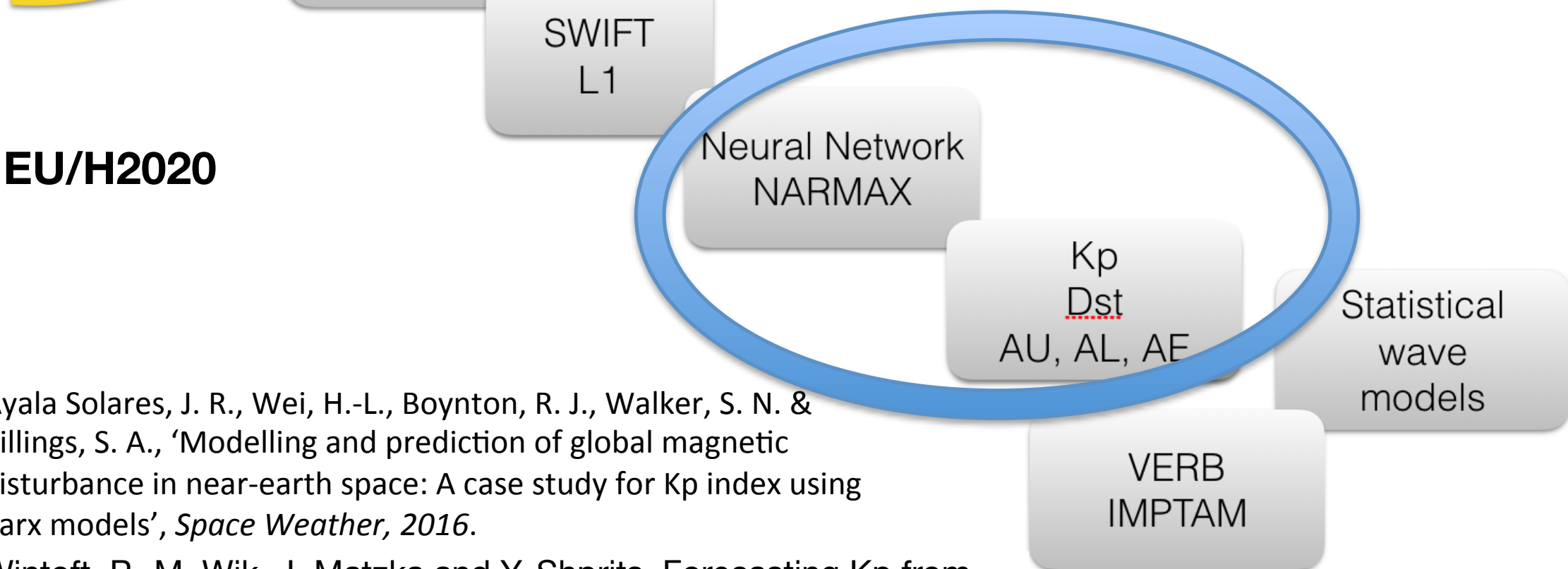
Forecasting the ring current Dst in real time  
T. P. O'Brien and R. L. McPherron  
Journal of Atmospheric and Solar-Terrestrial Physics 62 1295-1299 (2000)

# The PROGRESS project



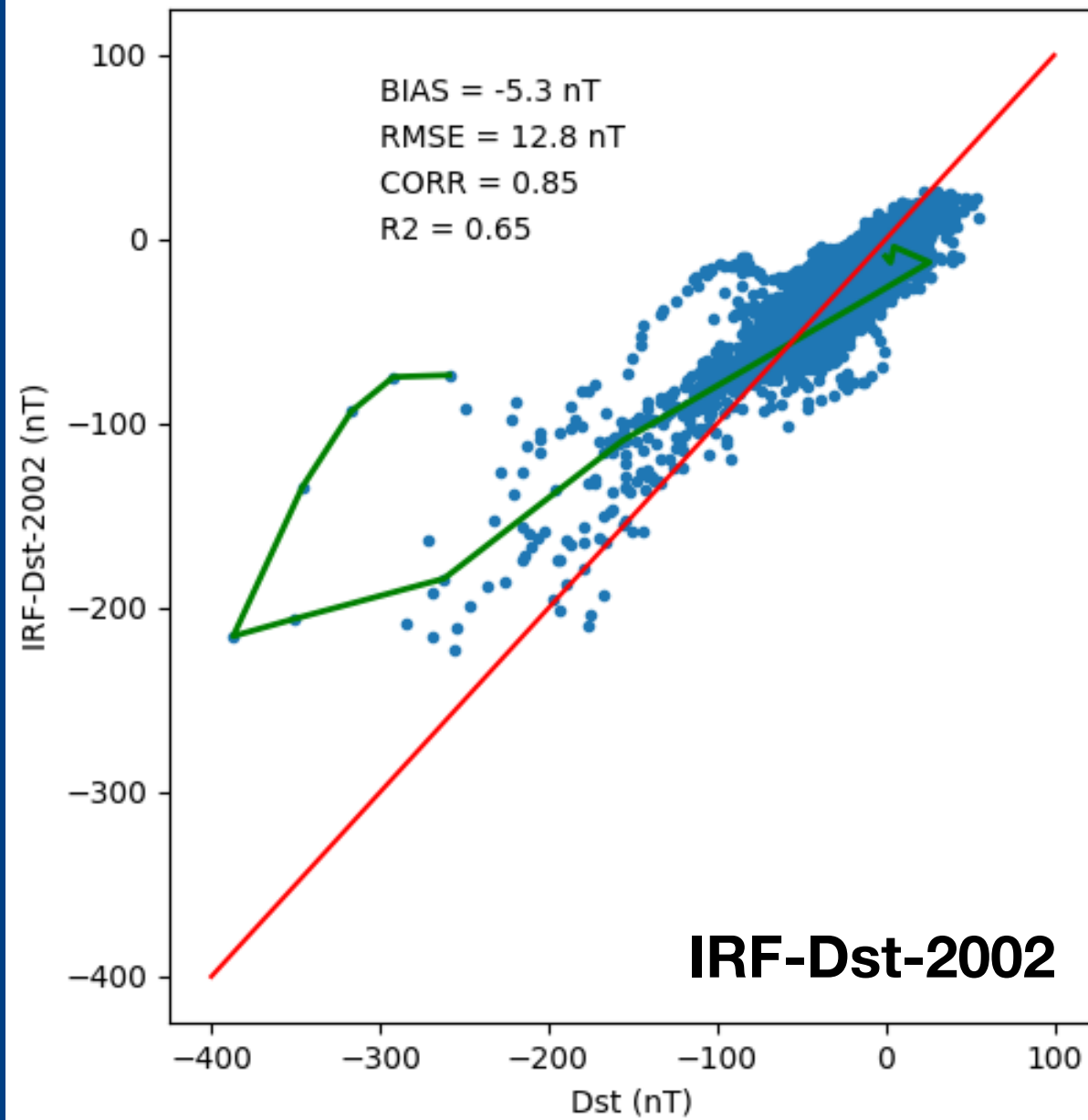
**EU/H2020**

- Ayala Solares, J. R., Wei, H.-L., Boynton, R. J., Walker, S. N. & Billings, S. A., 'Modelling and prediction of global magnetic disturbance in near-earth space: A case study for Kp index using narx models', *Space Weather*, 2016.
- Wintoft, P., M. Wik, J. Matzka and Y. Shprits, Forecasting Kp from solar wind data: input parameter study using 3-hour averages and 3-hour range values, *J. Space Weather Space Clim.* Volume 7, A29, 2017



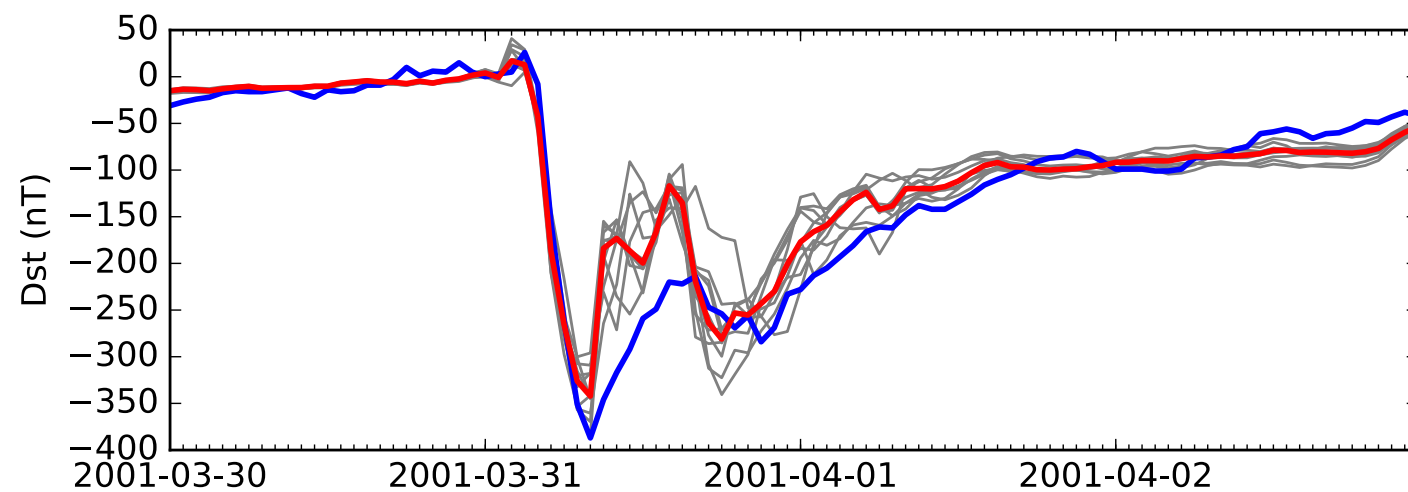
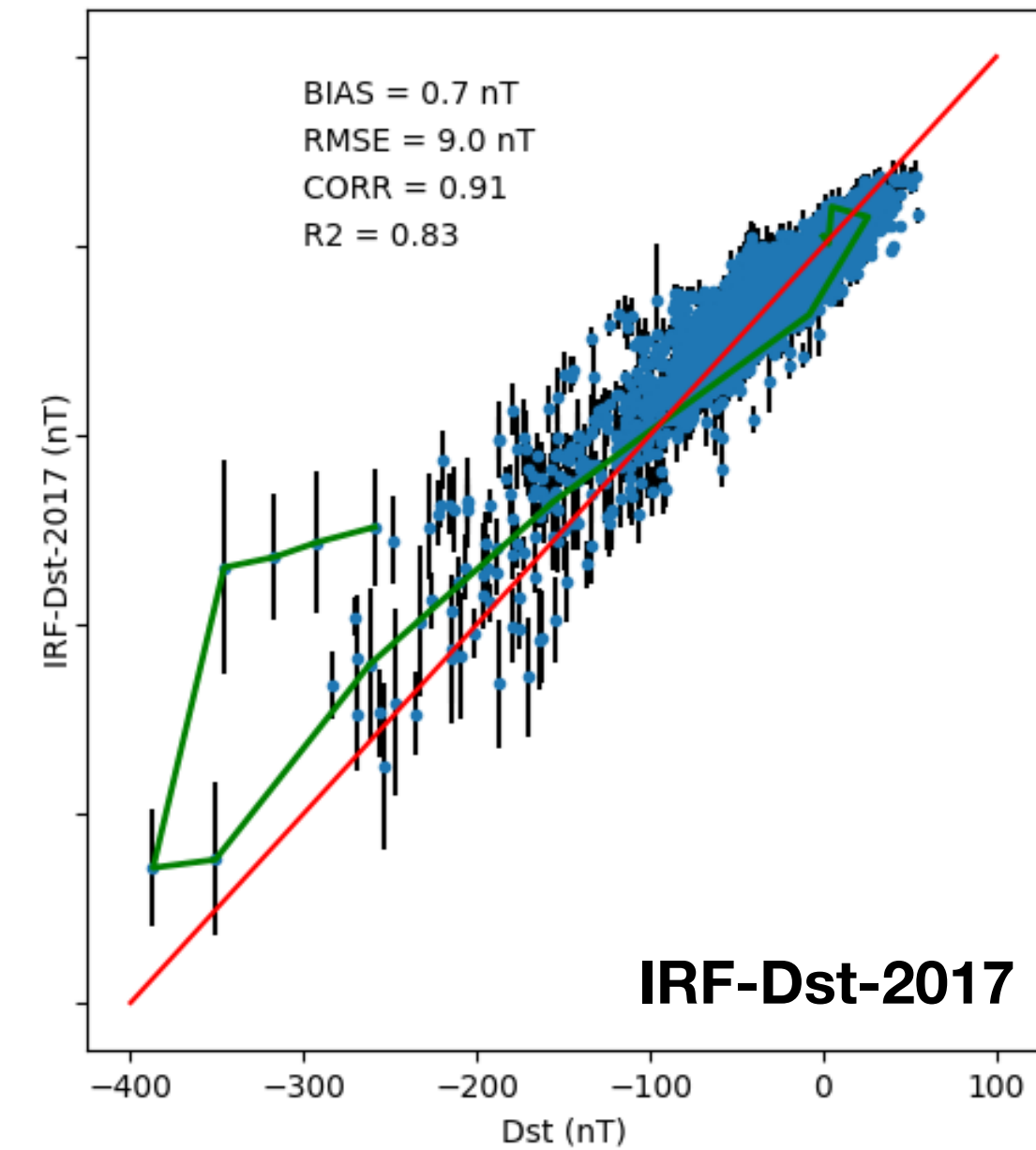
## B, Bz, n, V

Years [1981, 1996, 2001, 2008]



## B, By, Bz, n, V, DOY, UT

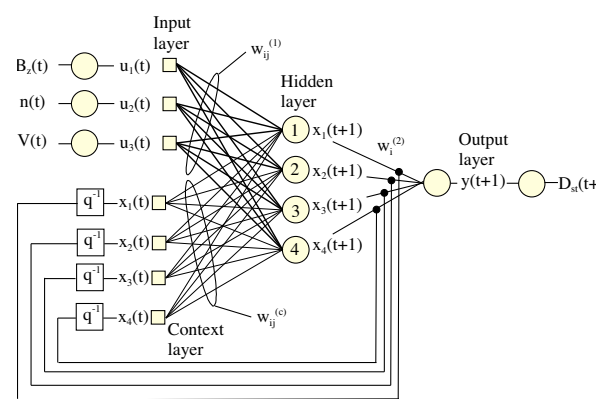
Years [1981, 1996, 2001, 2008]



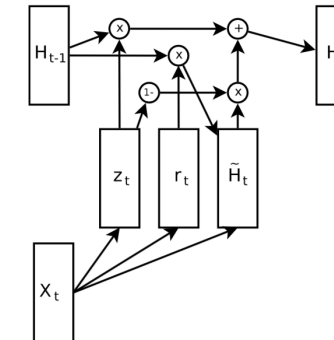
Evaluation of K<sub>p</sub> and Dst  
Predictions Using ACE and  
DSCOVR Solar Wind Data  
P. Wintoft and M. Wik  
Space Weather 16  
1972-1983 (2018)

# Recurrent NN

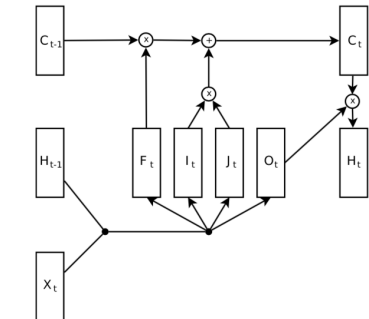
## Elman



## Gated Recurrent Unit (GRU)



## Long-Short Term Memory (LSTM)



Optimization of RNN becomes extremely difficult only after 10 to 20 time steps [Bengio et al., 1994].

An Empirical Exploration of Recurrent Network Architectures

R. Jozefowicz and W. Zaremba and I. Sutskever

Proceedings of the 32nd International Conference on Machine Learning, Lille, France (2015)

LSTM: A Search Space Odyssey

K. Greff and R. K. Srivastava and J. Koutník and B. R. Steunebrink and J. Schmidhuber

Transactions on neural networks and learning systems 28 2222-2232 (2017)

Multiple-Hour-Ahead Forecast of the Dst Index Using a Combination of Long Short-Term Memory Neural Network and Gaussian Process

M. A. Gruet and M. Chandorkar and A. Sicard and E. Camporeale

Space Weather 16 (2018)

Geomagnetic index Kp forecasting with LSTM

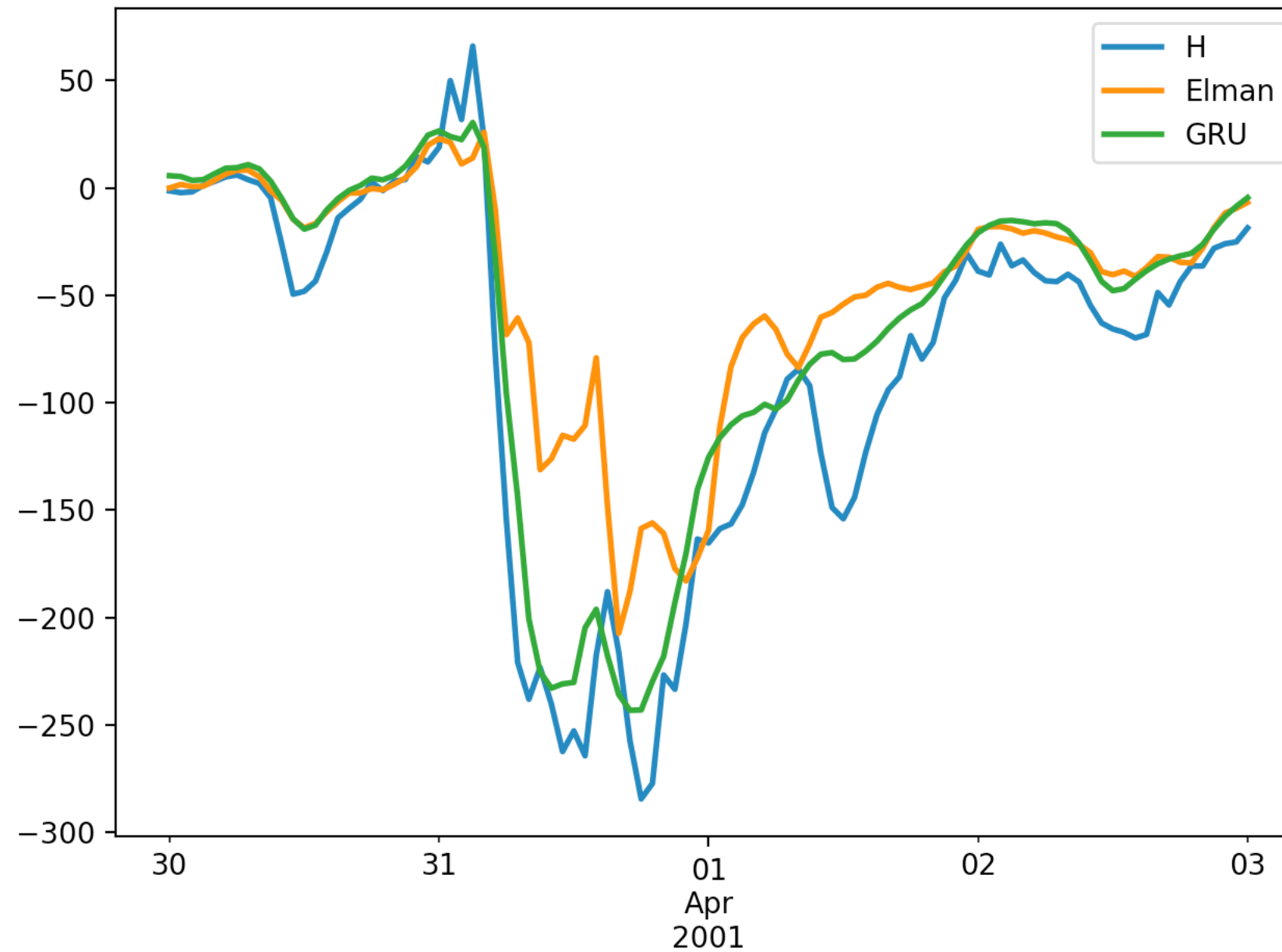
Y. Tan and Q. Hu and Z. Wang and Q. Zhong

Space Weather 16 406-416 (2018)

“Which pieces of the LSTM architecture are actually necessary?” [Goodfellow et al., 2016]

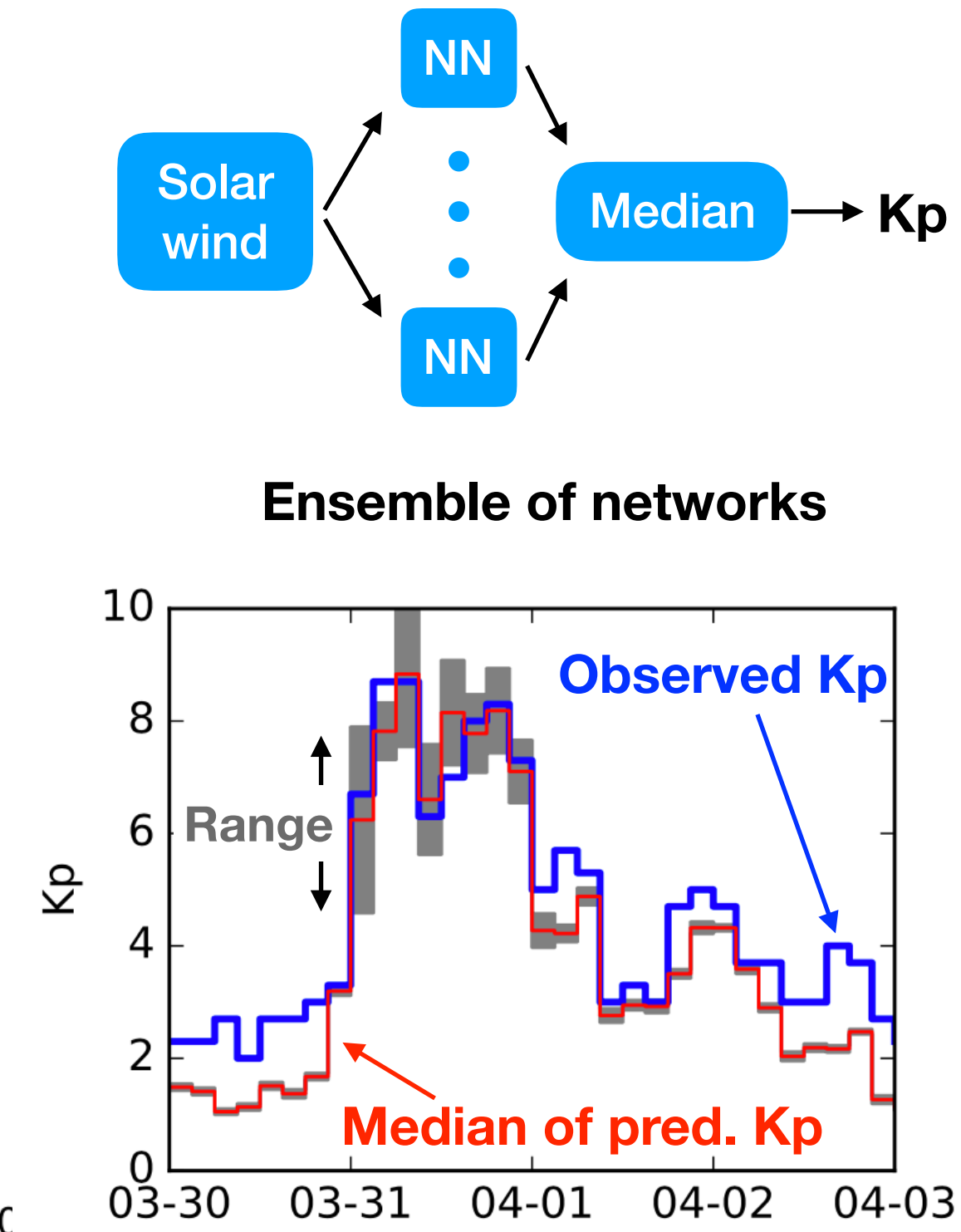
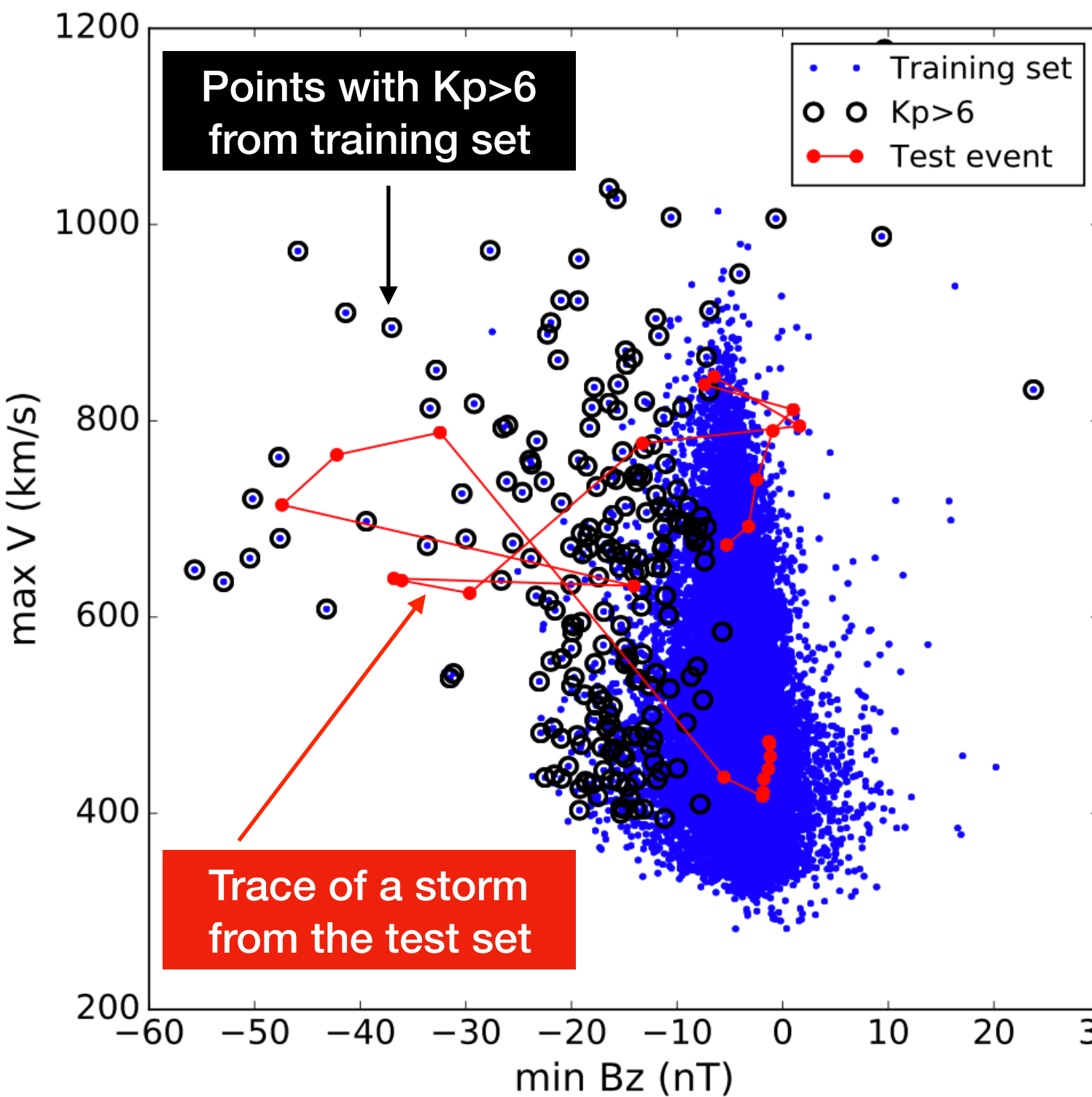
# Solar wind to local H

Hermanus hourly magnetic field (one of the four Dst stations).

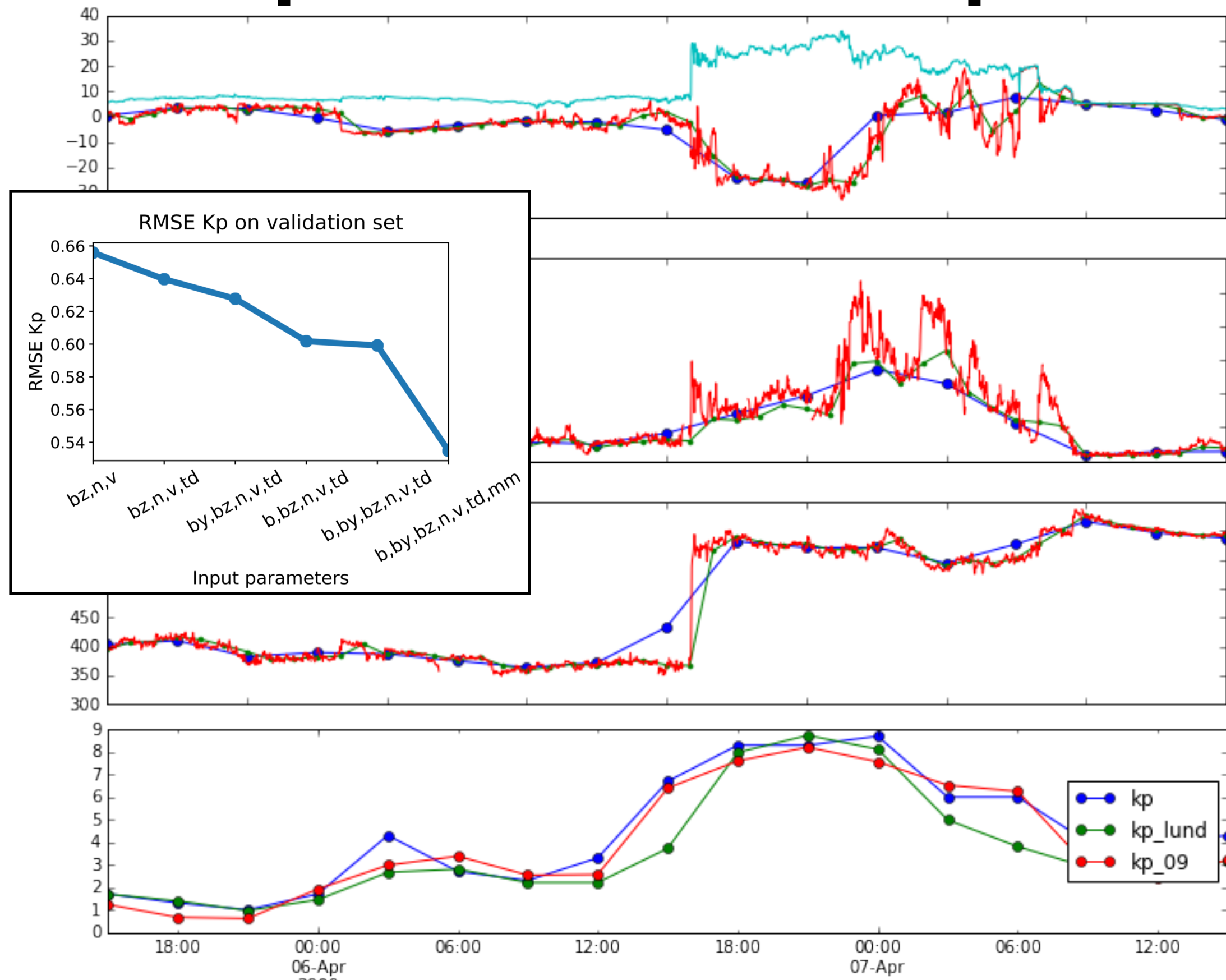


Wintoft, P, and M. Wik, Prediction of local ground magnetic field using recurrent neural networks, To be submitted to Frontiers and Space Sciences, 2020.

# Function estimation in low-density state-space

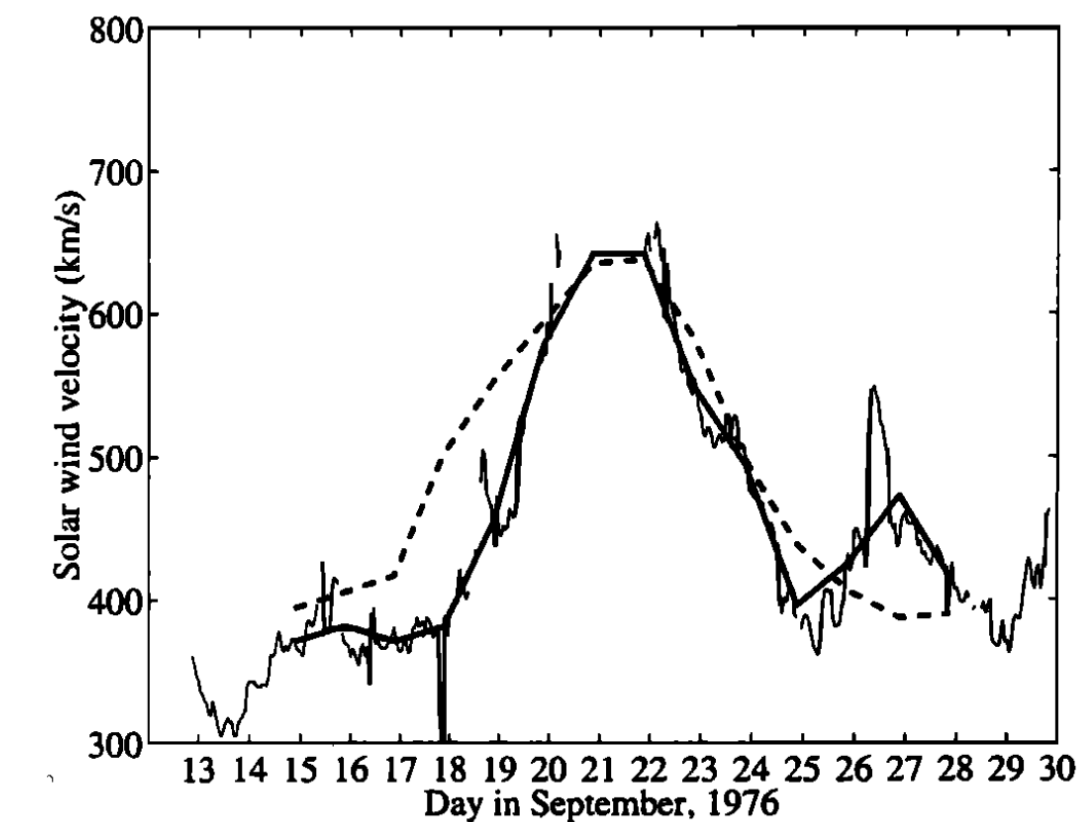


# Importance of inputs



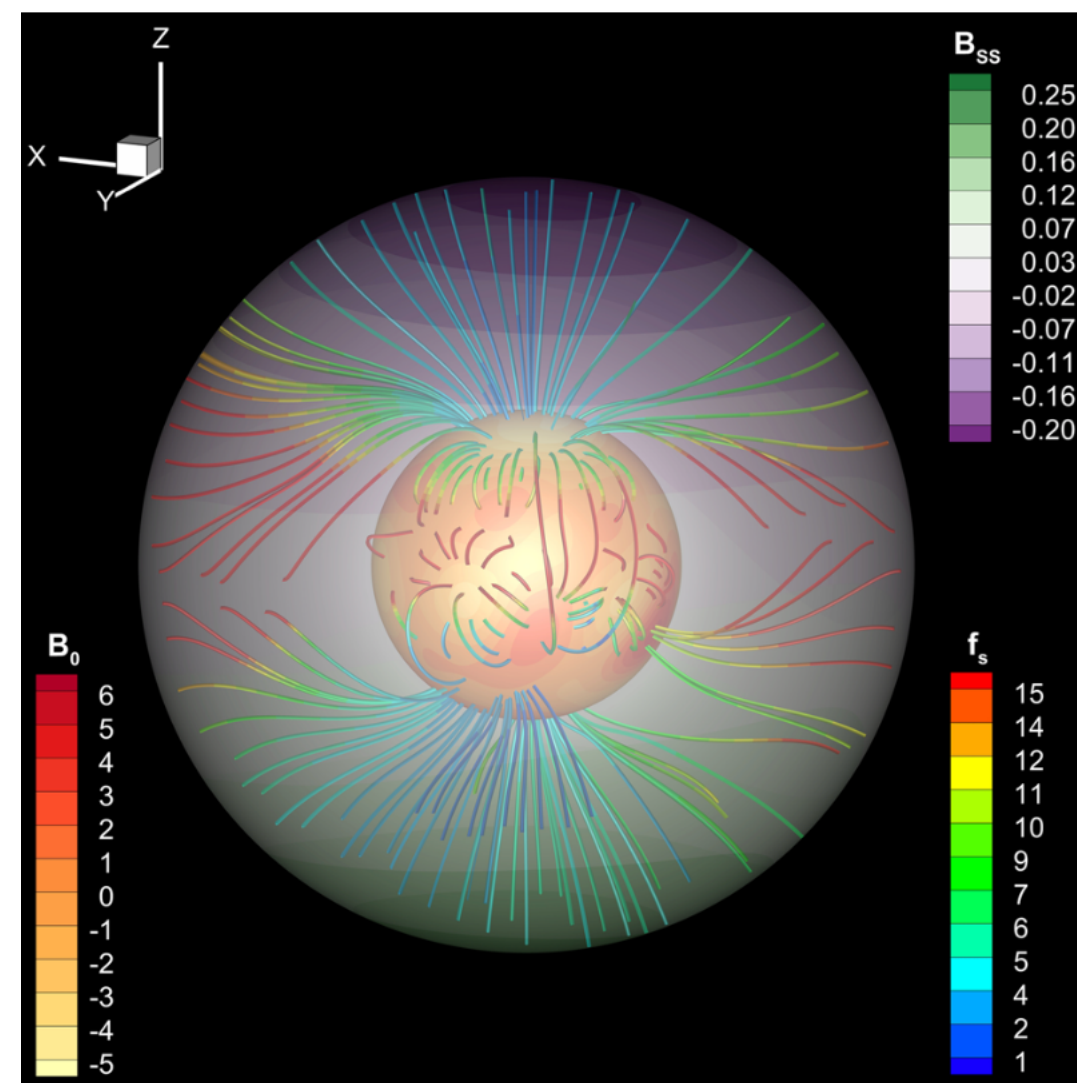
$$z^\mu = w_0 + \sum_{i=1}^{N_H} w_i \exp \left( - \sum_{j=1}^{N_I} \frac{(x_j^\mu - v_{ij})^2}{\sigma^2} \right)$$

A neural network study of the mapping from solar magnetic fields to the daily average solar wind velocity  
 P. Wintoft and H. Lundstedt  
 Journal of Geophysical Research 104 6729--6736 (1999)



$$f_s = \left( \frac{B_0}{B_{ss}} \right) \left( \frac{R_\odot}{R_{ss}} \right)^2$$

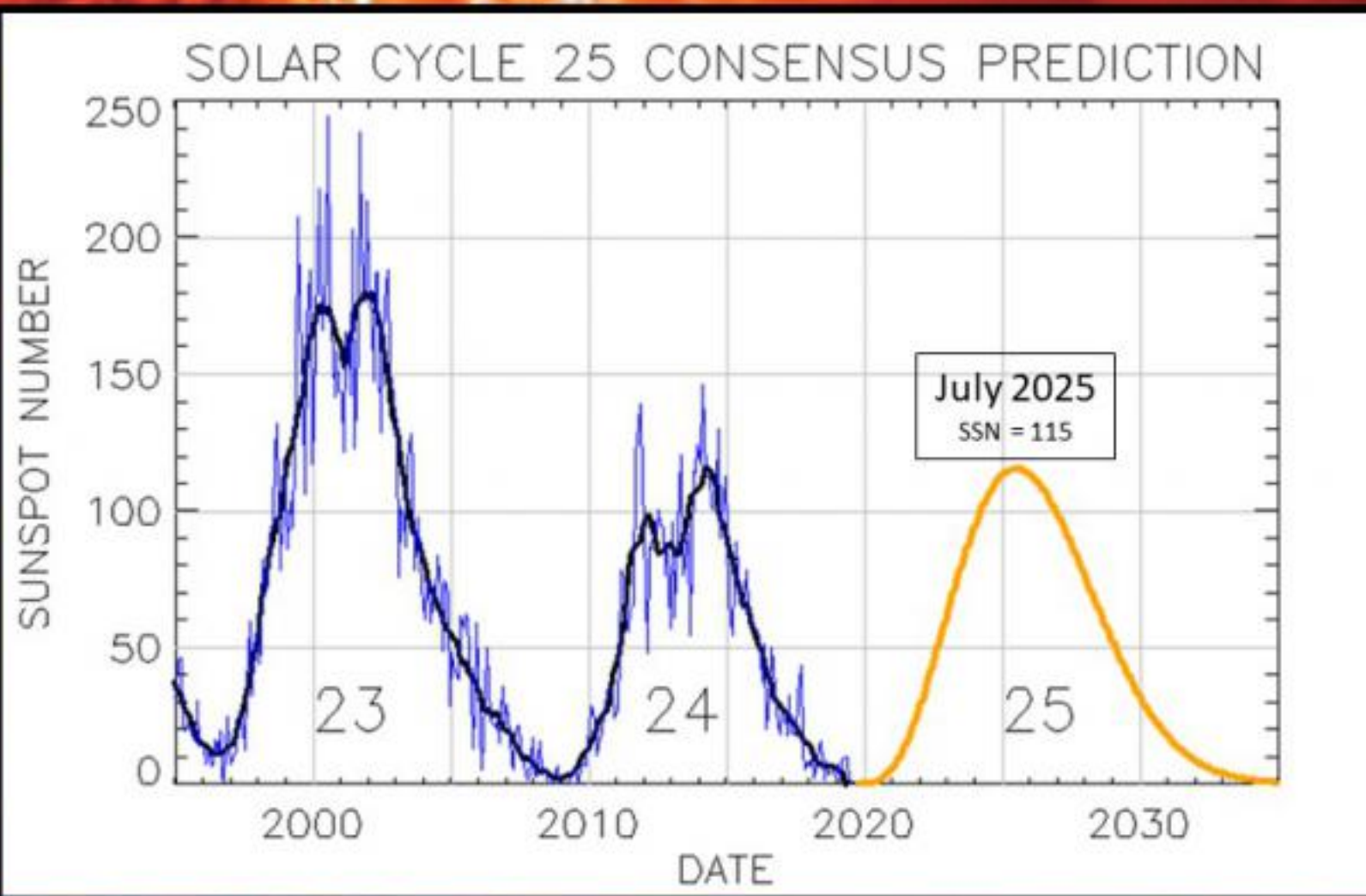
Modeling the Global Distribution of Solar Wind Parameters on the Source Surface Using Multiple Observations and the Artificial Neural Network Technique  
 Y. Yang and F. Shen  
 Solar Physics 2914 (2019)



# Solar cycle 25

## Solar Cycle 25 Forecast Update

- Released December 9<sup>th</sup>, 2019 -

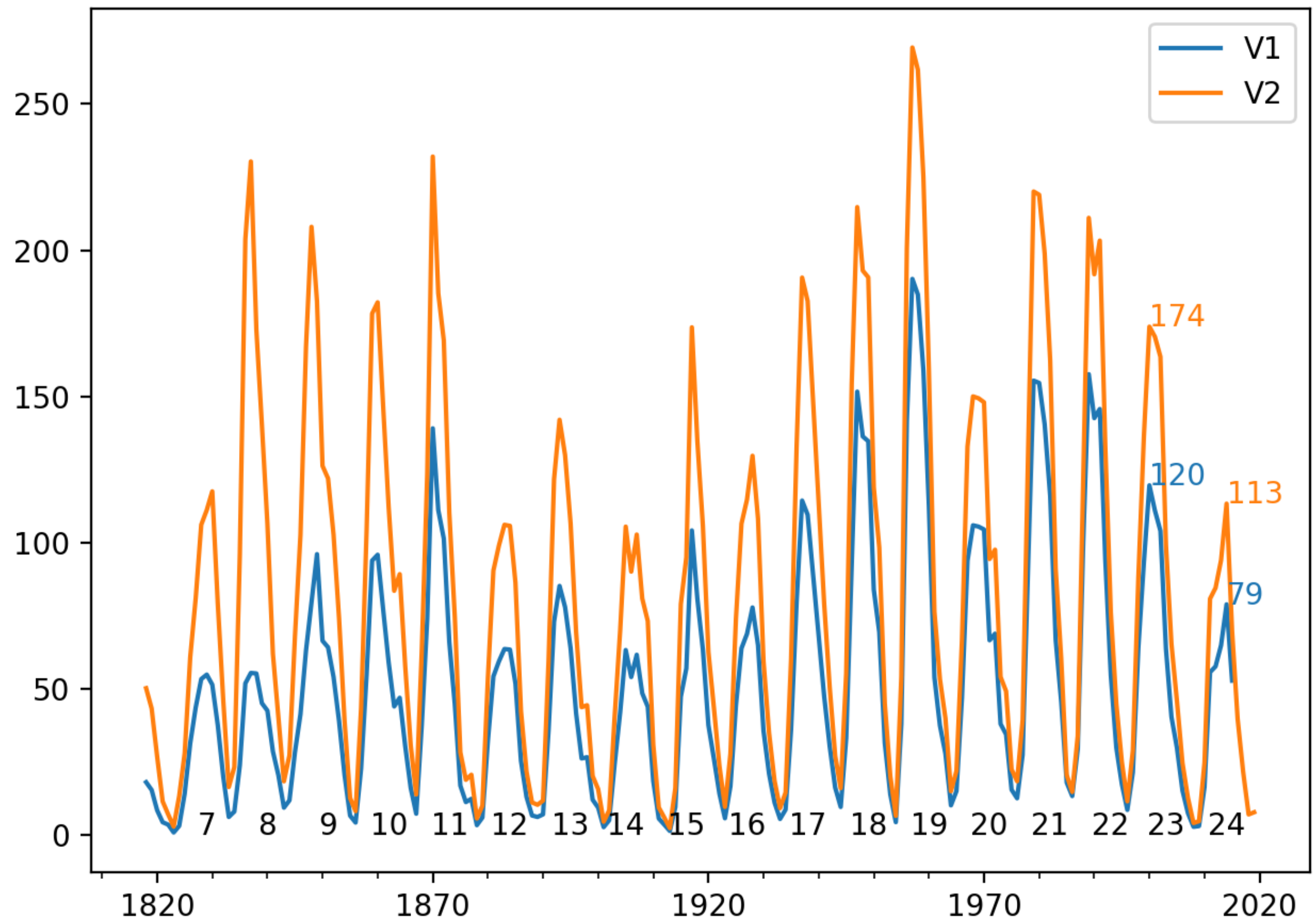


Solar Cycle 25 will have a peak SSN of 115 ( $\pm 10$ ) in July 2025

Solar Cycle 24/25 minimum will occur in April, 2020 ( $\pm 6$  months)

<https://www.swpc.noaa.gov/news/solar-cycle-25-forecast-update>

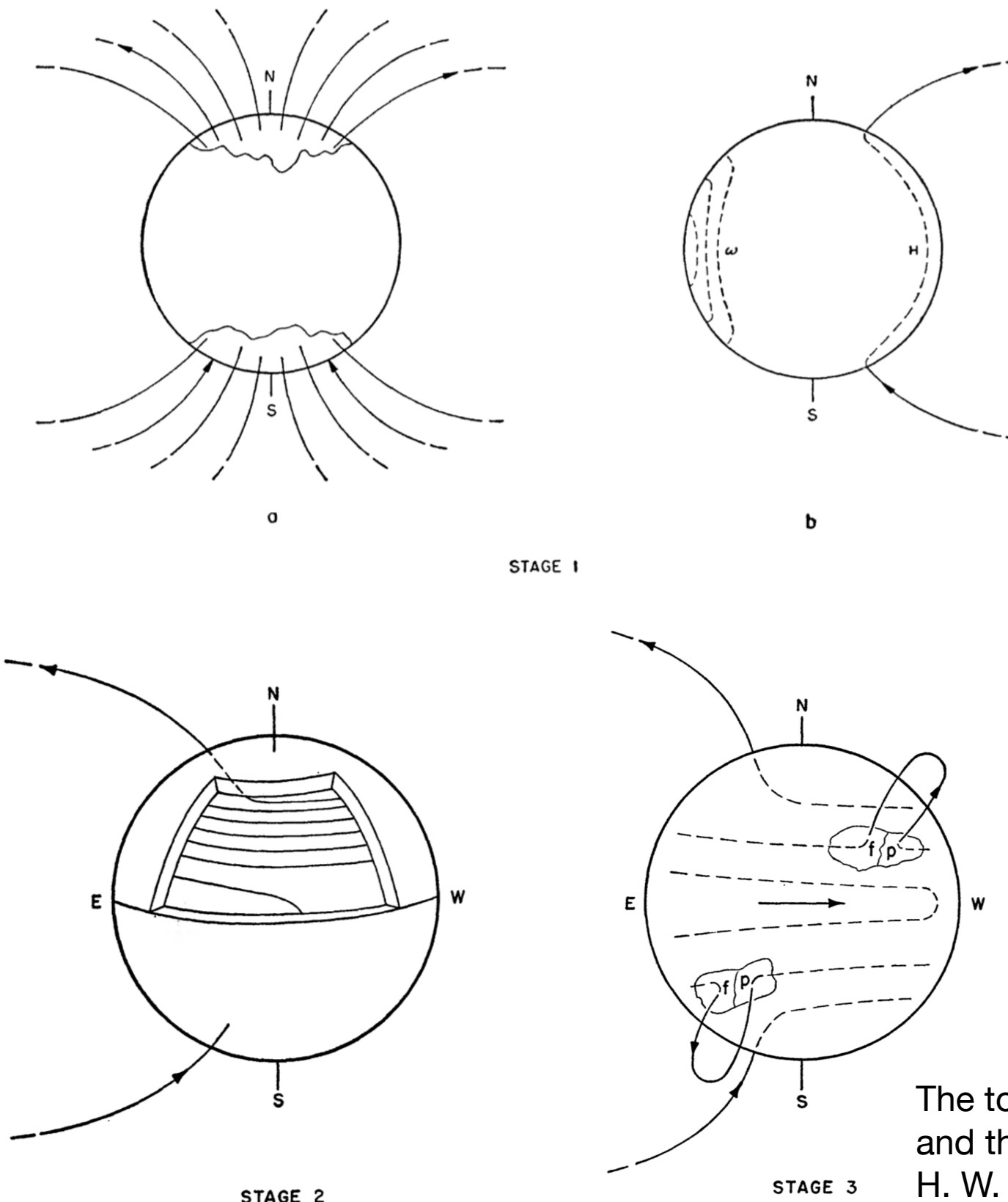
## Yearly average SSN



# ML-SSN predictions

- Lots of papers using different ML techniques to predict SSN.
- Many of the old papers contain the essential ideas.
- New algorithms, architectures (units and transfer functions), regularisation (dropout), and “view” on weights (non-parametric, Bayesian, GP).
- Validation and cross-validation for hyper-parameter search.
- Filtering (averages, wavelets, ...), temporal resolution, embedding dimension, (useful) prediction horizon.
- “But predictions based only on the statistics of the sunspot number are not adequate for predicting the next solar maximum.” W.D. Pesnell, 2015.

# Solar dynamo



$$\frac{\partial \rho}{\partial t} + \nabla \cdot (\rho \mathbf{u}) = 0,$$

$$\frac{\partial \mathbf{u}}{\partial t} + (\mathbf{u} \cdot \nabla) \mathbf{u} = -\frac{1}{\rho} \nabla p - 2\boldsymbol{\Omega} \times \mathbf{u} + \mathbf{g} + \frac{1}{\mu_0 \rho} (\nabla \times \mathbf{B}) \times \mathbf{B} + \frac{1}{\rho} \nabla \cdot \boldsymbol{\tau},$$

$$\frac{\partial e}{\partial t} + (\gamma - 1)e \nabla \cdot \mathbf{u} = \frac{1}{\rho} \{ \nabla \cdot [(\chi + \chi_r) \nabla T] + \phi_u + \phi_B \},$$

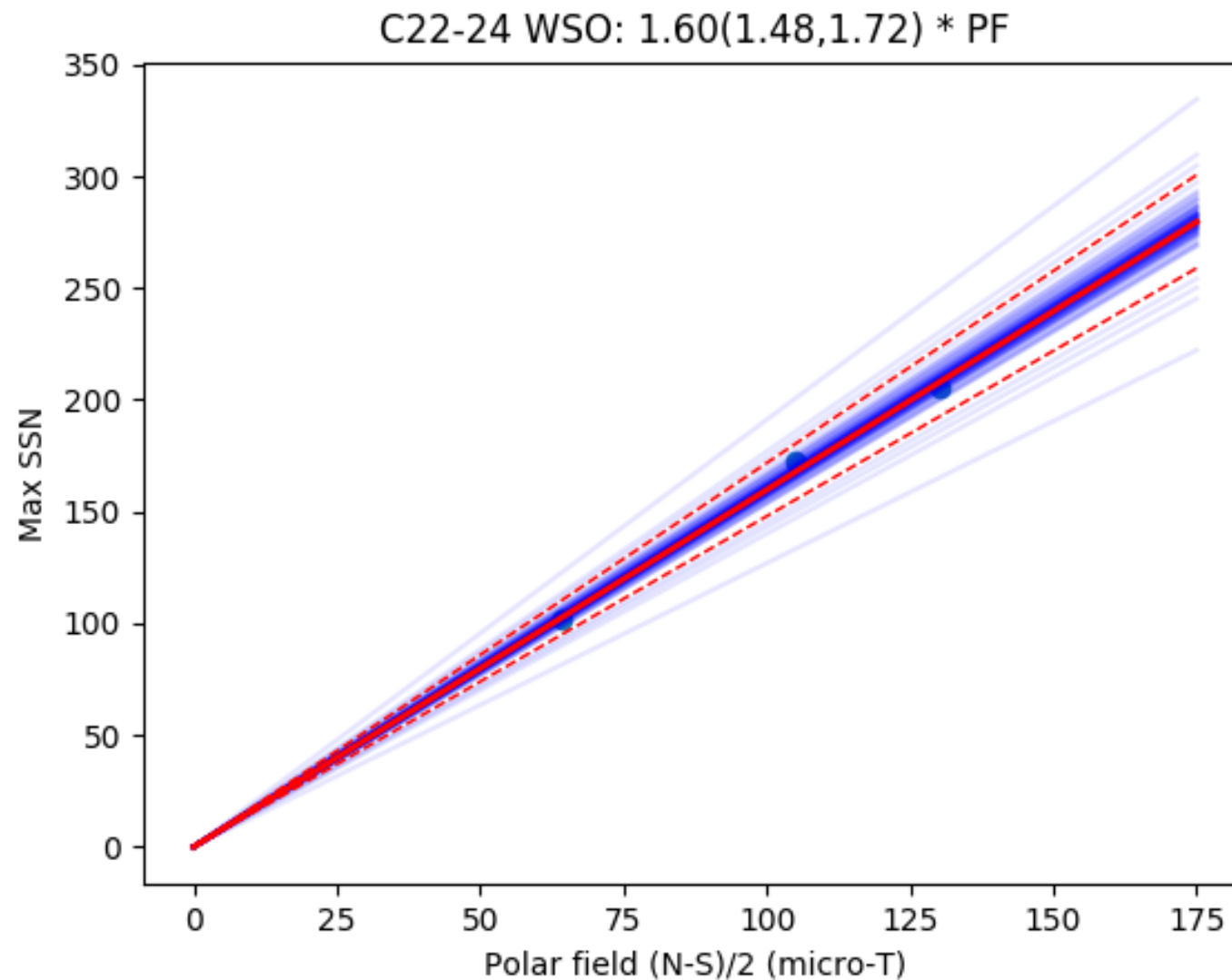
$$\frac{\partial \mathbf{B}}{\partial t} = \nabla \times (\mathbf{u} \times \mathbf{B} - \eta \nabla \times \mathbf{B}).$$

Solar dynamo theory  
 P. Charbonneau  
 Annual Review of Astronomy and Astrophysics 52 251-90  
 (2014)

The topology of the Sun's magnetic field and the 22-year cycle.  
 H. W. Babcock  
 Astrophysical Journal 133 572 (1961)

# Polar field as precursor of coming SSN maximum

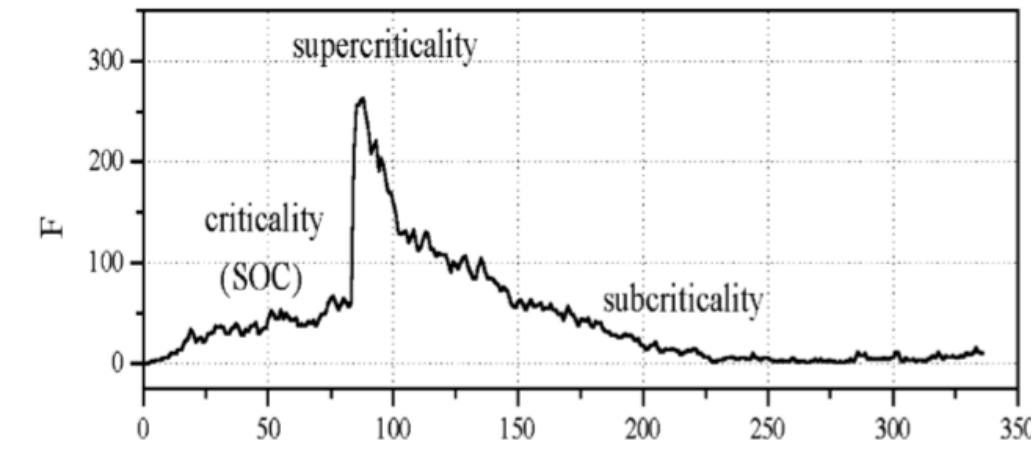
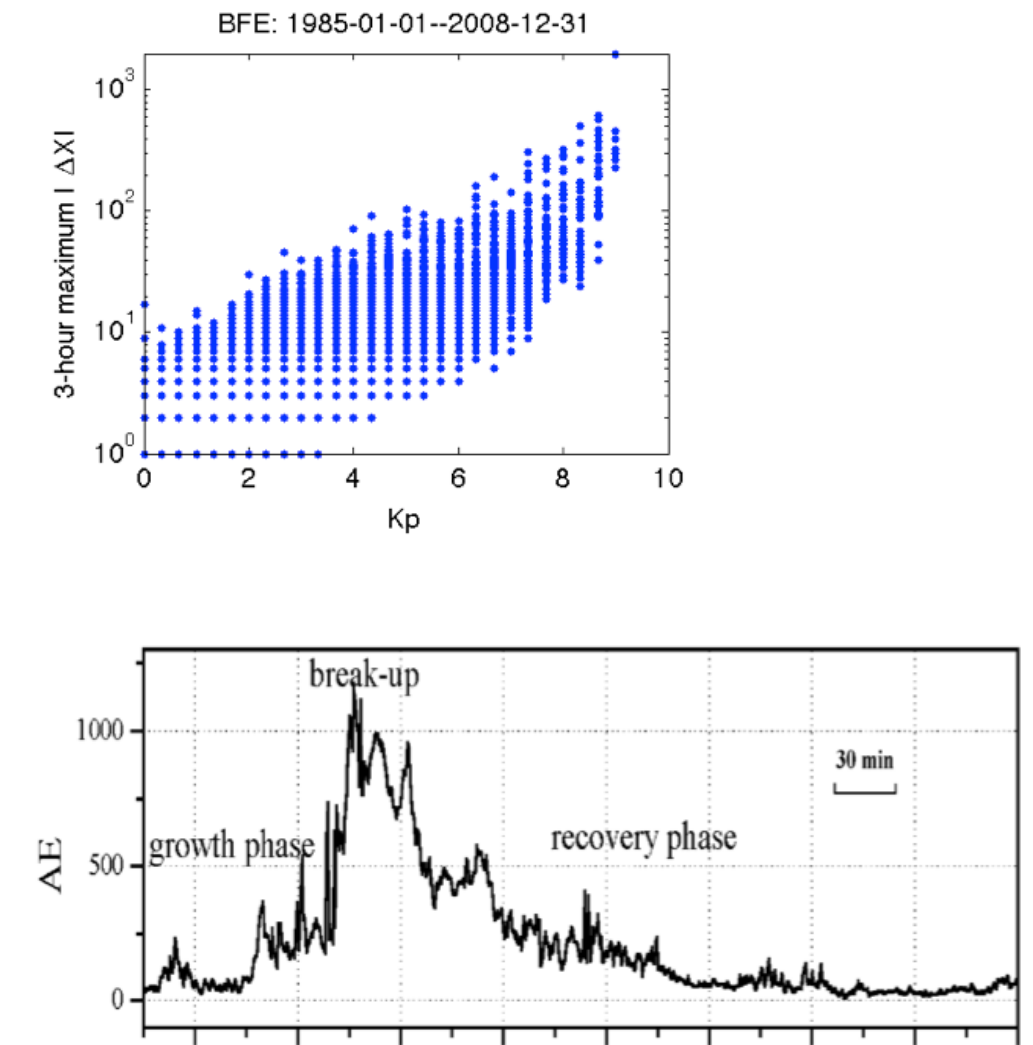
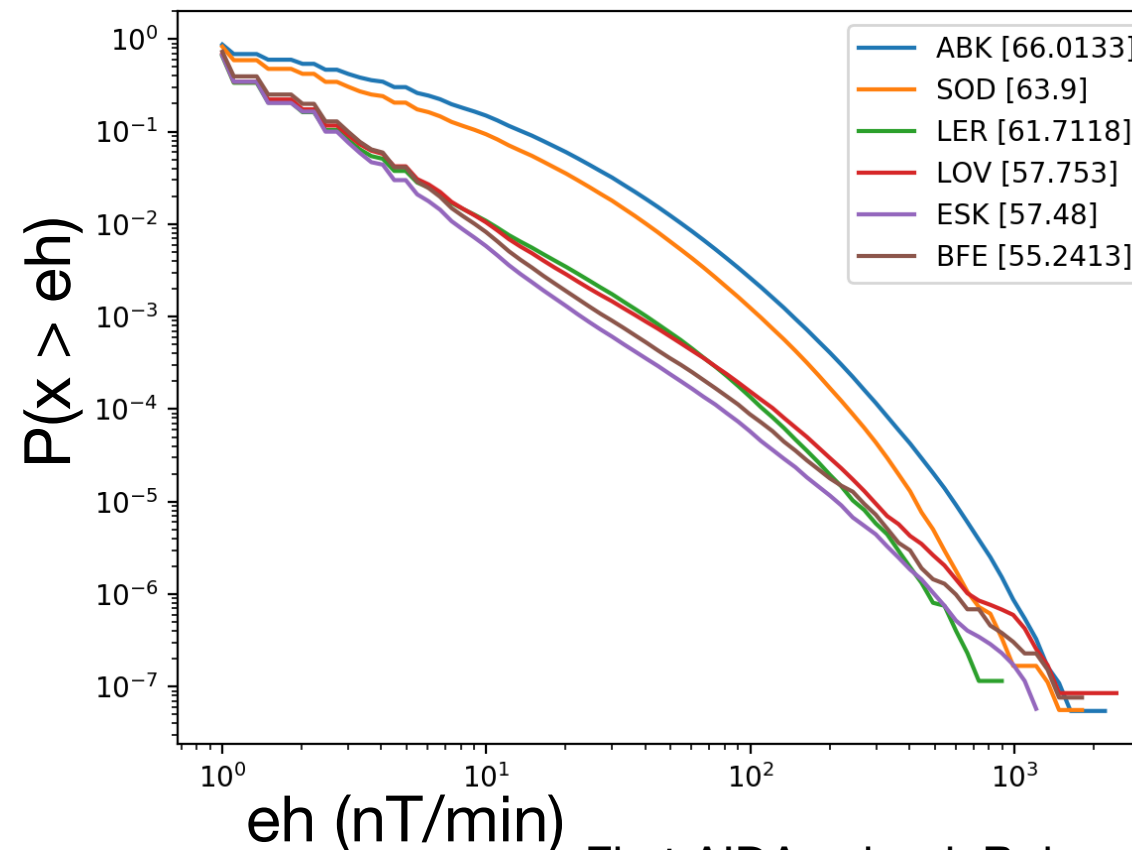
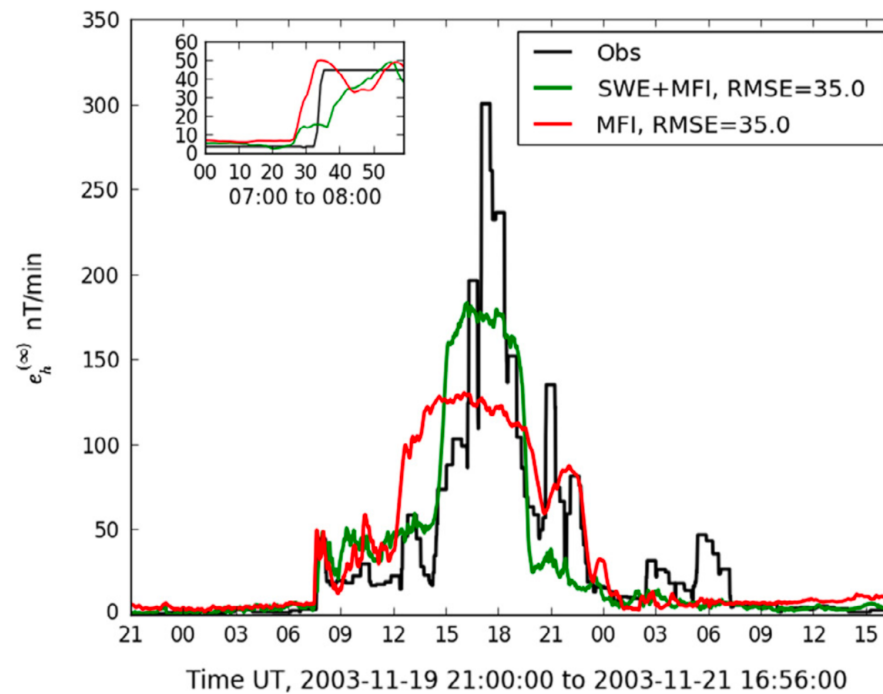
L Svalgaard, E W Cliver, and Y Kamide. Sunspot cycle 24: Smallest cycle in 100 years? Geophysical Research Letters, 32:L01104, 2005. doi: 10.1029/2004GL021664.



**Polar field data from Wilcox Solar Observatory (Stanford) and SSN data from WDC-SILSO, Royal Observatory of Belgium, Brussels**

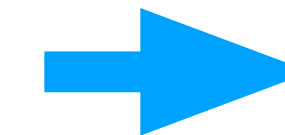
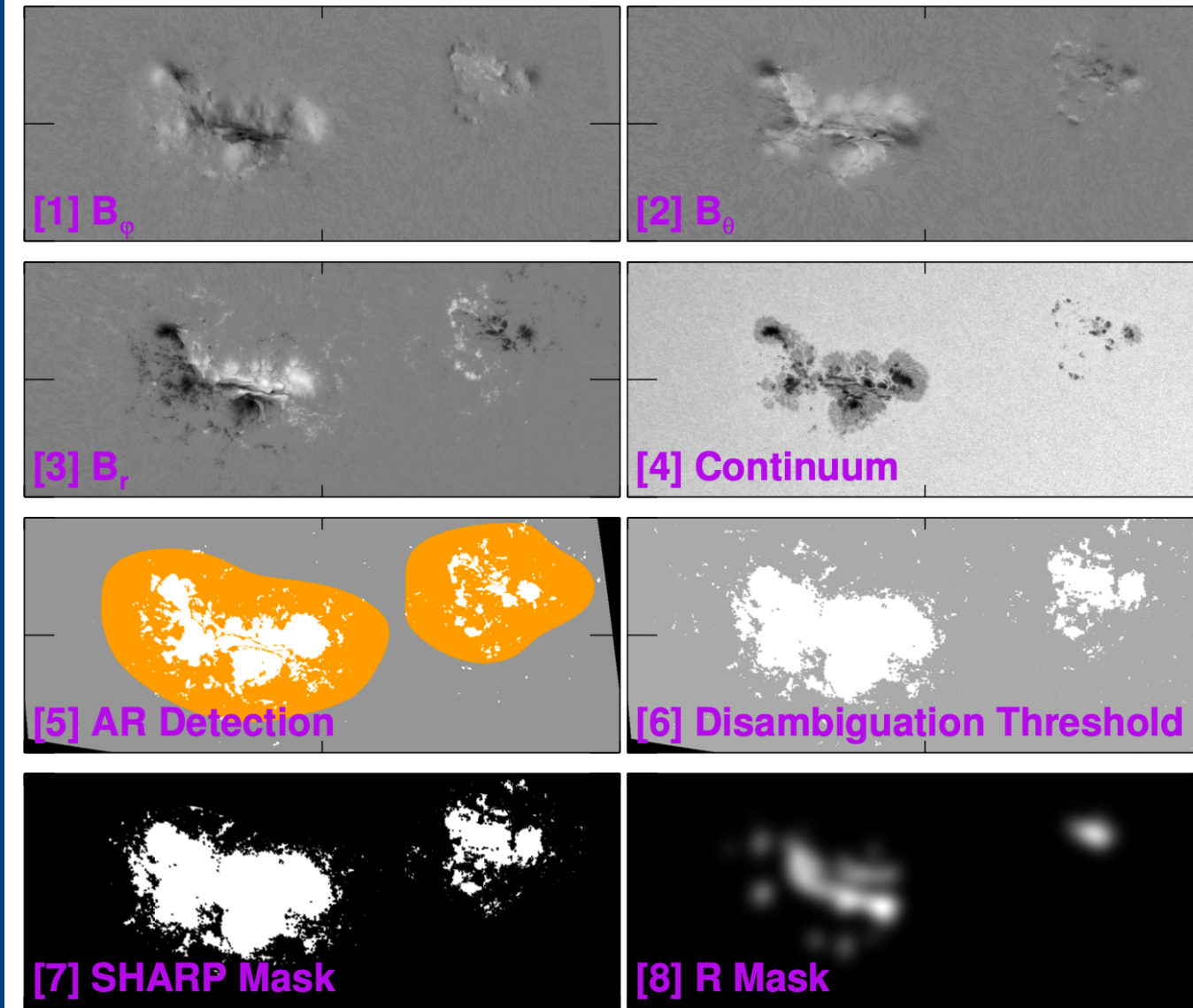


Solar wind driven empirical forecast  
models of the time derivative of the ground  
magnetic field, P. Wintoft and M. Wik and  
A. Viljanen, Journal of Space Weather and  
Space Climate 5 A7 (2015)



Geomagnetic substorms as perturbed self-organized critical dynamics of the magnetosphere, V. Uritsky and M. Pudovkin and A. Steen, Journal of Atmospheric and Solar-Terrestrial Physics 63 1415-1424 (2001)

# Solar flares



**SHARP**

Keyword	Description	Formula	F-Score	Selection
TOTUSH	Total unsigned current helicity	$H_{total} \propto \sum (B_z \cdot J_z)$	3560	Included
TOTBSQ	Total magnitude of Lorentz force	$F \propto \sum B^2$	3051	Included
TOTPOT	Total photospheric magnetic free energy density	$\rho_{tot} \propto \sum (\vec{B}^{obs} - \vec{B}^{pot})^2 dA$	2996	Included
TOTUJZ	Total unsigned vertical current	$J_z \propto \sum  J_z  dA$	2733	Included
AHSNZH	Absolute value of the net current helicity	$H_{total} \propto  \sum B_z \cdot J_z $	2618	Included
SAVNCP	Sum of the modulus of the net current per polarity	$J_{z,sum} \propto \left  \sum B_z dA \right  + \left  \sum J_z dA \right $	2448	Included
USFLUX	Total unsigned flux	$\Phi = \sum  B_z  dA$	2437	Included
AREA_ACR	Area of strong field pixels in the active region	Area = $\sum$ Pixels	2047	Included
TOTFZ	Sum of z-component of Lorentz force	$F_z \propto \sum (B_z^2 + B_\theta^2 - B_\phi^2) dA$	1371	Included
MEANPOT	Mean photospheric magnetic free energy	$\bar{\rho} \propto \frac{1}{N} \sum (\vec{B}^{obs} - \vec{B}^{pot})^2$	1064	Included
R_VALUE	Sum of flux near polarity inversion line	$\Phi = \sum  B_{z,obs}  dA$ within R mask	1057	Included
EPSZ	Sum of z-component of normalized Lorentz force	$\delta F_z \propto \frac{\sum (B_z^2 + B_\theta^2 - B_\phi^2)}{\sum B^2}$	864.1	Included
SHRGT45	Fraction of Area with Shear > 45°	Area with Shear > 45° / Total Area	740.8	Included
MEANSIR	Mean shear angle	$\bar{\Gamma} = \frac{1}{N} \sum \arccos \left( \frac{\vec{B}_z}{\ \vec{B}^{obs}\  \ \vec{B}^{pot}\ } \right)$	727.9	Discarded
MEANGAM	Mean angle of field from radial	$\bar{\gamma} = \frac{1}{N} \sum \arctan \left( \frac{B_\theta}{B_z} \right)$	573.3	Discarded
MEANGBT	Mean gradient of total field	$ \nabla B_{tot}  = \frac{1}{N} \sum \sqrt{\left( \frac{\partial B}{\partial x} \right)^2 + \left( \frac{\partial B}{\partial y} \right)^2}$	192.3	Discarded
MEANGBZ	Mean gradient of vertical field	$ \nabla B_z  = \frac{1}{N} \sum \sqrt{\left( \frac{\partial B_z}{\partial x} \right)^2 + \left( \frac{\partial B_z}{\partial y} \right)^2}$	88.40	Discarded
MEANGBH	Mean gradient of horizontal field	$ \nabla B_h  = \frac{1}{N} \sum \sqrt{\left( \frac{\partial B_h}{\partial x} \right)^2 + \left( \frac{\partial B_h}{\partial y} \right)^2}$	79.40	Discarded
MEANIZH	Mean current helicity ( $B_z$ contribution)	$\bar{H}_z \propto \frac{1}{N} \sum B_z \cdot J_z$	46.73	Discarded
TOTFY	Sum of y-component of Lorentz force	$F_y \propto \sum B_y dA$	28.92	Discarded
MEANIZD	Mean vertical current density	$\bar{J}_z \propto \frac{1}{N} \sum \left( \frac{\partial B_y}{\partial x} - \frac{\partial B_x}{\partial y} \right)$	17.44	Discarded
MEANALP	Mean characteristic twist parameter, $\alpha$	$\alpha_{total} \propto \frac{\sum J_z \cdot B_z}{\sum B_z^2}$	10.41	Discarded
TOTFX	Sum of x-component of Lorentz force	$F_x \propto -\sum B_x B_z dA$	6.147	Discarded
EPSY	Sum of y-component of normalized Lorentz force	$\delta F_y \propto \frac{-\sum B_x B_z}{\sum B^2}$	0.647	Discarded
EPSX	Sum of x-component of normalized Lorentz force	$\delta F_x \propto \frac{\sum B_x B_z}{\sum B^2}$	0.366	Discarded

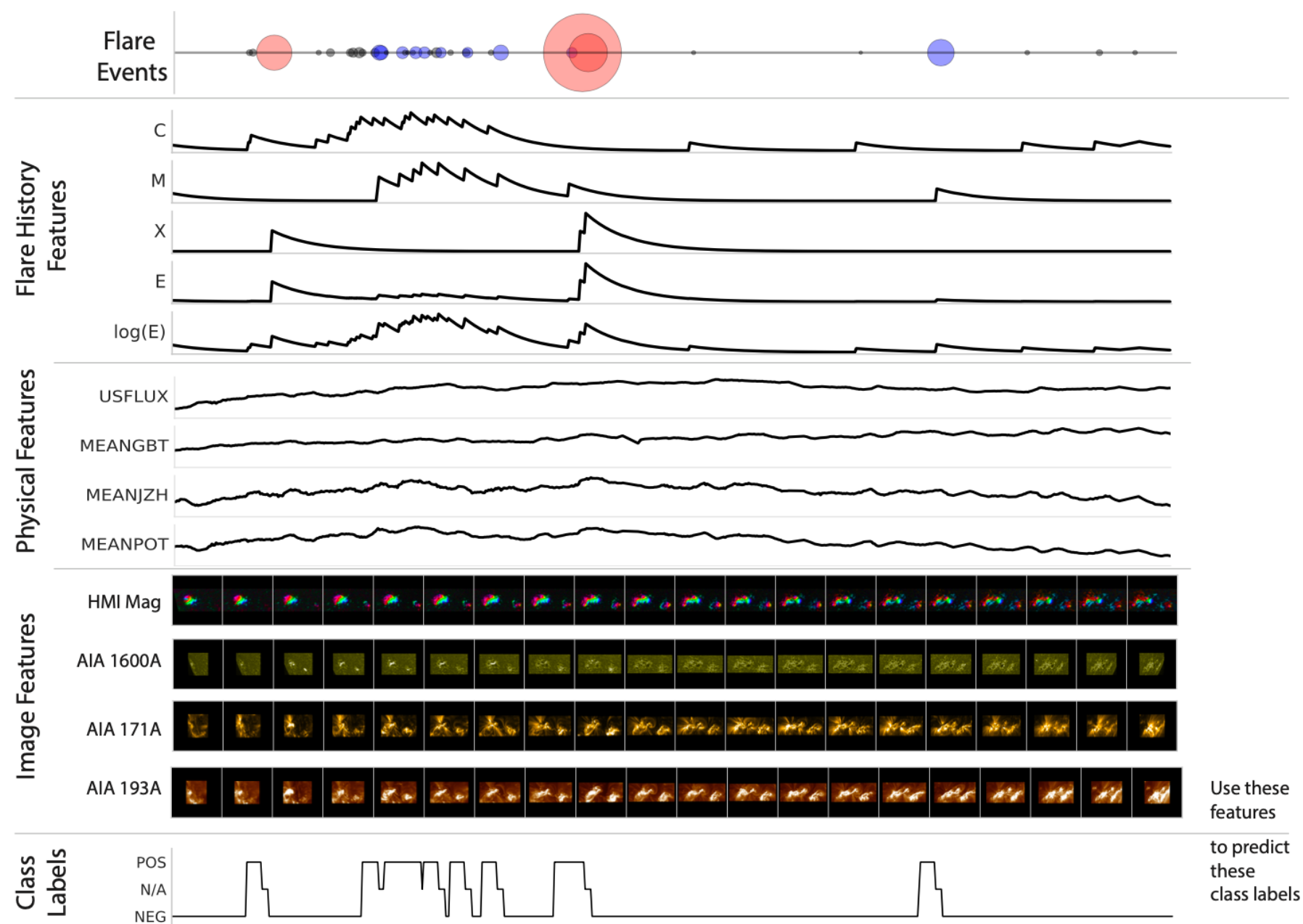


**SVM**

**M-flare or larger**

Solar flare prediction using SDO/HMI vector magnetic field data with a machine-learning algorithm  
M. G. Bobra and S. Couvidat  
The Astrophysical Journal 798 135 (2015)

# CNN for solar flare prediction



**“5.5 TB of SDO image data”**

Flare prediction using photospheric and coronal image data  
 E. Jonas and M. Bobra and V. Shankar and J. T. Hoeksema and B. Recht  
 Solar Physics 293 (2018)

# SOHO/MDI and SDO/HMI magnetograms to predict C, M, and X class flares within 6h to 48h windows

THE ASTROPHYSICAL JOURNAL, 856:7 (11pp), 2018 March 20

Huang et al.

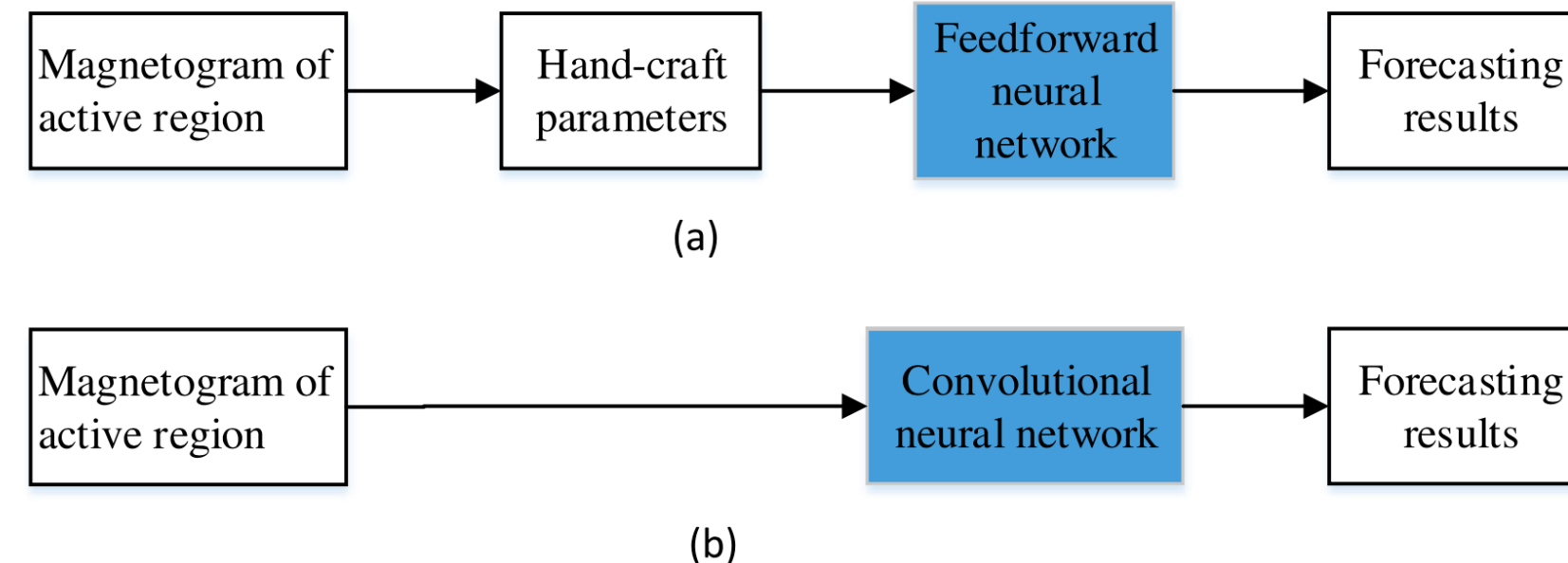


**Figure 1.** Difference between standard feed-forward neural network and convolutional neural network in solar flare forecasting. Components in shaded boxes need to be learned from the data set. (a) Standard feed-forward neural network for solar flare forecasting. (b) Convolutional neural network for solar flare forecasting.

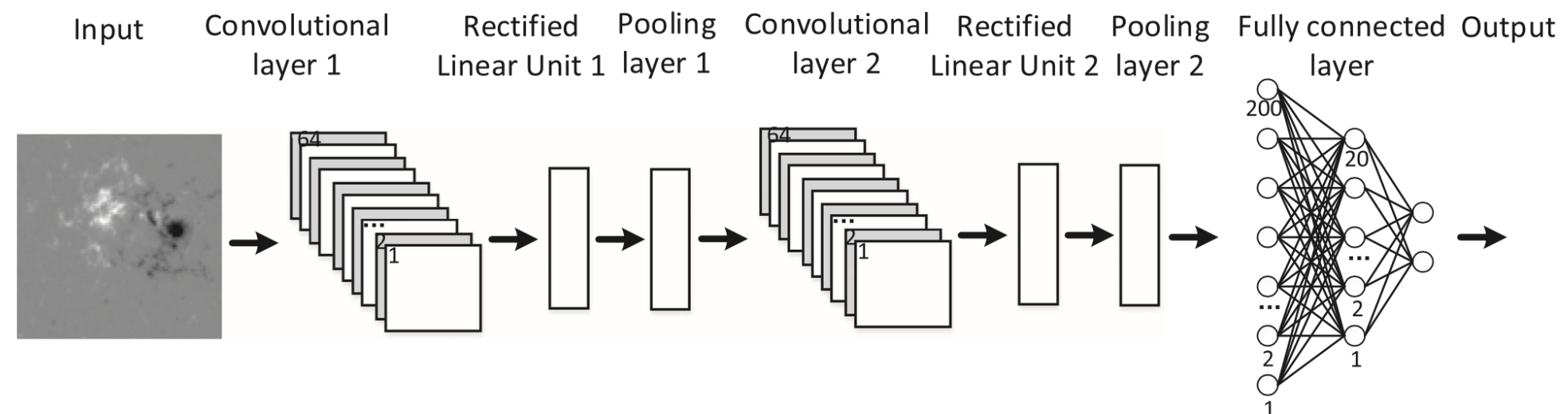
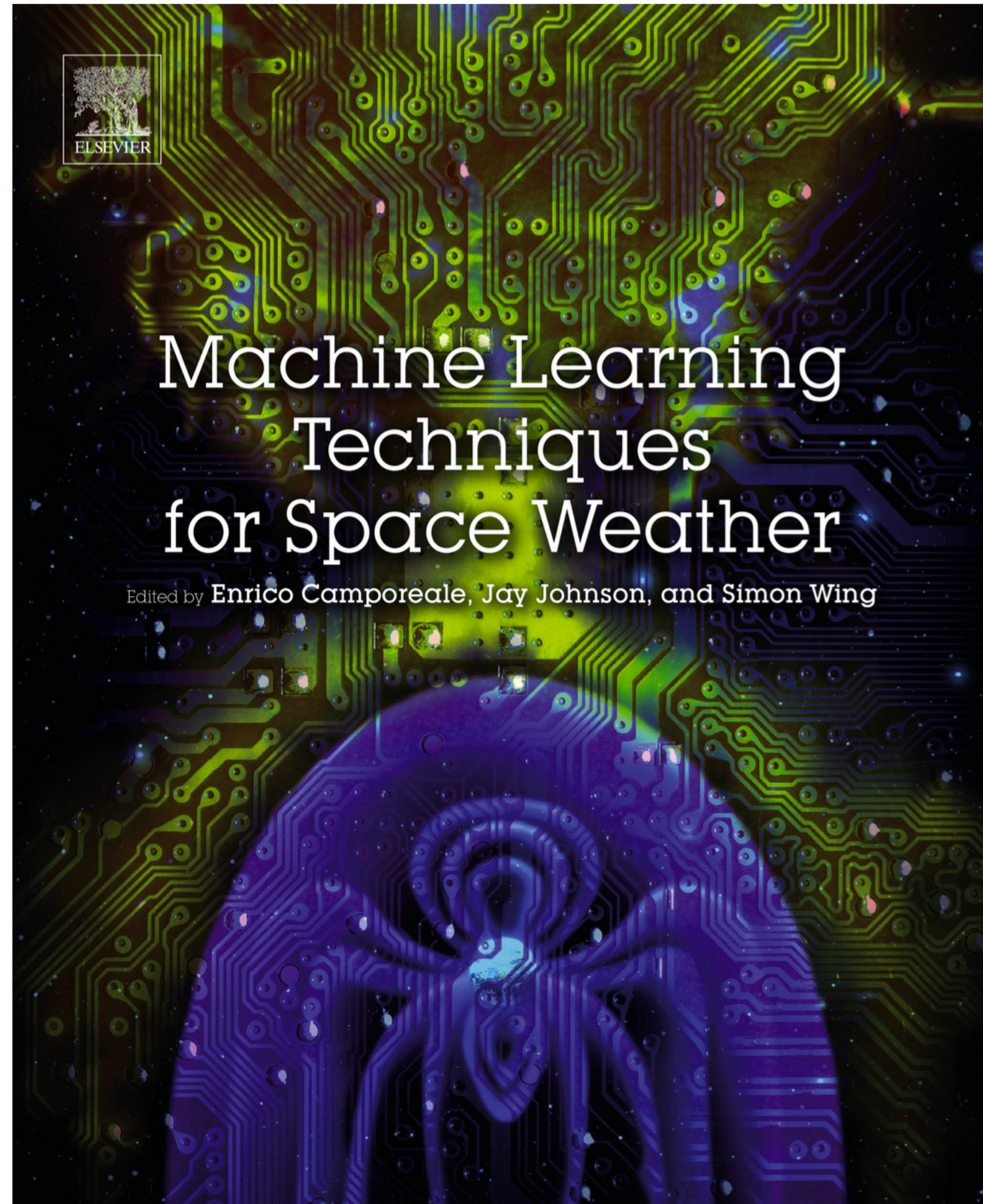


**Figure 2.** Structure of convolutional neural network for solar flare forecasting.

Deep Learning Based Solar Flare Forecasting Model. I. Results for Line-of-sight Magnetograms  
 X. Huang and H. Wang and L. Xu and J. Liu and R. Li and X. Dai  
 The Astrophysical Journal 856 (2018)

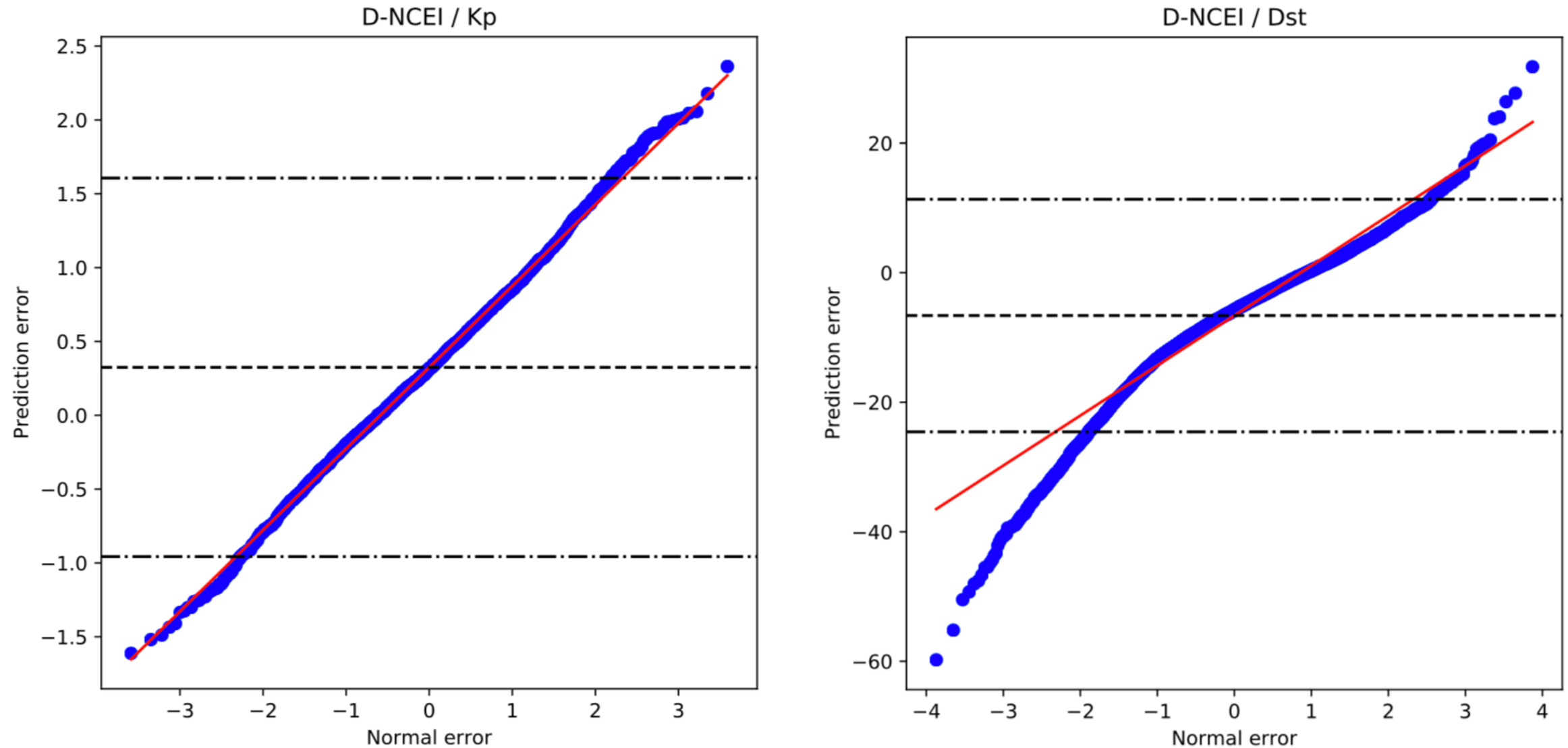


# List of some key questions/ research

- Comparing models?
- Develop simple baseline model for comparison.
- Dropout vs ensemble.
- Indices are useful but future work should target parameters closer to the phenomena.
- Increasing lead-time => solar data.
- Predicting solar magnetic field evolution.

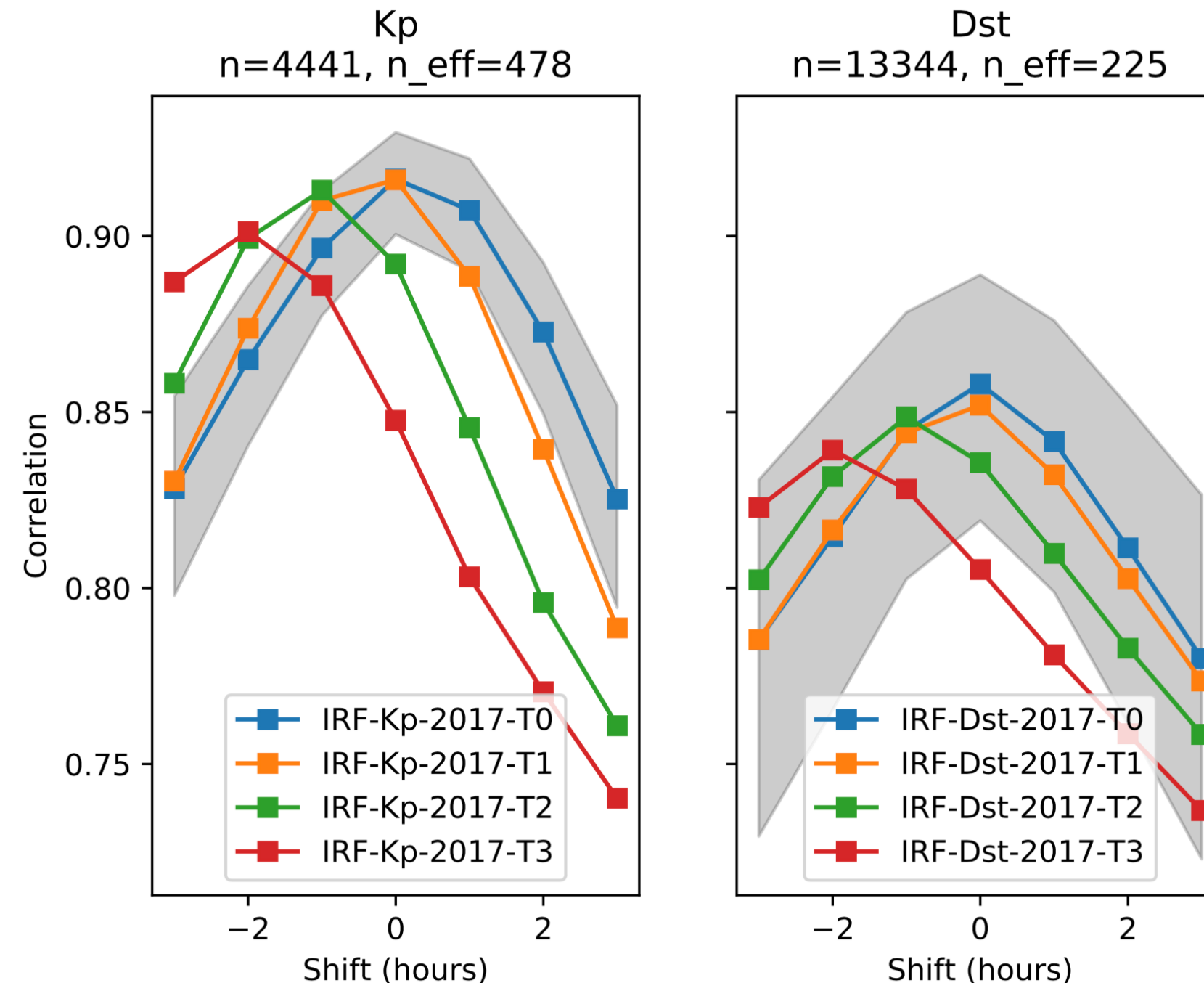
# Extra

# QQ plots



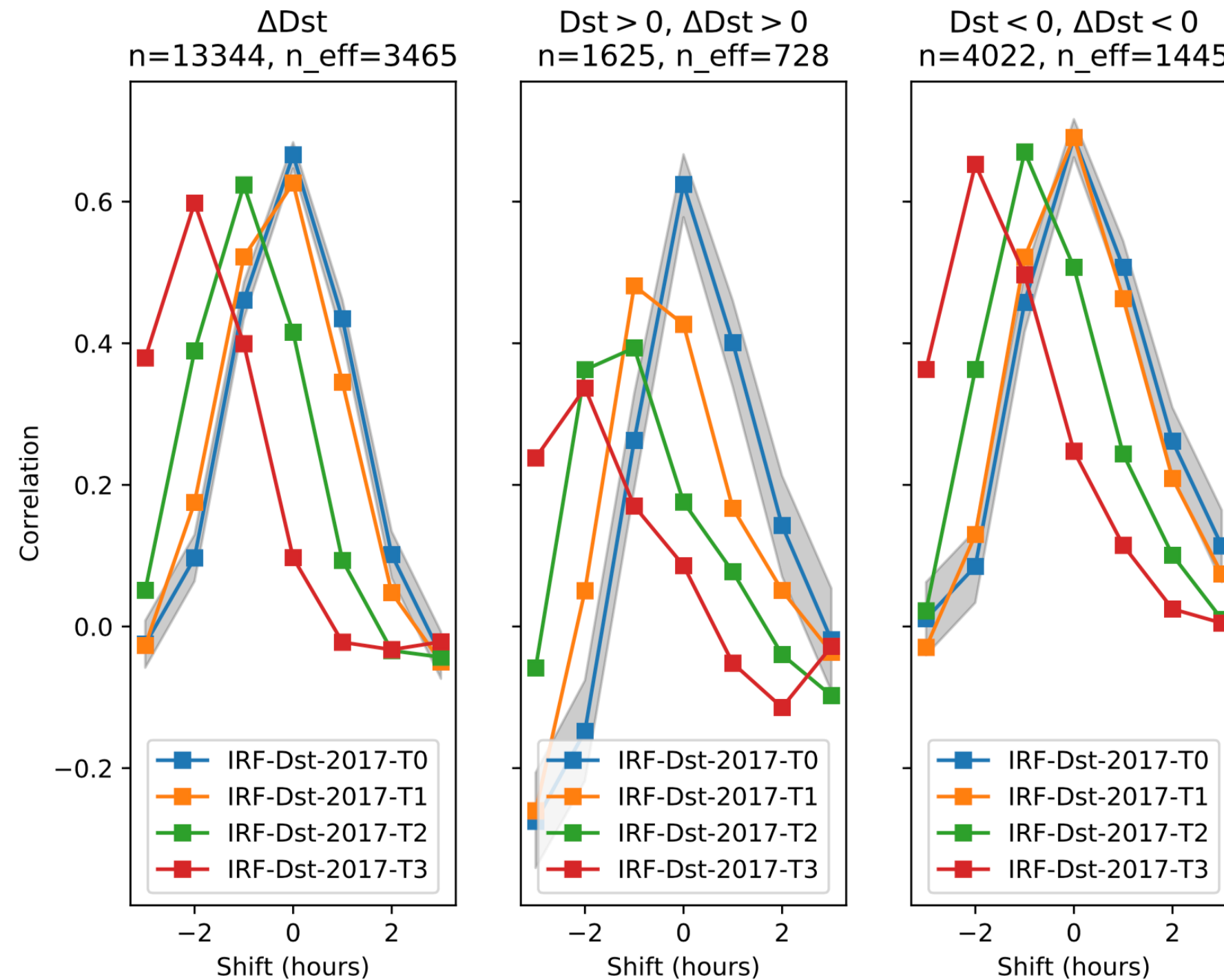
Evaluation of Kp and Dst Predictions Using ACE and DSCOVR Solar Wind Data  
P. Wintoft and M. Wik  
Space Weather 16 1972-1983 (2018)

# Prediction lead time



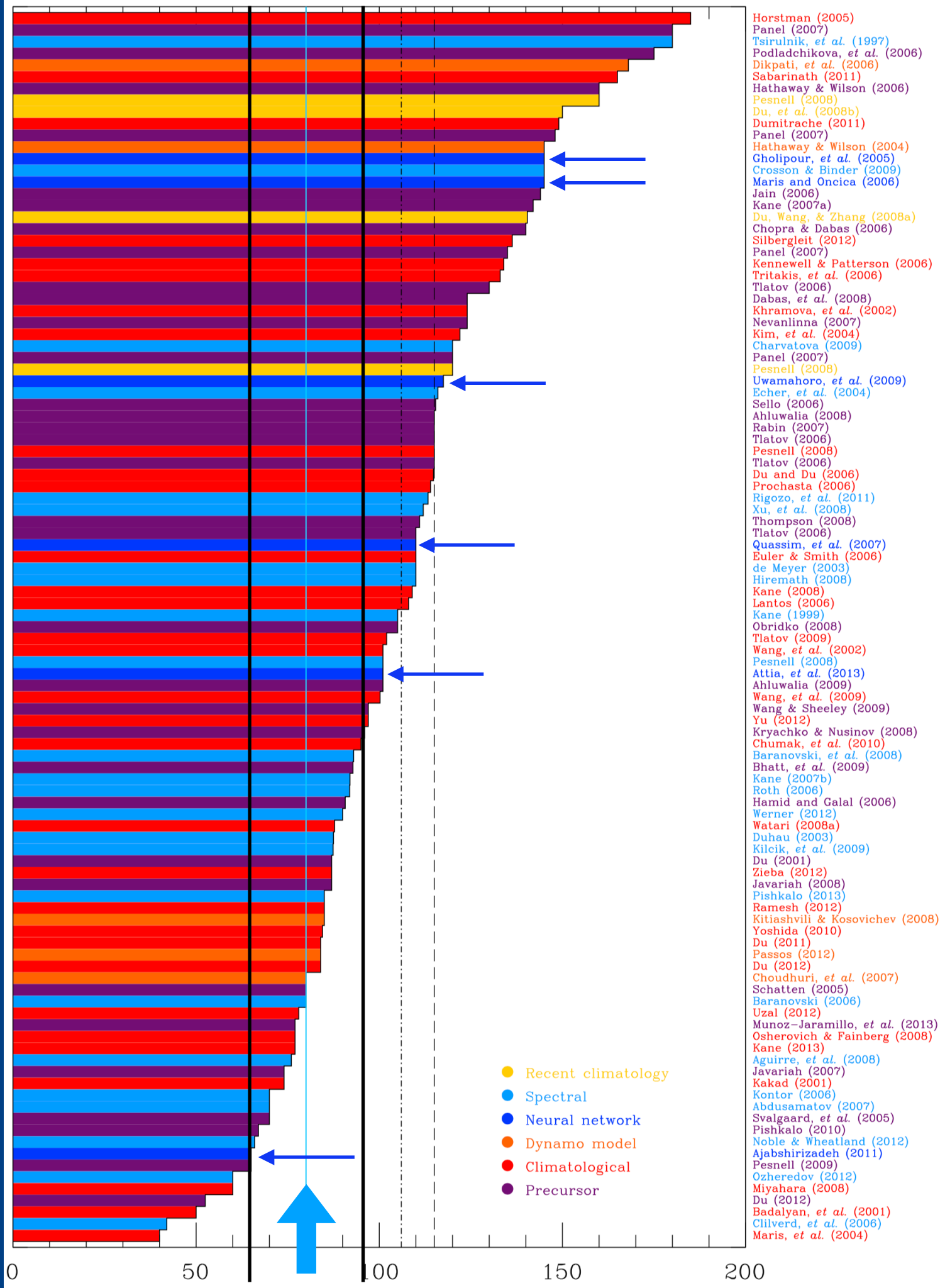
Evaluation of Kp and Dst Predictions Using ACE and DSCOVR Solar Wind Data  
 P. Wintoft and M. Wik  
 Space Weather 16 1972-1983 (2018)

# Prediction lead time

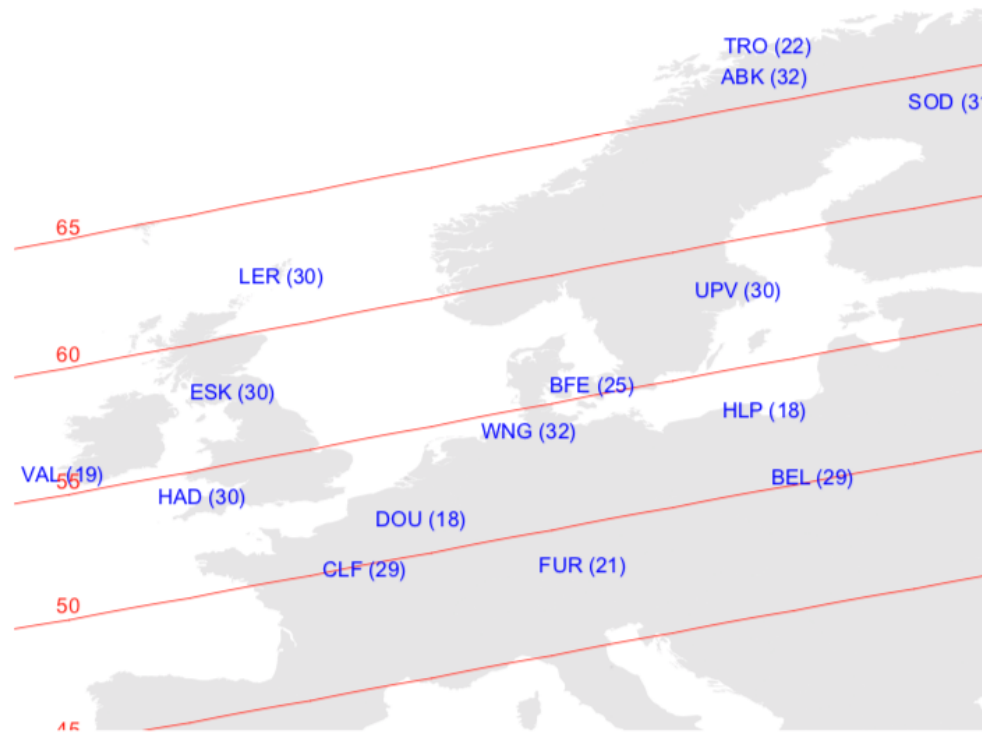


Evaluation of Kp and Dst Predictions Using ACE and DSCOVR Solar Wind Data  
P. Wintoft and M. Wik  
Space Weather 16 1972-1983 (2018)

# SC 24 Panel



# Extreme value analysis

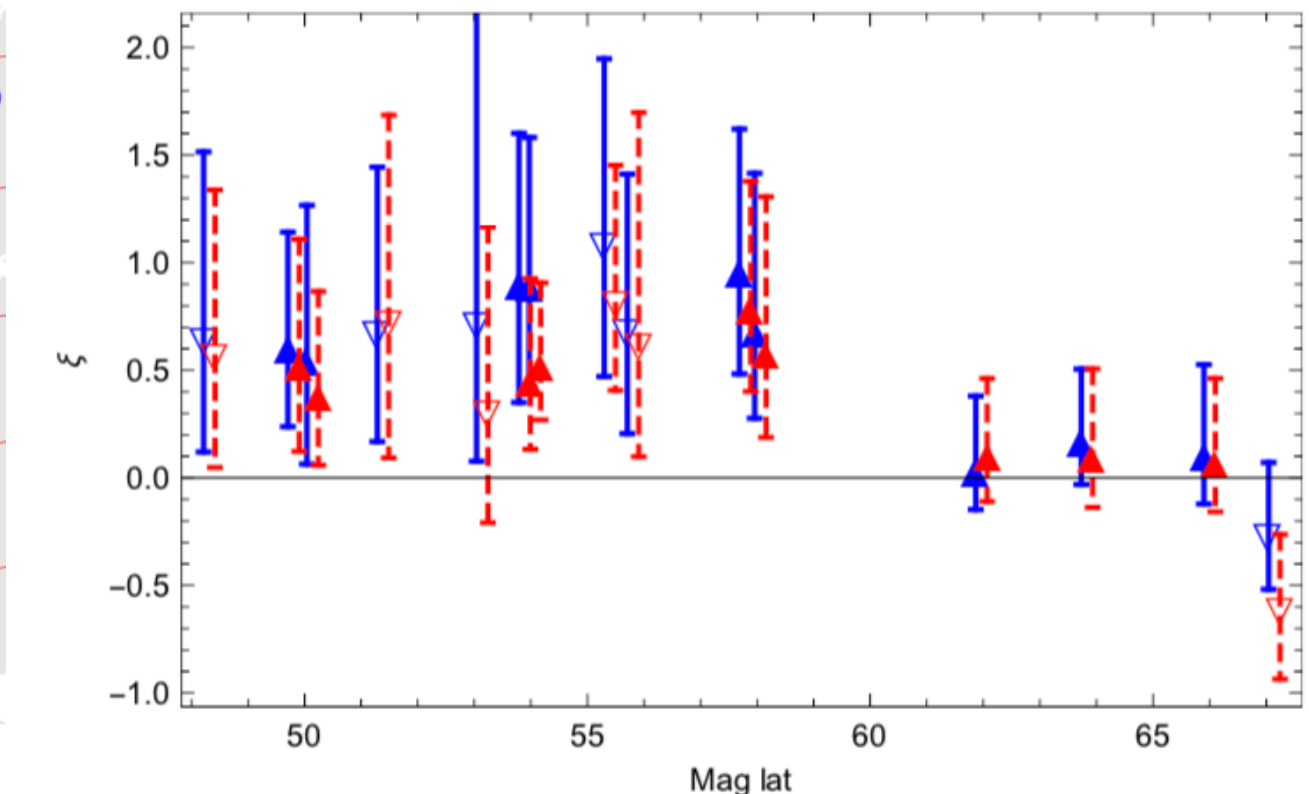


## PDF

$$g(z) = \left[ 1 + \xi \left( \frac{z - \mu}{\sigma} \right) \right]^{-(\xi+1)/\xi} e^{-\left[ 1 + \xi \left( \frac{z - \mu}{\sigma} \right) \right]^{-1/\xi}}$$

P. Wintoft and A. Viljanen and M. Wik, Extreme value analysis of the time derivative of the horizontal magnetic field and computed electric field, *Annales Geophysicae*, 34 ,485–491, 2016.

Quantifying extreme behavior in geomagnetic activity, A. Thomson and E. B. Dawson and S. J. Reay, *Space Weather*, 9, S100001 (2011)



## Distributions with

- **negative shape** are bounded
- **positive shape** are unbounded

